The Dissertation Committee for Tiffany Marcel Mott Certifies that this is the approved version of the following dissertation:

Characterization of the *Burkholderia mallei* Δ*tonB* Mutant and its Potential as a Backbone Attenuated Strain for Vaccine Development

Committee:

Alfredo G. Torres, PhD., Supervisor

Ashok Chopra, Ph.D., C.Sc.

Gustavo Valbuena, M.D., PhD.

Janice Endsley, Ph.D.

Shelley Payne, Ph.D.

Dean, Graduate School

Characterization of the *Burkholderia mallei* Δ*tonB* Mutant and its Potential as a Backbone Attenuated Strain for Vaccine Development

by

Tiffany Marcel Mott, B.S.

Dissertation

Presented to the Faculty of the Graduate School of

The University of Texas Medical Branch

in Partial Fulfillment

of the Requirements

for the Degree of

Doctor of Philosophy

The University of Texas Medical Branch

August

Dedication

I dedicate this dissertation to those whose constant support and sacrifice made this possible, including: my father, Richard Mott; my mother, Victoria Mott; my sister, Cassandra Goddard; my niece, Abigail Mott; my best friend, Ericka Verrett; and my dog, Nala.

Acknowledgements

I would like to acknowledge my mentors Dr. Alfredo Torres for his guidance and supervision. I would like to recognize my committee members Drs. Shelley Payne, Gustavo Valbuena, Ashok Chopra and Janice Endsley for their time, input and assistance. Also, I would like to thank past and present members of the Torres Lab Dr. Gregory Whitlock, Dr. Barbara Judy, Dr. Doug Botkin, Dr. Shane Massey, Dr. Sonja Lloyd, Dr. Anjana Kalita, Dr. Jia Hu, Roberto Cieza, Carla Blumentritt, Maricarmen Rojas-Lopez, Lieutenant Chris Hatcher, Brittany Ross, and Laura Muruato. All of the forgoing have my gratitude for their technical and creative assistance, in addition to having the patience of saints and wonderful listening skills when I needed to vent. Lastly, and most important, I would like to thank Rob Zombie and Xena Warrior Princess, who have from my early beginnings been a constant source of inspiration and provided me with entertainment and the motivation to complete my life goals. Without the support of all those listed, this accomplishment would not have been possible.

Characterization of the *Burkholderia mallei* Δ*tonB* Mutant and its Potential as a Backbone Attenuated Strain for Vaccine Development

Publication No._____

Tiffany Marcel Mott, Ph.D.

The University of Texas Medical Branch, 2014

Supervisor: Alfredo G. Torres

In this study, a *Burkholderia mallei* Δ*tonB* mutant deficient in iron acquisition was constructed, characterized and evaluated for its protective properties in acute inhalational mouse models of glanders and melioidosis infection. Compared to wild type, the *B. mallei* Δ*tonB* exhibits slower growth kinetics, siderophore hypersecretion and the inability to utilize hemin, hemoglobin and myoglobin as iron sources. A series of animal challenge studies showed an inverse correlation between percent survival in BALB/c mice and iron-dependent *B. mallei* Δ*tonB* mutant growth. Upon evaluation of the *B. mallei* Δ*tonB* mutant's potential as a protective vaccine, 100% survival was achieved after wild-type challenge in those animals previously immunized with $1.5x10^4$ CFU of the *B. mallei* Δ*tonB* mutant. At 21 days post immunization, *B. mallei* Δ*tonB* vaccinated animals showed significantly higher levels of *B. mallei* specific IgG1, IgG2a and IgM compared to PBS vaccinated animals. At 48 h post-challenge, PBS-treated animals exhibited higher levels of serum inflammatory cytokines and more severe pathological effects in target organs compared to animals immunized with the *B. mallei* Δ*tonB* mutant. In a cross-protection study with *Burkholderia pseudomallei*, *B. mallei* Δ*tonB* mutant-immunized animals showed significant protection when evaluated in an acute inhalational

melioidosis mouse model. While the wild-type was cleared in all the vaccination studies, animals failed to clear the *B. mallei* Δ*tonB* mutant, which was primarily recovered from the spleen. Although further work is need to reduce its long-term persistence, maintaining immunogenicity, the *B. mallei* Δ*tonB* mutant demonstrates great potential as backbone attenuated strain for vaccine development against both glanders and melioidosis.

TABLE OF CONTENTS

List of Tables

List of Figures

List of Illustrations

List of Abbreviations

2D2	*B. pseudomallei* strain 576 branch chain amino acid auxotroph
30:93	*B. pseudomallei* mutant containing a non-functional *purN* gene
56:65	*B. pseudomallei* mutant containing a non-functional *purM* gene
Δasd	*B. pseudomallei* mutant strain autotrophic for diaminopimelate (DAP)
ANOVA	Analysis of variance
aroB	3-dehydroquinate synthase gene
ATCC	American Type Culture Collection
BimA	*B. mallei* autotransporter protein
BopA	*B. mallei* type III secreted protein
Bp82	*B. pseudomallei* 1026b mutant containing a non-functional *purM*
BRI	*B. pseudomallei* strain 576
CapGB15	Irradiation inactivated *B. mallei* capsule negative mutant
CAS	Chrome azurol S
CFU	Colony Forming Units
CLDC	Cationic Liposome-Nucleic acid Complex
CO_2	Carbon dioxide
CpG	Cytosine-phosphate-Guanosine
CPS	Gram-negative capsular polysaccharides
CSM001	*B. mallei* strain carrying the *lux* reporter gene
DNA	Deoxyribonucleic acid
E8	*B. pseudomallei* non-l-arabinose-assimilating strain
ExbB	TonB accessory protein
ExbD	TonB accessory protein
ELISA	Enzyme Linked Immunosorbent Assay
Fe^{3+}	Ferric iron
Fe^{2+}	Ferrous iron
$FeSO_4$	Ferrous Sulfate
GSBS	Graduate School of Biomedical Science
H_2O_2	Hydrogen peroxide
H_2SO_4	Hydrogen Sulfate
HKGB15	Heat inactivated *B. mallei* ATCC 23344
IgG	Immunoglobulin G
IgG1	Immunoglobulin G subclass 1
IgG2a	Immunoglobulin G subclass 2a
IgM	Immunoglobulin M
ilvI	large subunit of the acetolactate synthase enzyme gene
Km	kanamycin
IL	Interlukin
i.n.	Intranasal
INF-γ	Interferon gamma

i.p.	Intraperitoneal
IRGB15	Irradiation inactivated *B. mallei* ATCC 23344
IVIS	*In vivo* Imaging System
LB	Luria-Bertani Broth
LBG	Luria-Bertani Broth with 4% D-Glucose
LD_{50}	Median lethal dose
LolC	*B. pseudomallei* ABC transporter protein
LPS	Lipopolysaccharide
MST	Mean survival time
MTTD	Mean time to death
NK	Natural Killer
OD_{600}	Optical Density at 600nm
ODN	Oligodeoxynucleotides
O-PS	LPS of *B. pseudomallei*
PBS	Phosphate Buffered Saline
PglB	*B. pseudomallei* oligosaccharyltransferase (OTase) enzymes
purM	gene that encodes step 5 of purine biosynthesis
purN	gene that encodes step 3 of purine biosynthesis
Pxb	Polymyxin B
s.c.	Subcutaneous
SD	Standard deviation
SCID	severe combined immunodeficient
serC	serine gene
T3SS	Type III secretion system
T6SS	Type VI secretion system
TDC	Thesis and Dissertation Coordinator
Th1	T helper cell 1 response
Th2	T helper cell 2 response
TonB	Energy transport protein
type I O-PS	*B. pseudomallei* capsular polysaccharide
type II O-PS	*B. pseudomallei* LPS O-antigen
type III O-PS	*B. pseudomallei* novel polysaccharide gene cluster 1
type IV O-PS	*B. pseudomallei* novel polysaccharide gene cluster 2
UTMB	University of Texas Medical Branch
UV	Ultraviolet
YT	Yeast tryptone

INTRODUCTION

Chapter 1: The Pathogens

Burkholderia mallei and *Burkholderia pseudomallei* are Gram-negative, intracellular pathogens that cause severe infections in humans and animals known as glanders and melioidosis, respectively [1,2]. *B. pseudomallei* is an environmental saprophyte endemic to the wet soil and stagnant water of Southeast Asia and Northern Australia [3-5]. *B. mallei* is an obligate mammalian pathogens in which solipeds (horses, mules and donkeys) in many parts of the world including the Middle East and Asia [6,7] serve as the natural reservoir for infection [8]. Human infections with either pathogen are associated with environmental exposure through inhalation, ingestion, cuts and skins abrasions [9-14]. The course and clinical manifestations of infection is dependent on the route of exposure. Direct contact with the skin can lead to a localized chronic suppurative infection of the skin. Inhalation of an aerosol containing either pathogen can lead to septicemic, pulmonary, or chronic infections of the muscle, liver and spleen. Melioidosis is typically treated with an aggressive regiment of antibiotic therapy for 20 weeks [4,15]. Even with early administration of therapy, an acute infection caused *B. pseudomallei* has a mortality rate of approximately 40% and a relapse rate of 10-15% among surviving patients [15]. Human cases of glanders have occurred rarely and sporadically among laboratory workers and those in direct contact with infected animals [16]. In these cases, glanders was also treated with an intense mixed antibiotic regimen that is has shown to be partially effective. Glanders has a 95% case fatality rate for untreated septicemia infections and 50% case fatality rate in antibiotic-treated individuals[17]. Treatment of both melioidosis and glanders is problematic due to the pathogen's high intrinsic resistance to many antibiotics [4,15]. Moreover, there is no prophylactic or therapeutic

vaccine available for man or animals [18,19]. Due to their potential for airborne transmission, ineffective treatment options and ability to cause a severe course of infection, the Centers for Disease Control have classified these two *Burkholderia* species as category B select agents. Furthermore, these pathogens are also considered a top candidate for bioterrorist use [20]. Their destructive potential has heightened concerns among public health officials due to the increased potential of opportunistic infection among growing populations of diabetic and immunocompromised people [21-23]. For military personnel and susceptible individuals, the availability of a vaccine would be the most efficacious and cost-effective way to protect from disease.

Chapter 2: Vaccines for Melioidosis and Glanders

INACTIVATED WHOLE CELL VACCINES

Historically representing a starting point for vaccine development, inactivated, whole cell vaccines have proven to be effective in the prevention of disease [24]. Composed of chemically or physically killed microorganisms, these vaccines are considered safe for immunocompromised individuals since there is no risk of wild type reversion or the onset of disease. Inactivated, whole cell vaccines induce robust antibodies responses and can general humoral immunity if boosters are given.

To test the protective efficacy of nonviable *B. mallei*, Amemiya et al. [25] made three cell preparations that consisted of heat inactivated *B. mallei* ATCC 23344 (HKGB15), irradiation inactivated *B. mallei* ATCC 23344 (IRGB15) or irradiation inactivated *B. mallei* capsule negative mutant (CapGB15). BALB/c mice were vaccinated subcutaneously (s.c.) with one of three *B. mallei* cell preparations and were given a boosted 21 days later. Four weeks after the boost, vaccinated mice were challenged intraperitoneal (i.p.) with 329 times the median lethal dose (LD_{50}) and observed for survival up to 21 days post challenge. All but one animal failed to survive

the challenge. The spleen of the surviving mouse vaccine with IRGB15 was greatly oversized and heavily colonized with bacteria. When lowering the challenge dose to 34 LD_{50}, all but one animal vaccinated with HKGB survived. Despite these results, it was unclear whether the increase in survival was due to the vaccine treatment or the combination of using older animals, which are more tolerant to infection, and lowering the challenge dose. Overall, it was concluded that none of the *B. mallei* cells preparations were unable to protect vaccinated mice against wild type challenge (X >300 LD_{50}).

In a similar study, Sarkar-Tyson et al. [26] tested the protective efficacy of heat inactivated *B. thailandensis, B. mallei* and *B. pseudomallei* against an aerosol challenge model of murine melioidosis and glanders. BALB/c mice were immunized i.p. with $1x10^7$ CFU of heat inactivated bacteria followed by two boost separated by two-week intervals. Five weeks after the last boost, vaccinated mice were i.p. or aerosol challenged with wild type bacteria. Heat-inactivated *B. pseudomallei* (K96243) vaccinated mice challenged i.p. with 100 LD_{50} of *B. pseudomallei* (K96243) showed 80% greater survival three weeks after challenge compared to control mice that all died by day 4. Similar results were seen in a parallel study using heat-inactivated *B. pseudomallei* strain 576. Vaccinated mice challenged i.p. with 100 LD_{50} of *B. pseudomallei* 576 showed even greater protection with 100% survival out to three weeks post challenge compared to control mice that all died by day 4. To investigate the protective potential of these heat-inactivated strains against strain composed of different O-antigen serotypes, mice were vaccinated either heat-inactivated *B. pseudomallei* K96243 or *B. pseudomallei* 576. Vaccinated mice were then i.p. challenged with the 100 LD_{50} of heterologous strain. In both experiments, all control mice died by day 4 whereas all vaccinated mice survival three weeks post challenge. Investigator in this study next examined the ability of *B. mallei* or *B. thailandensis* to cross protect against *B. pseudomallei* infection. Five weeks after the last boost, vaccinated mice were challenged i.p. with 40 LD_{50} of *B. pseudomallei* K96243. Vaccination with heat-inactivated *B. mallei* or *B. thailandensis* provided

77 comparable protection against *B. pseudomallei* K96243 challenge compared to both *B.*
78 *pseudomallei* strains when followed out to 45 days. Lastly, the protective capability of
79 heat-inactivated formulations composed of each of these *Burkholderia* species against
80 aerosolized *B. pseudomallei* and *B. mallei* was evaluated. Vaccinated mice were
81 challenged with 18 LD_{50} of B. pseudomallei K96234 or 3.5 LD_{50} of *B. mallei* five weeks
82 after the last boost. Challenge by the aerosol route resulted in much lowered protection
83 with heat-inactivated *B. thailandensis* conveying the least protection. The varying rates
84 of survival observed in treatment mice suggest that different heat inactivated
85 *Burkholderia* species/strains generate alternative immune responses. From the result of
86 the last three studies, Sarkar-Tyson et al. [26] concluded that three factors, bacterial
87 strain, route of vaccine administration, and route of challenge, must be considered to
88 generate an optimal immune response.
89 In a follow up study by Sarkar-Tyson et al. [27], *B. pseudomallei* mutants
90 carrying different inactivated polysaccharides gene clusters were generated and
91 investigated for their role in virulence and protective potential as heat inactivated whole
92 cell vaccines. *B. pseudomallei* strains used in this study carried an insertional
93 inactivation in one of four polysaccharide gene clusters: capsular polysaccharide (type 1
94 O-PS), LPS O-antigen (type II O-PS) and two novel polysaccharide gene clusters (type
95 III O-PS and type IV O-PS). Previously, *B. pseudomallei* type I O-PS and type II O-PS
96 cluster mutants have been showing to be attenuated in animal models of disease [25,28-
97 30]. To ascertain the roles of the type III O-PS and type IV O-PS polysaccharides in
98 virulence, mice were challenge with the *B. pseudomallei* ΔBPSS0421 or ΔBPSS1883
99 mutant, respectively, at 10^4 CFU via the i.p. route. Control mice all died 3 days post *B.*
100 *pseudomallei* wild type challenge. Mice challenged with *B. pseudomallei* ΔBPSS0421 or
101 ΔBPSS1883 resulted in an increased mean time to death (MTTD) of 7.8 and 11.6 days,
102 respectively. Next Sarkar-Tyson et al. [27] determined the protective potential of each
103 polysaccharide gene cluster individually by immunizing mice three times at two week

intervals with 10^8 CFU of heat-inactivated *B. pseudomallei* wild-type or one of the 4 polysaccharide gene cluster (type I-IV O-PS) mutants. Five weeks after the last boost, vaccinated mice were challenged with 10 LD_{50} of wild-type *B. pseudomallei* and monitored for survival for 35 days. The MTTD of vaccinated mice increased approximately three fold compared to PBS vaccinated mice that had a MTTD of 9.2 days. The MTTD for mice vaccinated with the heat-inactivated *B. pseudomallei* wild-type or *B. pseudomallei* mutants with nonfunctioning polysaccharide gene clusters type I O-PS, type II O-PS, type III O-PS and type IV O-PS are the following: 26.6, 32.5, 33, 29.7 and 28.3 days, respectively [27]. The varying levels of protection seen among vaccinated mice were attributed to their exposure to the distinct antigen profile of heat inactivated *B. pseudomallei* strain used for immunization. In addition, these results could be used to extrapolate the relative importance of each polysaccharide in protection against murine melioidosis.

LIVE ATTENUATED VACCINES

Given the facultative intracellular life style of *B. pseudomallei* and *B. mallei*, it has been proposed that live attenuated vaccines are best suited for protecting against infection. A live attenuated vaccine consists of an altered, viable version of a pathogen that can generate protective immunity without causing disease. Live attenuated vaccines work by mimicking natural infection which allows the production of both cellular and humoral immune responses that are highly specific, effective and long lasting.

The efficacy of using live attenuated vaccines against both *B. pseudomallei* and *B. mallei* has been investigated with some success. In 2002, Atkins et al. [31] identified and characterized a *B. pseudomallei* strain 576 branch chain amino acid auxotroph (2D2) that was generated by mutating the *ilvI* gene encoding the large subunit of the acetolactate synthase enzyme. Survival studies showed the *B. pseudomallei* 2D2 mutant to be highly attenuated in mice and effectively cleared from all organs by 30 days post challenge.

Mice vaccinated i.p. with *B. pseudomallei* 2D2 mutant (10^6 CFU) and subsequently challenged i.p. five weeks later with *B. pseudomallei* strain 576 or strain BRI (10^6 CFU) showed significant, yet partial protection. At 32 days post challenge with *B. pseudomallei* 576, vaccinate and naïve mice showed 80% and 0% survival, respectively. Vaccinated and naïve mice challenged with *B. pseudomallei* strain BRI had survival rates of 100% and 20% respectively. Differential protection conferred by the *B. pseudomallei* 2D2 mutant was speculated to result from the intrinsic differences in virulence between the challenge strains, clinical isolates of human melioidosis that produce immunologically distinct forms of LPS. This group reported a similar outcome in a parallel study where the *B. pseudomallei serC* mutant, a serine autotroph, was evaluated as a vaccine candidate. Results of this study showed 80% and 78.5% protection mice immunized i.p. with the *B. pseudomallei serC* mutant at 28 days post i.p. challenge with *B. pseudomallei* strains 576 and K96243, respectively [32]. In both studies, not only it was illustrated that live attenuated *B. pseudomallei* mutant auxotroph vaccination could provide cross-protection against heterologous strains of *B. pseudomallei*, but also highlighted the ability of antigens other than LPS to generate protective immunity. To make these auxotroph's clinical useful, Rodrigues et al [32] speculated the need to introduce additional mutations, such as the generation of a *B. pseudomallei serC ilvI* double auxotroph, to confer an irreversibly attenuated virulence phenotype. In a follow up study on the *B. pseudomallei* 2D2 mutant, Haque et al. [33] evaluated it's potential to provide long term protection against murine melioidosis. Performing the same vaccination and challenge studies outlined by Atkins et al. [31], Haque et al. [33] reported a median survival time (MST) of 3 days and high bacterial burdens in unvaccinated mice. Conversely, vaccinated mice had an increased MST of 52 days with significantly reduced bacterial burdens. However, vaccinated mice began to succumb to infection about 30 days post challenge, a finding which may mean the *B. pseudomallei* 2D2 vaccine is only able to protect against the acute phase of melioidosis.

Since parenteral vaccination does not always protect against inhalation exposure, Ulrich et al. [34] generated a *B. mallei* branch chain amino acid auxotroph (ILV1) to evaluate its potential to protect against aerosol-initiated murine glanders. Similar to what was seen with *B. pseudomallei* 2D2 mutant, survival studies showed the *B. mallei* ILV1 mutant to be highly attenuated and cleared by mice within 7 days post aerosol exposure. Mice vaccinated and then boosted 22 days later with the *B. mallei* ILV1 mutant at a predicted inhalational dose of $7.3x10^4$ and $4.7x10^4$ CFU, respectively, were challenged with 440 LD_{50} of aerosolized *B. mallei* ATCC 23344. By day 4 post challenge, all naïve animals had succumbed to infection where as 90% of vaccinated mice were still alive. However, vaccinated mice expired over time and by one-month post challenge only 25% survived. When exposed to a lower dose of *B. mallei* ATCC 23344 (5 LD_{50}), 50% of vaccinated mice survived till one-month post challenge. Necropsies revealed abscesses and pyogranulomas present on all the spleens, which were enlarged, and livers of surviving mice. Vaccinate mice were chronically infected with the challenge strain, which was detected in the lungs, liver and spleen. Although the *B. mallei* ILV1 mutant was unable to provide full protection against both high and low dose *B. mallei* aerosol challenge, it did increase the MST of vaccinated animals compared to naïve controls. Ulrich et al. [34] postulated that the *B. mallei* ILV1 mutant was cleared too rapidly to provide the antigenic exposure needed to generate a fully protective immune response. Cuccui et al. [35] came to a similar conclusion to rationalize the minor protection seen in i.n. *B. pseudomallei* K96243 ($1x10^3$ CFU) challenged mice that were i.n. vaccinated 35 days prior with the *B. pseudomallei aroB* mutant ($1x10^5$ CFU), an aromatic compound auxotroph. Subsequent colonization studies showed complete clearance of the *B. pseudomallei aroB* mutant ($6.5x10^5$ CFU) by day 3 post i.n. challenge. Thus, the generation of an auxotroph that can persist longer *in vivo* may be required to generate protective immunity against aerosolized exposure to *B. mallei*.

183 The hypothesis that the persistence of a live attenuated vaccine is important for
184 the protective potential is further supported in a study by Breitbach et al. [36], which
185 evaluated the vaccine potential of two live attenuated *B. pseudomallei* E8 mutants
186 deficient in different steps of purine biosynthesis. The *B. pseudomallei* prototrophic
187 mutant 30:93 contains a non-functional *purN* gene that encodes step 3 and the *B.*
188 *pseudomallei* auxotrophic mutant 56:65 contains a non-functional *purM* gene that
189 encodes step 5. Mice challenged i.p. with wild-type *B. pseudomallei* E8 (10^6 CFU)
190 showed greater protection when vaccinated i.n. four weeks prior with $5x10^3$ CFU the *B.*
191 *pseudomallei* 30:93 *purN* mutant vs. the *B. pseudomallei* 56:65 *purM* mutant. However,
192 the same level of protection was achieved in mice vaccinated i.n. with a higher dose
193 ($5x10^5$ CFU) of the *B. pseudomallei* 56:65 *purM* mutant. The *B. pseudomallei* 30:93
194 *purN* mutant was also reported to establish a 10^2-10^3-fold higher bacterial burden in the
195 spleen and liver of challenged mice compared to the *B. pseudomallei* 56:65 *purM* mutant.
196 It was speculated that prolonged persistence of the *B. pseudomallei* 30:93 *purN* mutant
197 resulted in more sufficient protection against i.p. challenge. The enhance burden of the
198 *B. pseudomallei* 30:93 *purN* mutant could be attributed to its prototrophic nature, which
199 is theorized to result from its expression of an alternative third step pathway of purine
200 synthesis. The *B. pseudomallei* auxotrophic 56:65 *purM* mutant has no way to
201 compensate for its loss of function, which could explain its rapid clearance *in vivo*. To
202 examine a possible link between persistence and protective potential, Breitbach et al. [36]
203 compared the survival of wild-type *B. pseudomallei* ($5x10^4$ CFU) i.p. challenged mice
204 vaccinated i.p. with live, heat-killed or UV-irradiated preparations of the *B. pseudomallei*
205 30:93 *purN* mutant. All mice immunized with 10^8 CFU of killed preparations perished
206 by four weeks post challenge whereas mice immunized with 10^5 CFU of live bacteria
207 showed 100% survival. The inability of killed preparations to provide protection
208 comparable to that of live preparation supports the theory that persistence of viable
209 bacteria is important for protective potential. As these results are in agreement with

previous reports [37-40], it was proposed that increased short-term persistence of a live attenuated vaccine enhances the immune system's exposure to protective antigens that result in the generation of a more educated, protective response. Although the *B. pseudomallei* 30:93 *purN* mutant was shown to provide protection during the acute phase of melioidosis, like many vaccine candidates previously tested, it failed to prevent against the development of chronic forms [30-32,35,36,41].

Investigating an alternative approach to increasing short-term vaccine persistence, Norris et al. [42] employed an i.n. prime-boost vaccination strategy in an effort extend protection and prevent the development of chronic melioidosis. Ten mice primed via i.n. vaccination with $1x10^7$ CFU of the *B. pseudomallei* 1026b *Δasd* mutant, a strain autotrophic for diaminopimelate (DAP), were then boosted in the same manner two weeks later. Vaccinate mice i.n. challenged with $4x10^3$ CFU of wild-type *B. pseudomallei* 1026b three weeks post boost showed enhanced protection compared to the naïve controls, which all perished by day 3. However, despite this enhanced protection, all vaccinated animals developed chronic infection and perished by 60 days post challenge. Despite the incorporation of a boost to increase antigenic exposure, the failure to generate protective immunity against chronic melioidosis was attributed to the *B. pseudomallei* 1026b Δ*asd* mutant's inability to persist long enough or disseminate and proliferate enough *in vivo*. Further, Norris et al. [42] suggested the i.n. route of vaccination may have been insufficient to provide systemic protection. This could account for the fact that the mice were protected from the initial lung infection during the acute phase but eventually succumbed to the systemic infection of the chronic phase. The incorporation of an intramuscular or subcutaneous vaccination with the inhaled vaccination could be a means to produce the systemic dissemination need to generate protection against chronic and/or latent infection.

Subcutaneous administration of the attenuated *B. pseudomallei* mutant Bp82 was evaluated by Silva et al. [43] for its ability to generate systemic protection in an

inhalational model of murine melioidosis. The previously characterized Bp82 mutant is a *B. pseudomallei* 1026b derivative containing a *purM* gene deletion that makes it auxotrophic for adenine and thiamine [44]. Keeping with the prime-boost strategy, BALB/c and C57BL/6 mice were immunized twice s.c. with $5x10^6$ CFU of the *B. pseudomallei* mutant Bp82 10 days apart. Vaccinated BALB/c and C57BL/6 mice challenged i.n. with 5 LD_{50} of wild-type *B. pseudomallei* 1026b showed 60% and 100%, respectively, survival till the experimental end of 60 days. The difference in protection can be attributed to the differential intrinsic resistances between mice strains, in which C57BL/6 mice are more resistant to *B. pseudomallei* infection where as BALB/c are more susceptible. These findings indicate that subcutaneous administration can effectively generate systemic protection from inhalational *B. pseudomallei* challenge. However, the inability to achieve 100% survival in susceptible murine models of infection necessitates further study to optimize protection.

SUBUNIT VACCINES

As indicated above, *Burkholderia* infections are difficult to treat with antibiotics and there are several reports indicating it is feasible to protect against melioidosis, at least in animal models of disease, with non-living vaccines [79]. There has also been some progress in identifying partially protective subunits. Current evidence indicates that other surface-expressed or secreted proteins are immunogenic and structural similarity exists between the proteins in *B. pseudomallei* and *B. mallei* [80,81]. Therefore, a recent study was aimed to identify *Burkholderia* protective proteins that could be administered in vaccines to generate cross-protective immunity against both *B. mallei* and *B. pseudomallei* [38]. The genes encoding each *B. mallei* protein, BimA (autotransporter protein), BopA (type III secreted protein), and *B. pseudomallei* LolC (ABC transporter protein), were cloned into pCDNA3.1+ and pET28a and the His-tag proteins were purified by chromatography. Six to eight week old female BALB/c mice were primed

with 10 μg of recombinant proteins mixed with Cytosine-phosphate-Guanosine (CpG) adjuvant and mixed with ISCOM, followed by a 2 week boost of 5 μg recombinant proteins with adjuvant. Four weeks post-boost, animals were infected by intranasal inoculation with 2 LD_{50} of *B. mallei* ATCC 23344. It was found that immunization with the recombinant *B. mallei* proteins generated significant protection against lethal inhaled *B. mallei* ATCC 23344 and survival of 100% up to 21 days post-infection, in mice vaccinated with recombinant BimA or BopA [38]. Experiments were also conducted to determine whether the *Burkholderia* recombinant antigens were also capable of generating protective immunity against *B. pseudomallei* challenge. For these experiments BALB/c mice were immunized with 2 μg of the purified recombinant BimA, BopA, or LolC proteins given with cationic liposome-nucleic acid complex (CLDC) adjuvant, and then boosted 2 more times. Mice were subjected to lethal intranasal challenge with 2 LD_{50} of *B. pseudomallei* strain 1026b. Immunization with BopA elicited the greatest protective activity, resulting in 60% survival against *B. pseudomallei* challenge [38]. Moreover, sera from recovered mice demonstrated reactivity with the recombinant proteins. Dendritic cells stimulated with each of the different recombinant proteins showed distinct cytokine patterns. In addition, T cells from immunized mice produced IFN-γ following in vitro re-stimulation. This study demonstrated that it was possible to elicit cross-protective immunity against both *B. mallei* and *B. pseudomallei* by vaccinating animals with one or more novel recombinant proteins identified in *B. mallei* and the serological results suggest that an optimal level of Th1 (IgG2a) and Th2 (IgG1) responses are important for protection in *B. mallei* infection [38].

PROTEIN-POLYSACCHARIDE CONJUGATE VACCINES

Gram-negative capsular polysaccharides (CPS) and lipopolysaccharides (LPS) are important virulence factors and major targets of the immune response to infection. Polysaccharides make excellent vaccines, as evidenced by the number of capsule-based

vaccines that are currently licensed for humans, including those to combat *Haemophilus influenzae, Streptococcus pneumoniae, Neisseriae meningitidis,* and *Salmonella enterica* serovar Typhi infection. Although effective in some groups of individuals, polysaccharides alone are generally poor vaccinogens that do not produce an anamnestic response because of the lack of T-cell involvement in the generation of immunity. The T-independent immune response generated by polysaccharide-based vaccines is generally associated with the production of IgM. To elicit a more favorable T-dependent response, polysaccharides are often conjugated to proteins. This is particularly important when polysaccharide vaccines are to be used in children, since this group generally responds poorly to this type of vaccine in the absence of a protein carrier. Using current technology, it is difficult to produce and manufacture these glycoconjugate vaccines, which require purification of capsular polysaccharide from the native pathogen and chemical coupling to a protein carrier. Demonstrating that it can be used to produce recombinant glycans, pioneering studies on PglB promises to resolve these technological problems [45]. It is worth noting that an experimental conjugate of *B. pseudomallei* O-antigen linked to flagellin protein was immunogenic and able to provide protection against melioidosis. Unfortunately, *B. mallei* are not motile, and this limits the utility of this conjugate for protecting against glanders.

Although surface polysaccharides are proven human vaccines, different polysaccharides amongst strains of the same bacterial species make the development of vaccine difficult. In contrast, in *B. pseudomallei* and *B. mallei* the CPS appears to be conserved across all strains and only two types of LPS O-antigen have been reported. Against this background the prospect is excellent for devising a *B. pseudomallei / B. mallei* vaccine based on CPS and/or LPS O-antigen.

Cellular and Humoral immunity against *Burkholderia* infection

Although host immune responses to *B. mallei* and *B. pseudomallei* infection, including the innate, the humoral and the cellular components, have been studied for a number of years, immune components of protection remain largely undetermined. As facultative intracellular pathogens, the capability of both species to invade, replicate and survive within host cells suggests that cell-mediated responses combined with a humoral response are linked to protection. Elicitation of the T helper 1 (Th1)-mediated immune response has been extensively reported in the literature as an essential link in protection against *B. mallei* and *B. pseudomallei* infections. Th1-mediated immune responses produce a cytokine profile that supports inflammation and cell-mediated responses.

Investigating the protective effects of 3 different *B. mallei* killed, whole-cell vaccine treatments in BALB/c mice, Amemiya et al. analyzed cytokine and antigen-specific isotype profiles in an attempt to define protective responses against *B. mallei* infection. Researchers reported a mixed Th1/Th2 cytokine profile, a higher IgG1/IgG2a ratio of serum immunoglobulin and inefficient protection against infection in treatment animals [25]. The initial protection was correlated to the increased production of Th1-like cytokines (IL-2 and IFN-γ) and Th2-like cytokines (IL-4, IL-5, and IL-10) [25]. However, the failure to protect against *B. mallei* infection was attributed to the treatment's inability to generate a polarized Th1 or Th2 cytokine profile [25]. Furthermore, the Th2 skew indicated by the higher IgG1/IgG2a ratio suggest elicitation of Th1 immunity may provide better protection. Therefore, Amemiya et al. [46] next incorporated interlukin-12 (IL-12) into the vaccine regimen with inactivated *B. mallei*. Secreted by macrophages and dendritic cells, IL-12 enhances the cytotoxic activity of natural killer cell and CD8+ cytotoxic T lymphocytes, stimulates production of IFN-γ and promotes the Th1 subset of adaptive immunity. Upon the addition of IL-12, researchers reported greater protection against wild-type challenge with an increased mean survival time of 11 days [47]. This protection was attributed to the increased IL-12-mediated

production of IgG2a, a more Th1-like antibody response, and IFN-γ, a cytokine critical for protection against intracellular bacteria [47]. Similar results were reported in the aforementioned vaccination studies where CpG-containing oligodeoxynucleotides (ODN), cationic liposome DNA complexes (CLDC) and *Burkholderia* auxotrophs were used as treatment prior to *Burkholderia* wild-type challenge. Eliciting production of IL-12 and type 1 interferon via Toll-like receptor 9 pathways, CpG-containing ODNs were reported to result in 100% protection when used as a pretreatment compared to the 70% mortality observed in control BALB/c mice [48]. Potent activators of innate immunity, CLDCs were reported to provide 100% protection against both *B. mallei* and *B. pseudomallei* infection surviving till the experimental end on day 21 whereas control mice demonstrated 100% mortality by day 3 [49]. To define the components in CLDC mediated protection against infection, researchers used antibody depletion and/or BALB/c knockout mice to study the roles of IFN-γ and NK cells. Neutralization of both IFN-γ and NK cells abrogated CLDC-mediated protection [49]. Thus, CLDC-mediated protection was reported to be dependent on the production of IFN-γ and NK cells activation [49]. Overall, studies for *B. pseudomallei* and T cell-mediated immunity suggest that IFN-γ expressing cells should be the targets for an effective vaccination strategy.

Mutants of *B. pseudomallei* and *B. mallei*, auxotrophic in the branch chain amino acid biosynthetic pathway, have shown to be protective in challenge studies. Compared to 100% mortality in control mice, vaccination studies show 50% and 80% survival in auxotroph pretreated animals after infection with wild type *B. mallei* and *B. pseudomallei*, respectively [50,51]. As evident by the high IgG2a/IgG1 ratio, the *B. mallei* auxotrophic mutant's skewing of Th1 immunity was attributed to the protection seen in vaccinated animals [51]. Investigating further the cellular involvement in protection conferred by the *B. pseudomallei* auxotroph (2D2) vaccination, Haque et al. [52] compared the survival times of severe combined immunodeficient (SCID) mice

adoptively transferred with T cells from immunized mice to that of naïve T cell recipient counterparts after wild type challenge. Increased survival in SCID mice that received T cells from 2D2 immunized mice suggests that T cell mediated responses play an important role in the protection conferred by 2D2 immunization [53]. In the same study, to determine the role of specific T cell subtypes, 2D2 immunized mice antibody depleted of either CD4+ or CD8+ T cells were challenged with wild type *B. pseudomallei* and then monitored for survival [53]. No change in 2D2-mediated protection was seen in mice depleted of CD8+ T cells [53]. On the other hand, immunized CD4+ T cell depleted mice displayed an increased susceptibility to infection, as seen with the naive control mice, compared to that of immunized mice receiving isotype control antibodies [53]. These data demonstrated that 2D2 vaccine induced immunity was mediated by CD4+, but not CD8+ T cells.

B. mallei iron transport systems implicated as essential virulence determinants by comparative genomic analysis.

To date, virulence factors utilized by *B. mallei* for infection, dissemination and colonization within the body remain relatively unknown. Thus far, only four virulence factors, the capsule, the quorum sensing system, the type III (T3SS) and type VI (T6SS) secretion systems, have been shown to be essential for virulence in animal models [21,54-60]. Comparative analysis of the sequenced *B. mallei* ATCC 23344 genome has provided further insight into its mechanisms of pathogenesis and evolutionary history. To elucidate factors essential for survival in the host, Nierman et al. [21] used DNA microarray analysis to compare gene expression profiles of *B. mallei* collected from the livers of Syrian golden hamsters to *B. mallei* grown in Luria-Bertani (LB) medium. Among the genes with the most notable differential expression in the hamster, an environment where free iron concentrations are deficient for bacterial survival, were iron

storage and iron acquisition proteins [21]. The down-regulated expression of iron storage proteins and up-regulated expression of iron acquisition proteins illustrates the adjustments necessary for optimal *B. mallei* survival in the host. In a similar experiment conducted by Kim et al. [61], *B. mallei* collected from mouse livers and spleens were evaluated for differential gene expression when compared to *B. mallei* grown in LB. Substantiating the findings of Nierman et al. [21], *B. mallei* genes involved in iron acquisition were among the most up-regulated genes identified by Kim et al. [61]. Iron is an essential factor for bacterial growth and survival, as it is involved in a multitude of biological processes, e.g., electron transport, oxygen activation, H_2O_2 reduction [62]. To evaluate iron-regulated gene expression in *B. mallei*, Tuanyok et al. [63] used DNA microarray analysis to compare gene expression profiles of *B. mallei* grown in iron-depleted or replete conditions. In iron-depleted conditions, the genes encoding most respiratory metabolic systems and proteins of related function were down-regulated in expression. Conversely, genes encoding siderophore-mediated iron transport systems, heme-hemoglobin receptors and alternative metabolic enzymes were up-regulated [63]. Taken as a whole, findings from these studies suggest that iron acquisition systems are essential for *B. mallei* adaptive survival with host. Therefore, an aim of the current study was to investigate this hypothesis. To our knowledge, this is the first investigation into *B. mallei* iron acquisition systems and their contribution to virulence. This work is significant because the information gained from this study could not only enhance the overall knowledge of *B. mallei* pathogenesis, but also lead to the identification of new targets for vaccine development.

TonB is an essential determinate for virulence and target of attenuation and vaccine development.

Iron is the only transition metal known to be growth limiting and to play an essential role in bacterial virulence [20,62,64-70]. The removal of free iron from the environment on the part of the host has been theorized to be a primary defense mechanism against infection. Known as iron withholding, this mechanism functions to deprive invading pathogens of iron in a way that this growth-essential element is still accessible for host metabolism [71]. In the host, iron is bound by proteins such as ferritin, transferrin, and lactoferrin, or sequestered within hemoglobin. Heme, the most abundant form of iron-containing complex, is first synthesized by the host and then is either incorporated into hemoglobin or bound by hemoplexin [71]. Ferritin is the primary intracellular iron-storage protein that acts as a buffer between iron deficiency and iron overload. Transferrin and lactoferrin are important extracellular binding proteins that attach to iron so tightly that, when in equilibrium, only one iron ion per liter remains free [62]. As a result, free iron levels in the mammalian host under normal conditions are only available at growth-limiting concentrations for microorganisms estimated to be as low as 10^{-24} M [72-74]. Upon infection, the host responds defensively by lowering free iron levels an additional 30% [71]. To replicate in the host, bacteria generally need to acquire 10^5 to 10^6 iron ions per cell division [62]. To fulfill this requirement, bacteria have multiple iron acquisition systems that are grouped under four categories of iron uptake: siderophore, heme, Fe^{3+} and Fe^{2+} (Illustration 1) [18]. These iron acquisition systems attain this element by using one of two general mechanisms. In the first mechanism, bacteria synthesize and secrete siderophores. These high-affinity, iron-chelating compounds competitively bind extracellular iron ions and transport them back into the cell as an iron complex via specific transport systems [62]. In the second mechanism, bacteria synthesize high-affinity transferrin and lactoferrin outer-membrane receptors that are able to seize iron from host transferrin and lactoferrin for transport across the outer membrane [62]. For both mechanisms, the import of iron from the extracellular space requires the energy-dependent process of active transport. Since there

is no energy source in the outer membrane, nearly all Gram-negative bacteria depend upon the function of the cytoplasmic membrane-bound, energy-transducing protein TonB for iron acquisition [75].

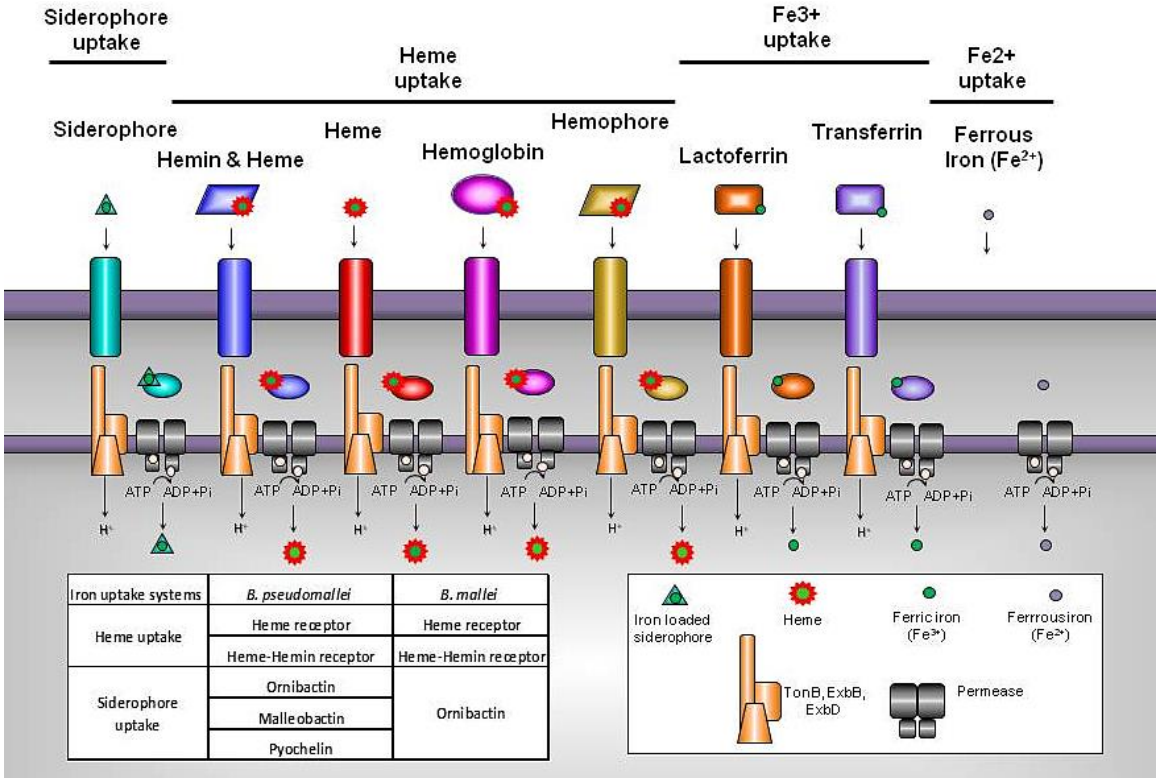

Illustration 1: Bacterial iron transport. A schematic view of Gram-negative iron uptake systems is shown. Inset table depicts the specific iron transport systems of *B. mallei* and *B. pseudomallei*.

TonB, along with its accessory proteins ExbB and ExbD, functions to transport energy derived from the proton motive force in the cytoplasm to outer-membrane receptors for active transport of iron into the periplasm [76-81]. When assessed in models of infection, all null mutations in the *tonB* gene resulted in attenuation, a conserved phenotype among all plant, animal and human Gram-negative pathogens evaluated thus far [82-95]. When studying the *tonB* mutation in *Klebsiella pneumoniae*, Hsieh et al. [86] reported the mutant's inability to grow in iron-deficient media, reduced capability to grow on blood agar or LB media, and severe attenuation of virulence, which

460 resulted in a higher LD_{50} when inoculated in mice [86]. Furthermore, when used to
461 immunize mice in vaccination studies, the *K. pneumoniae tonB* mutant was reported to
462 provide 100% protection against wild-type challenge [86]. These results provide proof of
463 concept that Gram-negative *tonB* mutants are attenuated and, in one case, can provide
464 protection against infection. In all these studies, among the genes with the most up-
465 regulated expression *in vivo* or under iron-depleted conditions were those involved in
466 TonB-dependent transport, including *tonB* itself [21,61,63]. Thus, from what little is
467 known, *B. mallei* iron-transport systems, specifically their contribution to virulence and
468 potential as targets for vaccine development, necessitate further investigation with a
469 focused emphasis on the TonB-dependent iron transport. As to our knowledge, this is the
470 first investigation into TonB-dependent iron transport in *Burkholderia*. Results from
471 these studies could further solidify TonB as a desirable target for *B. mallei* vaccine
472 development. In addition, the knowledge gained from this study is applicable to the
473 development of vaccines for any pathogen that employs the TonB-dependent iron
474 transport system.

OBJECTIVES OF THIS STUDY

The long-term objective of this research is to develop an appropriate vaccine that is not only protective but also provides sterile immunity against *B. mallei* infection. In order to develop an appropriate vaccine for *B. mallei*, research should be focused on gaining a better understanding of its virulence factors and pathogenesis within the host in addition to host protective innate and adaptive responses, which, at present, are relatively unresolved for *B. mallei*. Thus, a more immediate goal of this research is to evaluate gene targets for live attenuated vaccine development. Whole genome DNA microarray studies suggest that iron acquisition systems play an important part in host adaption [21,61,63]. Iron is only present in growth limiting concentrations within the host; therefore, in order to establish infection, most Gram negative bacteria employ TonB-dependent active transport for iron uptake [62]. TonB functions to transport energy derived from the proton motive force in the cytoplasm to outer-membrane receptors for the import of iron into the periplasm [62]. Studies on TonB have reported severe attenuation in null mutants and, when assessed as a live attenuated vaccine candidate, provided 100% protection in BALB/c mice against lethal wild type challenge [82-84,86-95]. Thus, I believe that eliminating iron uptake by mutating the *tonB* gene will generate an attenuated *B. mallei* mutant that elicits protective immunity. I have tested my central hypothesis by completing the following three aims: 1) to assess the fitness and characteristics of the *B. mallei* Δ*tonB* mutant, 2) determine the contribution of Δ*tonB* to *B. mallei* invasion, dissemination and establishment of infection in BALB/c mice and 3) to determine the protective effects of vaccinating BALB/c mice with the live attenuated *B. mallei* Δ*tonB* mutant. In addition to this work, I focused on implementing a new *in vivo* imaging system to monitor disease progression, host responses and treatment outcomes. For this, I chose to evaluate the protective potential of CpG pretreatment in an

acute respiratory BALB/c mouse model of *B. mallei* infection. For proof of concept, I chose the bioluminescent *B. mallei* reporter strain CSM001 to monitor real time bacterial infection in combination with a new technique that employs a Neutrophil-Specific Fluorescent Imaging Agent to visualize neutrophil trafficking *in vivo*. All *in vivo* observations were followed by quantitative studies for validation.

MATERIALS AND METHODS

B. mallei Δ*tonB mutant* studies

IN VITRO STUDIES

Bacterial Strains and Growth Conditions

The bacterial strains and plasmids used in this study are listed in Table 1. All *E. coli* strains were grown in Luria-Bertani (LB) media at 37ºC or 30ºC, as required. All manipulations of *B. mallei* were conducted in CDC/USDA-approved and registered biosafety level 3 (BSL3) facilities at the University of Texas Medical Branch and experiments with select agents were performed in accordance with BSL3 standard operating practices. For all the experiments, all *B. mallei* strains were taken from freezer stocks, plated on LB agar containing 4% glucose (LBG) and incubated at 37ºC in 5% CO_2 for 3 days. For liquid cultures, a few colonies (2-3) were inoculated into 20 mL of LBG broth and incubated overnight with agitation at 37ºC in 5% CO_2. When employing antibiotic selection, kanamycin and polymyxin B were used at concentration of 50 µg/mL and 30 µg/mL, respectively. For counter-selection, co-integrates were grown in YT broth (10 g of tryptone and 10 g of yeast extract in 1 L of dH_2O) and then plated on sucrose agar (YT agar supplemented with 5% sucrose) as described by Hamad et. al [96]. When appropriate, LBG broth and agar were supplemented with $FeSO_4$ at a concentration of 200 µM. Unless otherwise stated, *B. mallei* ATCC 23344 (WT) or *B. mallei* CSM001 (*B. mallei* Lux), *B. mallei* TMM001 (Δ*tonB*) and *B. mallei* TMM002 (pTonB-comp) were used in all experiments.

DNA Methods, PCR and Cloning

Cloning methods were performed as previously described [96]. Chromosomal

528 **Table 1: Bacterial Strains and Plasmids**

Strains	**Relevant features**	**Reference**
B. mallei ATCC 23344	Human clinical isolate; $Km^{S}Pb^{R}$	[97]
B. pseudomallei K96243	Human clinical isolate; $Km^{R}Gm^{R}Zeo^{R}$ Pb^{R}	[98]
B. mallei CSM001	*B. mallei* ATCC 23344 with a mini-Tn*5*::*lux*Km_2; $Km^{R}Pb^{R}$	[99]
B. mallei TMM001	*B. mallei* ATCC 23344 with an unmarked deletion of *bmaa1801 (*Δ*tonB*)	This study
B. mallei TMM002	Δ*tonB* complemented with pTonB-comp; Km^{R}	This study
E. coli S17-1	For conjugal transfer, *recA thi pro hsdRM*+ RP4:2-Tc:Mu:KmTn7 Tp^{R} Sm^{R}	[100]
E. coli S17-1(pTonB-allex)	*E. coli* S17.1 with the recombinant suicide plasmid pTonB-allex; Km^{R}	This Study
Plasmids		
pMo130	Suicide vector for allelic exchange in *Burkholderia*; used to construct pTonB-allex; pUC19 *ori*, RK2 *ori*T, *xylE*, *sacB*, Km^{R}	[96]
pTonB-allex	pMo130 derived recombinant suicide plasmid used to generate Δ*tonB*; Km^{R}	This study
pMo168	Replicative vector for *Burkholderia; ori*pBBR1, *mob*+, *xylE*, Km^{R}	[96]
pTonB-comp	pMo168 derived recombinant replicative vector used to complement Δ*tonB*; pMo168:: *bmaa1801;* Km^{R}	This study

529 and plasmid DNA were isolated using the DNeasy Qiagen Blood and Tissue kit, and the
530 QIAGEN Plasmid Mini Kit, respectively (Qiagen, Inc., Valencia, CA). Polymerase chain
531 reaction (PCR) products were purified with either the QIAquick PCR purification kit or
532 QIAquick gel extraction kit (Qiagen). Restriction enzymes and T4 DNA ligase were
533 purchased from NEB and used in accordance with manufacturer instruction (New
534 England Biolabs Inc., Ipswich, MA). All primers used in this study were purchased from
535 Sigma-Aldrich Co (St. Louis, MO). All fragments obtained for cloning were amplified
536 with Phusion High-Fidelity DNA polymerase (New England Biolabs) using the following
537 Touchdown PCR protocol: 1 cycle of 95ºC for 5mins, 29 cycles of 95ºC for 30 sec, 70ºC

to 55ºC (-5ºC/cycle) for 30 sec, 72ºC for 2 min, 29 cycles of 95ºC for 30 sec, 55ºC for 30 sec, 72ºC for 30 sec, 1 cycle of 72ºC for 7 min and 12ºC until the end.

Construction and Complementation of a *B. mallei* Δ*tonB* mutant

Matched adaptamers containing 3' enzyme restriction sites and 5' complementary sequences were amplified via touchdown PCR. The sequences of the PCR primers were as follows: Δ*tonB* US forward primer (5' AAG CTA GCC CTC GGC GCG GCG ATC CGC GAC GT) (underlined sequence indicates a newly introduced *Nhe*I site); Δ*tonB* US reverse primer (5' CGG TAT TGC CGA GAT TAA CGG TGC GGC ACG TCG T); Δ*tonB* DS forward primer (ACG ACG TGC CGC ACC GTT AAT CTC GGC AAT ACC G); Δ*tonB* DS reverse primer (CCA AGC TTT ACG AGC ATG ACG TCG ACG AGC GGC GTC ATG TTG) (underlined sequence indicates a newly introduced *Hind*III site). The adaptamers were fused together via splicing by overlap (SOE) PCR to create a 1794 bp chimeric fragment containing sequences flanking the *tonB* gene plus its first 33 codons. The chimeric fragment was digested with *Nhe*I and *Hind*III and ligated into the pMo130 vector to create the allelic exchange plasmid pTonB-allex. The pTonB-allex plasmid was then transformed into *E. coli* S17-1 and introduced into *B. mallei* via conjugal transfer. Merodiploids were selected based on their growth on kanamycin (Km) agar plates and ability to turn yellow after exposure to pyrocathecol. Single deletion mutants were counter selected on 5% sucrose YT agar supplemented with 200 μM $FeSO_4$ (Illustration 2). The Δ*tonB* mutant was then confirmed via PCR amplification, followed by sequencing, of the *tonB* gene and flanking DNA regions using the following primers: Confirmation forward primer (5' GCG CCA CGC GGC CGA TTG CCG CTT TCT); Confirmation reverse primer (ACA GAA CCG TGC CGT CGC TTT). To restore the Δ*tonB* mutant to wild-type function, pMo168 carrying a functional *tonB* gene plus its native promoter was used for complementation. Briefly, a fragment containing the wild-

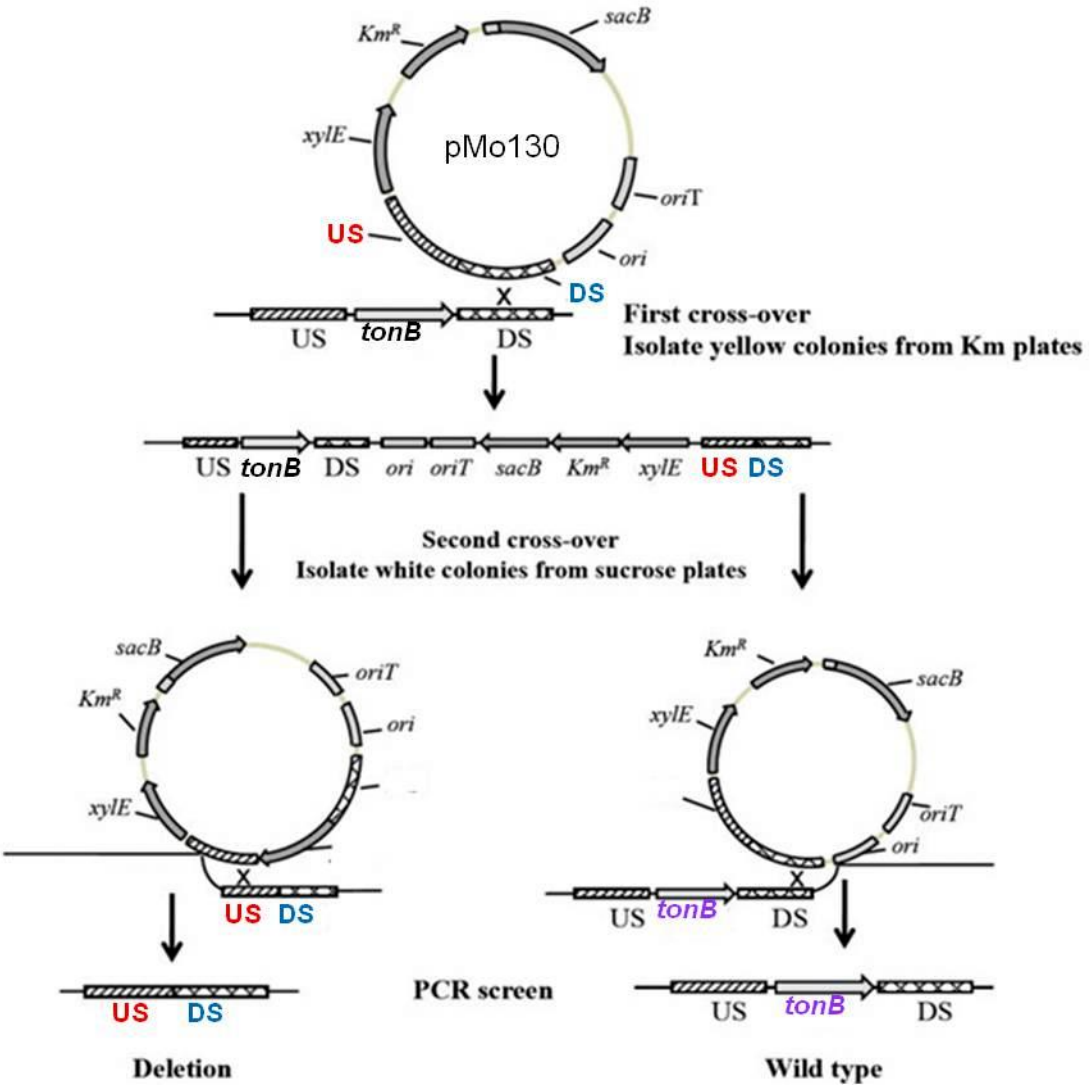

Illustration 2: Mutagenesis schematic. Diagramed are the pMo130 plasmid map and the processes used to generate an unmarked deletion of the *tonB* gene via allelic exchange. Figure adapted and used with permission from Hamad et al. [96].

type *bmaa1801* gene plus approximately 120 bp of its upstream sequence flanked by enzyme restriction sites was amplified using the following PCR primers: Complementation forward primer (CCG CTA GCC TGA TTT TCC GCA AGT GAT GCA GCA CT) (underlined sequence indicates a newly introduced *Nhe*I site); Complementation reverse primer (CCA AGC TTT TAA TCG GTC AGA GTG AAG TCA TAA GGC) (underlined sequence indicates a newly introduced *Hind*III site). The

fragment was then digested with *Nhe*I and *Hind*III and ligated into the pMo168 plasmid (Addgene plasmid 27389) to create pTonB-comp. After transformation into *E. coli* S17-1, pTonB-comp was introduced into *B. mallei* via conjugal transfer. The Δ*tonB* mutant containing pTonB-comp was isolated via selection on LBG Km agar plates and confirmed by PCR amplification, followed by sequencing, of the region flanking the *tonB* gene using the same primers used to confirm the Δ*tonB* mutant.

Growth Kinetics

Overnight cultures were used to inoculate 50 mL of LBG with $6x10^6$ CFU of each strain. Inoculated cultures were then incubated with agitation at 37°C. At the indicated time points, 1 mL aliquots from each culture taken to measure optical density at 600 nm (using a spectrophotometer). Individual data points represent the OD_{600} mean ± standard deviation (SD) of three independent experiments. A significant difference due to treatment over time was ascertained via two-way ANOVA. *S*ignificant differences of each OD_{600} reading at every time point compared to wild type was ascertained via one-way ANOVA followed by Dunnett's multiple comparisons test. A p-value of $x < 0.05$ was considered significant.

Iron Utilization Assay

Overnight cultures were diluted to 1×10^5 bacteria mL^{-1} in LBG containing 200 μM of 2,2'-dipyridyl and poured onto plates, as previously described [91]. Disks containing iron sources were placed on the surface of the LBG plates, which was incubated at 37°C for 48 h. Iron utilization was quantified by the measuring the diameter of growth around the disk. Disks contained 10 μL of the following compounds at the specified concentrations: hemin 8.0 μM, hemoglobin 4.5 μM, myoglobin 4.5 μM transferrin and lactoferrin, 30 μM; or $FeSO_4$, 10 mM [91].

Siderophore Secretion Assay

598 Ten µl samples of overnight cultures, grown in LBG or LBG supplemented with
599 200 µM $FeSO_4$ or 200 µM 2, 2'-dipyridyl, were spotted onto Chrome azurol S (CAS)
600 agar plates and incubated at 37°C. Halos were then monitored and diameter of color
601 change was measured over the course of the next 4 days. For one liter of CAS agar,
602 solutions 1-4 were prepared as previously described [101]. Solutions 1-3 were
603 autoclaved and then cooled to 50°C. Solutions 2 and 4 were added to solution 3 and
604 solution 1 was added last with constant stirring to mix the ingredients without forming
605 bubbles. An unpaired t test with equal standard deviation was performed on halo
606 measurements to ascertain a significance difference between the strain specific halos
607 produced.

608 **Animal Studies**

609 Female, 6- to 8-week-old, BALB/c mice obtained from Harlan Laboratories
610 (Indianapolis, IN, USA) were housed in microisolator cages under pathogen-free
611 conditions. Animals were provided with rodent feed, water *ad libitum* and maintained on
612 a 12 h light cycle. Before experiments, mice were afforded an adaption period of at least
613 1 week. This study was carried out in strict accordance with the recommendations in the
614 Guide for the Care and Use of Laboratory Animals of the National Institutes of Health.
615 The protocol was approved by the Animal Care and Use Committee of the University of
616 Texas Medical Branch (Protocol Number: 0503014A).

617 **Survival Study**

618 Anesthetized BALB/c mice (n=8 per treatment) were challenged by the intranasal
619 (i.n.) route with the indicated colony forming unit (CFU) of *B. mallei* Δ*tonB* mutant,
620 grown in LBG ± 200 µM $FeSO_4$ and diluted in phosphate buffered saline (PBS) in a total
621 volume of 50 µL (25 µL/ nare). BALB/c mice were monitored and deaths were recorded
622 over a period of 14 days. Survival curves were generated and analyzed using the Kaplan-

623 Meier method. A significant difference in survival curves was ascertained via a Log-rank
624 test. A *p*-value of $x < 0.05$ was considered significant.

625 **Colonization Study**

626 Anesthetized BALB/c mice (n=8 per treatment) were challenged i.n. with $1.5x10^4$
627 CFU/50 µL of the wild-type CSM001 strain and the Δ*tonB* mutant grown in LBG ± 200
628 µM $FeSO_4$. At 24, 48 and 72 h post challenge, BALB/c mice were euthanized and
629 necropsied for organ collection. The lungs, liver and spleen were homogenized in 1 mL
630 of PBS using a tissue grinder (Covidien, Mansfield, MA) and then the bacteria were
631 enumerated by standard plate counts on LBG supplemented with 200 µM $FeSO_4$.
632 Significant differences in colonization at 24 h and 48 h were individually ascertained via
633 one-way ANOVA followed by Tukey's multiple comparisons test. Significant difference
634 in colonization at 72 h was extrapolated using an unpaired t test with equal standard
635 deviation. A *p*-value of $x < 0.05$ was considered significant.

636 **Vaccine Study**

637 Anesthetized BALB/c mice (n=8 per treatment) were immunized i.n. with PBS or
638 the indicated CFU of *B. mallei* Δ*tonB* mutant diluted in PBS in a total volume of 50 µL
639 (25 µL/ nare). BALB/c mice were challenge 21 days post immunization with $1.5x10^5$
640 CFU of a *B. mallei* WT luminescent reporter strain (CSM001) or $9 x10^2$ CFU of wild-
641 type *B. pseudomallei*, diluted PBS in a total volume of 50 µL (25 µL/ nare). BALB/c
642 mice were monitored and deaths were recorded until the end of the study. Survival
643 curves were generated and analyzed using the Kaplan-Meier method. A significant
644 difference ($p \leq 0.05$) in survival curves was ascertained via a logrank test. To ascertain
645 significant differences in individual treatment as compared to the PBS-treatment control,
646 an additional logrank test was employed using an adjusted definition of significance ($p \leq$
647 0.05 of pairwise comparisons).

In vivo Imaging

Bioluminescent images were acquired using an IVIS Spectrum (Caliper Corp., Alameda, CA, USA), as previously described [99]. Briefly, anesthetized BALB/c mice placed in the isolation chamber were transferred to the imaging chamber and connected an internal anesthesia delivery system that maintained 1-2% isoflurane. Bioluminescent signal was measured after three minutes exposure with no excitation (filters blocked) and an open emission filter to capture all luminescent signals from labeled bacteria. To depict the differences in intensity of the signal, bioluminescence is represented in the images with a pseudocolor scale ranging from red (most intense) to violet (least intense). Scales were manually set to the same values for every comparable image to normalize the intensity of the bioluminescence across time points.

B. mallei specific IgG1, IgG2a and IgM titer analysis

Serum extracted from PBS- or *B. mallei* Δ*tonB* mutant-vaccinated BALB/c mice 21 days post treatment was evaluated for *B. mallei* specific IgG1, IgG2a and IgM using the Ready-Set-Go!® ELISA Kit (Affymetrix eBioscience, San Diego, CA) as instructed by the manufacturer. Briefly, microplates (Costar, Cambridge, MA) were coated with 10 μg/ml of heat inactivated *B. mallei* and incubated overnight at 4°C. Wells were then washed twice with 1x PBS, 0.05% Tween-20 and then blocked over night with the 2x Assay Buffer provided in the kit. After the wells were washed, a 1:10,000-fold dilution of the serum samples were added to the appropriate wells followed by the detection antibody provided by the kit. After 3 h incubation, the wells were washed four times before 100 μL of the substrate solution was added. After 15 min incubation, 100 μL of stop solution consisting of 2 N H_2SO_4 was added and absorbance was measured at 450 nm with the Epoch microplate spectrophotometer (Winooski, VT).

Histopathological Evaluation

673 At the indicated time points, anesthetized BALB/c mice were euthanized and
674 necropsies were preformed to collect the lung, liver and spleen. Organs were instilled
675 with 10% formalin, paraffin-embedded and processed for histopathology. Hematoxylin
676 and Eosin stained slides were examined and blindly scored by a pathologist (Dr. Sbrana)
677 for the follow observations: perivascular and peribronchial inflammatory infiltrates,
678 necrosis and microabscesses in the lung; granulomas, necrosis and histocytosis in the
679 spleen; and inflammation and necrosis in the liver. Severity of pathology was scored
680 using the follow scale: 0 (unremarkable), 1 (minimal), 2 (mild), 3 (moderate) and 4
681 (severe). Pathology scores were added together to give the total score for each organ.
682 Each image is representative of three replicates per treatment. A two-way ANOVA was
683 performed on each organ individually to assess a significant difference in treatment over
684 time. Student's t test was performed to ascertain a significant difference between the
685 treatments of each organ, individually, at 0 and 48 h.

686 **Cytokine Quantification**

687 At the indicated time points, whole blood was collected by cardiac puncture from
688 anesthetized BALB/c mice. The blood was stored in microvette tubes without anti-
689 coagulant and incubated at room temperature for 20 min to permit clotting. Serum was
690 collected after centrifugation of the tubes and store at -80°C. Samples were inactivated
691 as previously described [102] and verified for sterility by plating 10% of the sample on
692 LBG supplemented with 200 μM $FeSO_4$. Serum chemokine/cytokine levels were
693 measured using the murine bioplex ELISA kit (BioRad Bio-Plex Pro™ Mouse Cytokine
694 23-plex Assay) according to the manufacturer's specification. Assaying samples diluted
695 1:4 in PBS, the following molecules were targeted: IL-1α, IL-1β, IL-2, IL-3, IL-4, IL-5,
696 IL-6, IL-9, IL-10, IL-12 (p40), IL-12 (p70), IL-13, IL-17A, eotaxin, G-CSF, GM-CSF,
697 IFN-γ KC, MCP-1 (MCAF), MIP-1α, MIP-1β, RANTES, and TNF-α. Data values
698 represent the SEM of 3 animals per treatment and were ascertained as previously

described [103]. A significant difference in individual serum cytokine levels in PBS vs. Δ*tonB* treated BALB/c mice was determined using the Mann-Whitney test.

CPG studies

Bacterial strains and growth conditions

B. mallei lux (CSM001), a previously constructed luminescent reporter strain [104], was cultured on LBG and 50 µg/ml of kanamycin (Km) for 48 h at 37°C followed by an overnight culture at 37°C with shaking to obtain an exponential growth phase inoculum. Optical density readings (OD_{600}) were used to calculate dose concentration. Bacterial colonies sub-cultured to LBG broth were centrifuged, washed and re-suspended in sterile PBS to obtain the desired infectious dose.

GpG treatment Study

Phosphorothioate-stabilized class-C CpG ODNs was purchased from InvivoGen, San Diego, CA, USA. Anesthetized BALB/c mice (n = 10) were treated i.n. with either 20 µg of CpG class-C 2395 (TCG TCG TTT TCG GCG CGC GCC G) or PBS in a 50 µL volume (25 µL/ nare). After 24 h post-treatment, BALB/c mice were then challenged i.n. with $1.0x10^4$ CFU of *B. mallei* WT CSM001 in a 50 µL volume (25 µL/ nare), a dose empirically determined to show luminescent signal 48 h after CSM001 infection [38]. BALB/c mice were monitored and deaths were recorded over a period of 21 days. Survival curves were generated and analyzed using the Kaplan-Meier method. A significant difference ($P \leq 0.05$) in survival curves was ascertained via a logrank test.

Bacterial Burden Analysis

BALB/c mice (n = 18) were treated with either CpG or PBS and then challenged with CSM001 as described above. At 24, 48 and 72 h post infection, following whole-

722 body imaging, BALB/c mice (n = 3) from each group were sacrificed and lungs, livers
723 and spleens were harvested. Organs were homogenized by fine mincing with surgical
724 scissors followed by pushing through a 70 μm pore nylon tissue strainer. The
725 homogenates were then serial diluted 10-fold for plating on LBG supplemented with 50
726 μg/ml of Km. Plates were incubated at 37°C for 48 h prior to CFU determination.

727 ***In vivo* Imaging**

728 Bioluminescent and fluorescence images were acquired at 24, 48 and 72 h post
729 infection, as described above, using an IVIS Spectrum (Caliper Corp., Alameda, CA,
730 USA). Three hours prior to imaging, the Neutrophil-Specific, near infrared (NIR)
731 Fluorescent Imaging Agent (Kerafast, Boston, MA) was administered to class-C CpG
732 ODN or PBS-pretreated BALB/c mice by way of tail vein injection. Images were
733 collected after 1 second of exposure utilizing a 745 nm excitation and 800 nm emission
734 filters. To depict the differences in intensity of the signal, bioluminescence and
735 fluorescence are represented in the images with a pseudocolor scale ranging from red
736 (most intense) to violet (least intense) and yellow (most intense) to dark red (least
737 intense), respectively. Scales were manually set to the same values for every comparable
738 image to normalize the intensity of the bioluminescence and fluorescence across time
739 points. Bioluminescent and fluorescent images were than superimposed to show co-
740 localization of bacteria and neutrophils.

741 **Cell Preparation and Flow Cytometry**

742 BALB/c mice treated with CpG or PBS 24 h prior to *B. mallei* CSM001 challenge
743 as described above were sacrificed at time 0 (right before challenge) and 72 h after
744 infection. Lungs were harvested and prepared as previously described [105] and used for
745 flow cytometric analysis. Briefly, a single cell suspension was prepared by fine mincing
746 the lung tissue with surgical scissors followed by pushing through a 100 μm, followed by

747 a 70 μM, pore nylon tissue strainer (BD Biosciences, San Jose, CA, USA). The resulting
748 homogenate was treated with RBC Lysis Buffer (Sigma) according to manufacturer's
749 instruction. Trypan blue exclusion was used to determine white blood cell counts and
750 viability. Single cell suspensions were than stained with fluorescent monoclonal
751 antibodies for flow cytometric analysis, using procedures previously described. The
752 following monoclonal antibodies (mAb) against mouse antigens were purchased from BD
753 Biosciences (San Jose, CA, USA), Ly6G/C-PE, CD11c-FITC, CD11b-PerCpCy5.5, and
754 F4/80-APC. Corresponding isotype controls included: IgG2b-PE, IgG2b-FITC, IgG2a-
755 APC, or IgG1-PerCPCy5.5. Cells were then washed and re-suspended in 400 μl of 4%
756 ultrapure formaldehyde (Polysciences Inc.). Samples were fixed for 48 h, with fresh 4%
757 formaldehyde replacement at 24 h, and sterility confirmed by selective plating. A total of
758 350 μL of sample was analyzed on a FACS Canto (BD Biosciences, UTMB Flow
759 Cytometry and Cell Sorting Core Facility) and compensation for spectral overlap was
760 performed using FACS DIVA software (BD Biosciences). Isotype- and fluorochrome-
761 matched non-specific control antibodies determined background fluorescence, and
762 analysis was performed using FCS Express v4.0 Flow Research ed. (De Novo Software)
763 as described previously. Data are presented as the number of gated events corresponding
764 to the expected live leukocyte side scatter and forward scatter gate. Assessment is based
765 on the number of $F4/80^{+}Ly6G/C^{+}$ (macrophages), $F4/80^{+}Ly6G/C^{+}$ (inflammatory
766 monocytes), and $F4/80^{-}CD11c^{-}CD11b^{+}Ly6G/C^{+}$ (neutrophils) cells in the live leukocyte
767 gate. Data are shown as mean ± SEM. One-way ANOVA followed by a Dunnett's
768 multiple comparison tests for group comparisons (GraphPad Software v4.0). Statistically
769 significant values are designated as *, $p < 0.05$.

770 **Histopathology**

771 After imaging, BALB/c mice were euthanized and their lungs removed. Lungs
772 were instilled with formalin, paraffin-embedded and processed for histopathology.

773 Hematoxylin and Eosin stained slides were examined by a pathologist (Dr. Sbrana) for
774 differences in inflammation, inflammatory infiltrates, microabscesses and necrosis in the
775 tissues.

RESULTS AND DISCUSSION

Chapter 6: A *Burkholderia mallei tonB* mutant as an effective vaccine conferring protective immunity against inhalational glanders and melioidosis

INTRODUCTION

Melioidosis and glanders are severe zoonotic diseases caused by two closely related Gram-negative pathogens known as *Burkholderia pseudomallei and Burkholderia mallei*, respectively [22,106]. The genomic relatedness between these two pathogens suggests that *B. mallei* is a host-adapted clone of *B. pseudomallei*, which evolved from a process of reductive evolution. Genes retained by *B. mallei* share 99% sequence identity with their *B. pseudomallei* orthologs and of those, 650 genes have been identified as putative virulence determinants via *in silico* genomic subtraction from non-pathogenic *Burkholderia* species [107]. In addition to this evidence, the presence of very few *B. mallei* specific genes suggest it's possible to generate a live attenuated vaccine with a *B. mallei* backbone that can cross-protect against both melioidosis and glanders [61].

Where *B. pseudomallei* is an environmental saprophytic pathogen ubiquitous in soil and fresh water surfaces, *B. mallei* is an obligate mammalian pathogen that typically infects solipeds (horses, donkeys and mules) [23,106]. Despite these differences in epidemiology, the clinical manifestations and pathological effects of *B. pseudomallei* or *B. mallei* infection bear striking resemblance. Both pathogens can be contracted via the cutaneous, oral and/or inhalational routes. Depending on the dose and route of transmission, *B. pseudomallei* or *B. mallei* infection may result in an acute or chronic disease. Clinical manifestations of acute infection, which include fever, malaise, abscess formation, pneumonia and sepsis, from either disease are non-specific. The lack of pathognomonic symptoms, which, in addition to their ability to cause silent infection,

makes rapid and accurate diagnosis problematic for these *Burkholderia* infections. Since mortality rates among severe infections are high, and there are no reliable antibiotic therapy or licensed pre- and post-exposure vaccines, both pathogens remain top candidates for bioterrorist use and thus have been classified as category B, tier 1, biothreat agents [106]. The destructive potential of *B. pseudomallei* and *B. mallei* has heightened concerns among public health officials due to the increased potential of opportunistic infection among growing populations of diabetic and immunocompromised people [22]. For military personnel and susceptible individuals, the availability of a vaccine would be the most efficacious and cost-effective way to protect from disease.

For a majority of bacterial pathogens, the acquisition of iron and iron complexes has long been recognized as major determinant in the pathogenesis and thus also represent promising targets for vaccine development. Iron is the only nutrient known to be generally growth-limiting, playing an essential role in bacterial virulence [62,70,108-111]. To replicate, bacteria need to acquire 10^5 to 10^6 iron ions per cell division [62]. This requirement for iron is based on its involvement in a variety of biological processes, such as DNA and protein synthesis, energy generation, and oxidative stress protection [70]. Thus, a pathogen's success of establishing infection in the host is contingent upon its ability to acquire iron. In the host, iron is tightly bound by proteins such as ferritin, transferrin, and lactoferrin, or by those sequestered within hemoglobin [71]. Upon infection, the host responds defensively by lowering free iron levels an additional 30% [71]. To fulfill this requirement, bacteria have evolved multiple mechanisms to seize and then actively transport host iron from the extracellular space into the periplasm. Bacterial acquisition systems attain iron by using one of two general mechanisms. In the first, bacteria synthesize and secrete siderophores, which are high-affinity, iron-chelating compounds that competitively bind extracellular iron ions for cell uptake [62]. In the second, bacteria synthesize high-affinity outer-membrane receptors that are able to seize iron from host iron-binding proteins for transport into the cell [62]. Because the ability to

acquire this element is directly linked to survival and thus to virulence, different components of the iron transport system have been targeted for vaccine and therapeutic development with some success. However, in the case of *B. pseudomallei* and *B. mallei*, very little information exists concerning iron uptake mechanisms in the host and their roles in virulence. In one study, Kvitko el at. [112] generated single, double and quadruple mutants defective in siderophores and/or hemoglobin utilization to elucidate their contribution to *B. pseudomallei* virulence. Contrary to similar studies performed on closely related pathogens, these mutants remained fully virulent in an acute model of murine melioidosis [112]. Failure to eliminate virulence was attributed to redundancy in the iron transport system, citing a reliance on alternative iron sources and acquisition mechanisms.

The import of iron from the extracellular space requires the energy-dependent process of active transport. Since the outer membrane lacks an energy source, most all Gram-negative bacteria depend upon the protein TonB, which functions to energize all outer-membrane iron receptors [69,80,81]. When assessed in multiple models of infection, *tonB* mutants displayed severe attenuation compared to their wild-type homologs [82,86,92,94]. However, the *K. pneumoniae* Δ*tonB* mutant, when used to immunize mice in vaccination studies, was reported to provide 100% protection against wild-type challenge [86]. Thus, *Burkholderia* TonB-dependent iron-transport systems, specifically their contribution to survival, persistence and potential as targets for vaccine development, should be investigated further. In this communication, we describe the construction and characterization of a *B. mallei* Δ*tonB* mutant as a protective vaccine candidate to prevent acute inhalational glanders and melioidosis in a murine model.

RESULTS

Mutant Construction and Phenotype

A previously described method for genetic manipulation via allelic exchange was used to create an unmarked *tonB* mutant in the *B. mallei* strain ATCC 23344 [96]. To ensure the mutant phenotype was not due to polar effects incurred during mutagenesis, the *tonB* deletion mutant was transformed with the plasmid pTonB-comp, which carries the intact *tonB* gene plus its native promoter (Table 1). Unlike the wild type, the *tonB* mutant appears as bright yellow colonies that discolor the surrounding media (Figure 1).

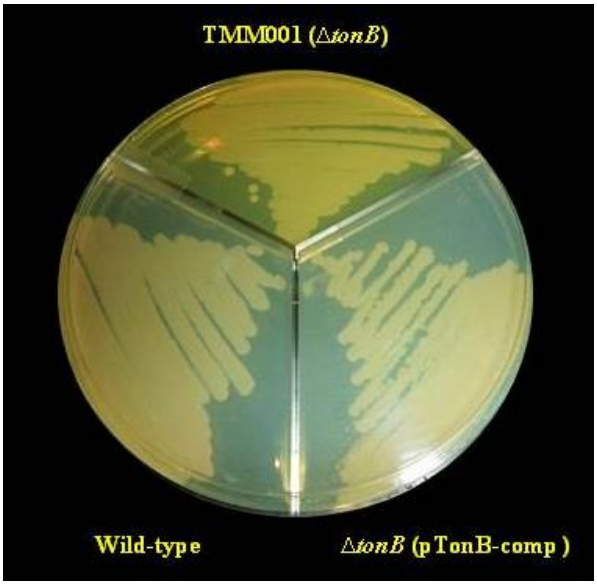

Figure 1: The *B. mallei* Δ*tonB* mutant displays an alternative phenotype. *B. mallei* strains wild-type (lower left), Δ*tonB* mutant (top) and the complement Δ*tonB* (pTonB-comp) (lower right) were grown on LBG + 200 μM $FeSO_4$ for 3 days at 37°C at 5% CO_2. The figure shows the differences in colony color and alteration of the media as a result of the *tonB* gene deletion.

The mutant phenotype was restored to wild-type levels in the complemented strain, which grew as muted yellow-beige colonies with no media discoloration.

Growth Rate Study

To determine the effect of the *tonB* deletion on growth rates and the iron requirement of the mutant, growth curves were initiated with the following strains and

broth conditions: wild type in LBG, Δ*tonB* in LBG, and Δ*tonB* in LBG + 200 μM $FeSO_4$ (Figure 2).

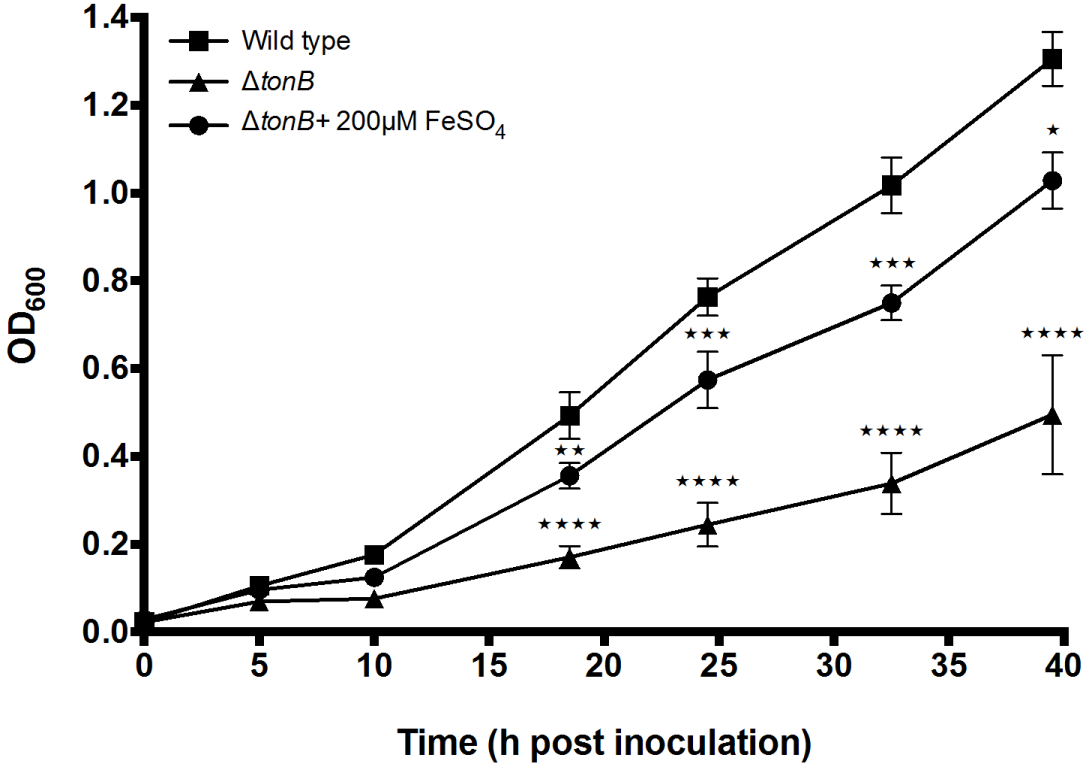

Figure 2: The attenuated *B. mallei* Δ*tonB* mutant's growth kinetics is partially rescued by iron supplementation. Overnight cultures of *B. mallei* wild type (■) and *B. mallei* Δ*tonB* (●) were diluted 1:100 in 50 mL of Luria broth with 4% glycerol (LBG). An additional overnight culture of Δ*tonB* (▲) was diluted 1:100 in 50 mL of LBG + 200 μM $FeSO_4$. At the indicated time points, optical densities at 600 nm of all strains were measured. The means plotted with their SD are representative of three independent experiments. Statistical significance was determined by Dunnett's test of multiple comparisons relative to wild-type. ★★ $p < 0.001$, ★★★ $p = 0.0001$, ★★★★ $p < 0.0001$.

When grown in LBG, the Δ*tonB* mutant exhibited an attenuated growth rate, displaying a longer lag phase, compared to that of the wild type. When grown in LBG enriched with 200 μM $FeSO_4$, the growth rates of the Δ*tonB* mutant increased substantially approaching that of the wild type. Notably, the Δ*tonB* mutant, when grown in iron rich media, maintained wild-type growth rates longer, showing statistical differences at 10 h vs. 5 h.

Siderophore Secretion Assay

To ascertain if the deletion of *tonB* in *B. mallei* results in the differential siderophore production, both the *B. mallei* wild-type and Δ*tonB* mutant were plated on CAS agar. The CAS media was used because when strong iron chelators, such as siderophores, are secreted, they are able to strip the dye complex of iron, which results in the formation of blue to orange/yellow zones (Figure 3). Siderophore secretion zones were measured after

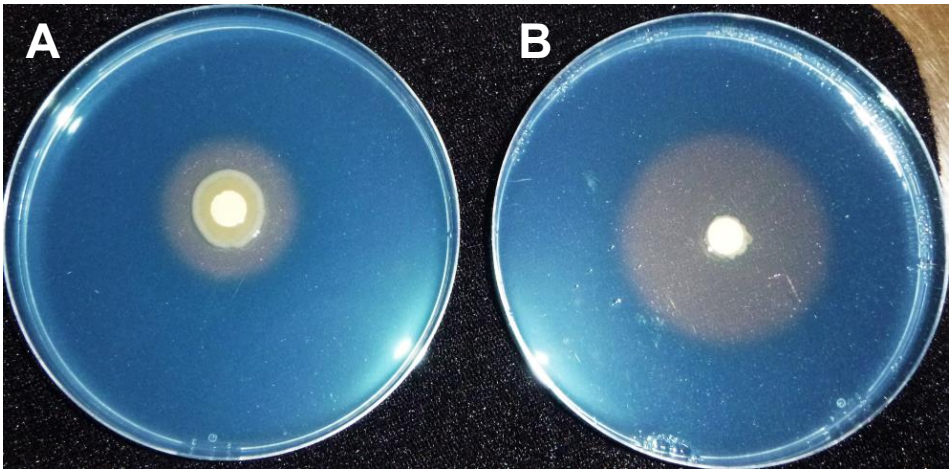

Figure 3. *B. mallei* Δ*tonB* mutant displays hyper-secretion of siderophores. Ten microliters of *B. mallei* wild-type (A) and Δ*tonB* mutant (B) overnight cultures grown in LBG were spotted on a filter disk that was then placed on CAS agar media. CAS agar plates were then incubated for at 37°C for 96 h.

96 h and calculated as the diameter of the yellow halo minus the diameter of colony growth or filter disk. The *B. mallei* Δ*tonB* mutant produced significantly larger halos (33.3 ± 0.5 mm) compared to those of the wild type (12.3 ± 0.6 mm).

Iron Utilization Assay

A disk diffusion assay was performed to examine the *B. mallei* Δ*tonB* mutant's ability to utilize the following sources of iron: $FeSO_4$, hemoglobin, hemin, lactoferrin, and transferrin. Iron assimilation was determined by measuring the diameter (mm) of bacterial growth around the disk containing specific iron sources placed on iron-depleted

media (Table 2). The *B. mallei* wild-type strain was able to grow by utilizing all iron sources, while the *B. mallei* Δ*tonB* mutant was only capable of utilizing $FeSO_4$, the only iron source acquired by a TonB-independent process.

Table 2. Diameter (mm) of *B. mallei* wild-type and Δ*tonB* mutant colonial growth utilizing individual iron sources.

Strain	$FeSO_4$	Hemoglobin	Hemin	Lactoferrin	Transferrin
B. mallei wild-type	25.8 ± 3.5	14.2 ± 1.8	17.7 ± 1.5	12.5 ± 0.5	12.8 ± 2.1
B. mallei Δ*tonB* mutant	14.7 ± 1.5	0	0	0	0

In vivo Survival Study

We determined in previous characterization studies of our acute respiratory murine inhalational glanders model that the 50% lethal dose using *B. mallei* strain ATCC 23344 is $7.4x10^4$ CFU/50 μL (unpublished data). To ascertain the role of *tonB* in *B. mallei* virulence, we challenged BALB/c mice intranasally (i.n.) with 1.5×10^5 CFU (~$2LD_{50}$), 1.5×10^6 CFU (~$20LD_{50}$) and 1.5×10^7 CFU (~200 LD_{50}) of *B. mallei* Δ*tonB* grown in LBG ± 200 μM $FeSO_4$ and monitored them for survival up to day 14. The Kaplan-Meier curve shows an inverse correlation between the Δ*tonB* mutant dose and/or iron concentration and the survival rate (Figure 4). Despite growth conditions, all BALB/c mice challenged with 1.5×10^7 CFU of the Δ*tonB* mutant succumbed to infection by 4 days post challenge. At lower doses, the effect of supplementing *B. mallei* Δ*tonB* with 200 μM $FeSO_4$ on survival was still apparent. At day 14, survival increased from 62.5% to 100% and 0% to 12.5% when BALB/c mice received a challenge dose of 1.5×10^5 CFU and 1.5×10^6 CFU of the Δ*tonB* mutant, respectively, when grown in LBG alone.

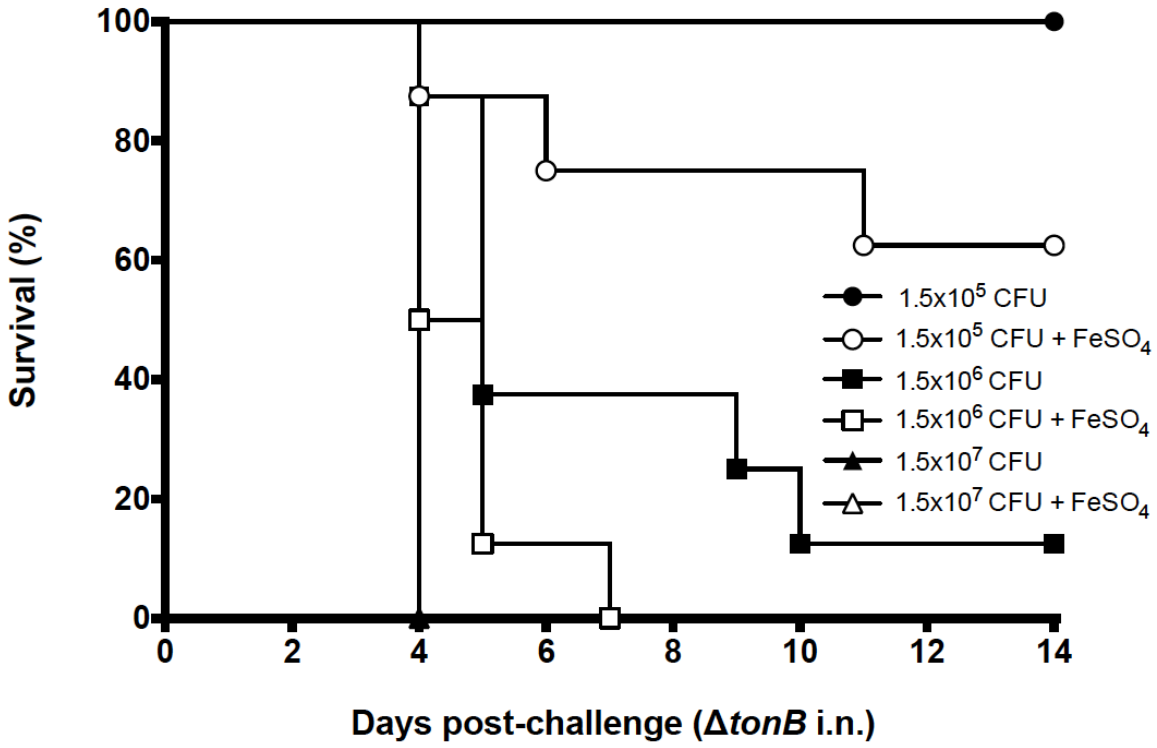

Figure 4. Attenuated virulence of the *B. mallei* Δ*tonB* is partially rescued by iron supplementation in growth media. Mice (n=8) were challenged i.n. with 1.5 x 10^5 CFU (solid circle/open circle), 1.5 x 10^6 CFU (solid square/open square) or 1.5 x 10^7 CFU (solid triangle/open triangle) of Δ*tonB* grown in LBG with (open) or without (closed) 200 µM $FeSO_4$. The statistical significance of differences in survival times was determined by plotting Kaplan-Meier curves, followed by a log rank test. **** $p \leq 0.0001$.

Colonization Study

By using the same murine infection model described in the previous section, we performed a colonization study to determine the role of TonB in *B. mallei's* ability to disseminate and colonize to target organs. BALB/c mice challenged i.n. with 1.5 x 10^4 CFU of the wild-type or Δ*tonB* mutant grown in LBG ± 200 µM $FeSO_4$ were euthanized at 24, 48 and 72 h post challenge. At each time point, the lungs and spleen were removed, homogenized, and plated for CFU elucidation. Compared to the wild-type strain, the numbers of the *B. mallei* Δ*tonB* recovered from the lungs were significantly reduced, independent of growth conditions, at 24 h (* $p \leq .05$) and 48 h (**** $p \leq .0001$)

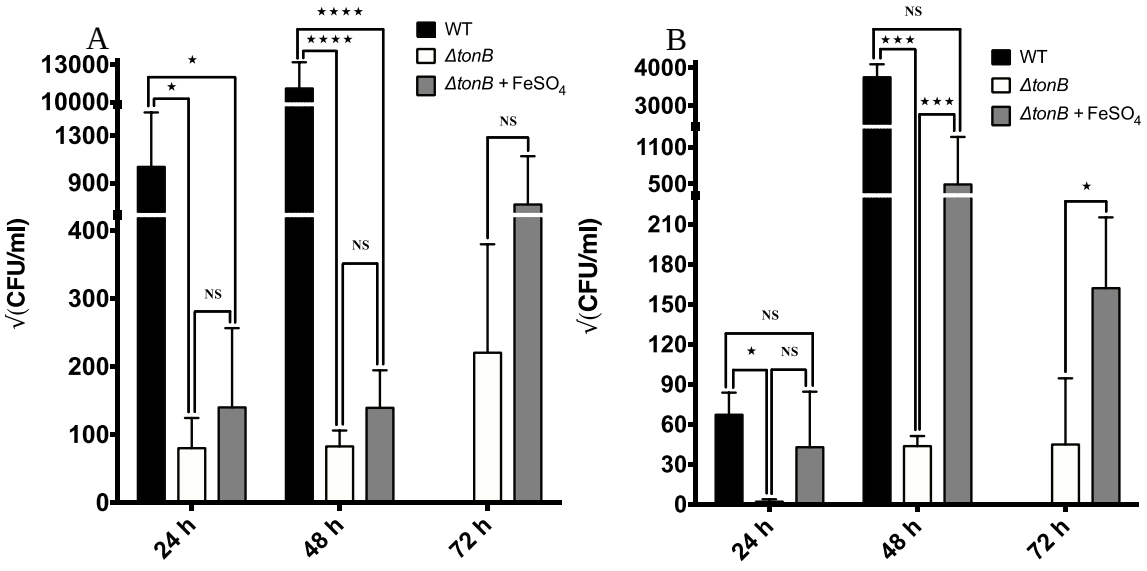

Figure 5. The attenuated ability of the *B. mallei* Δ*tonB* mutant to colonize target organs is partially rescued by iron supplementation in the media. Bacterial burden in the lungs (A) and spleen (B) of mice infected with *B. mallei* wild-type and Δ*tonB* mutant grown + 200 μM $FeSO_4$ at 24, 48 and 72 h post infection. Bars plotted with their SD represent the mean of three independent experiments. Significant differences in colonization at 24 and 48 h were individually ascertained via one-way ANOVA followed by Tukey's multiple comparisons test. Significant difference in colonization at 72 h was extrapolated by using an unpaired *t* test with equal SD. ★ $p \leq .05$, ★★★ $p \leq .001$, ★★★★ $p \leq .0001$, ns = no significance.

(Figure 5). A similar trend in the spleen showed significantly reduced numbers of the B. mallei ΔtonB mutant compared to the wild-type at 24 h (★ $p \leq .05$) and 48 h (★★★ $p \leq .001$). When grown in LBG + 200μM FeSO4 prior to challenge, the B. mallei ΔtonB resembles the wild-type strain, showing no statistical difference in the number of bacteria recovered from the lungs. However, a statistical difference was seen in the recovery of the ΔtonB mutant grown in LBG ± 200 μM FeSO4 in the spleen at 72 h (★ $p \leq .05$) (Figure 5). BALB/c mice challenged with the wild type expired before the last time point and are thus not represented in the 72 h time point.

Vaccine Studies

To evaluate the protective efficacy of Δ*tonB* mutant immunization against wild-

type challenge, BALB/c mice were immunized i.n. with PBS, 1.5 x 10^4 CFU or 1.5 x 10^5 CFU of the Δ*tonB* mutant grown in LBG only. At 21 days post-immunization, vaccinated BALB/c mice were challenged i.n. with 1.5x10^4 CFU of the *B. mallei* strain CSM001. The CSM001 strain, a wild-type homolog containing a luminescent reporter, was used instead of the wild type to assess the protective potential of Δ*tonB* mutant vaccination via real-time *in vivo* monitoring of CSM001 strain dissemination. All PBS-treated BALB/c mice died by day 4 with a calculated median survival of 3 days post challenge (Figure 6).

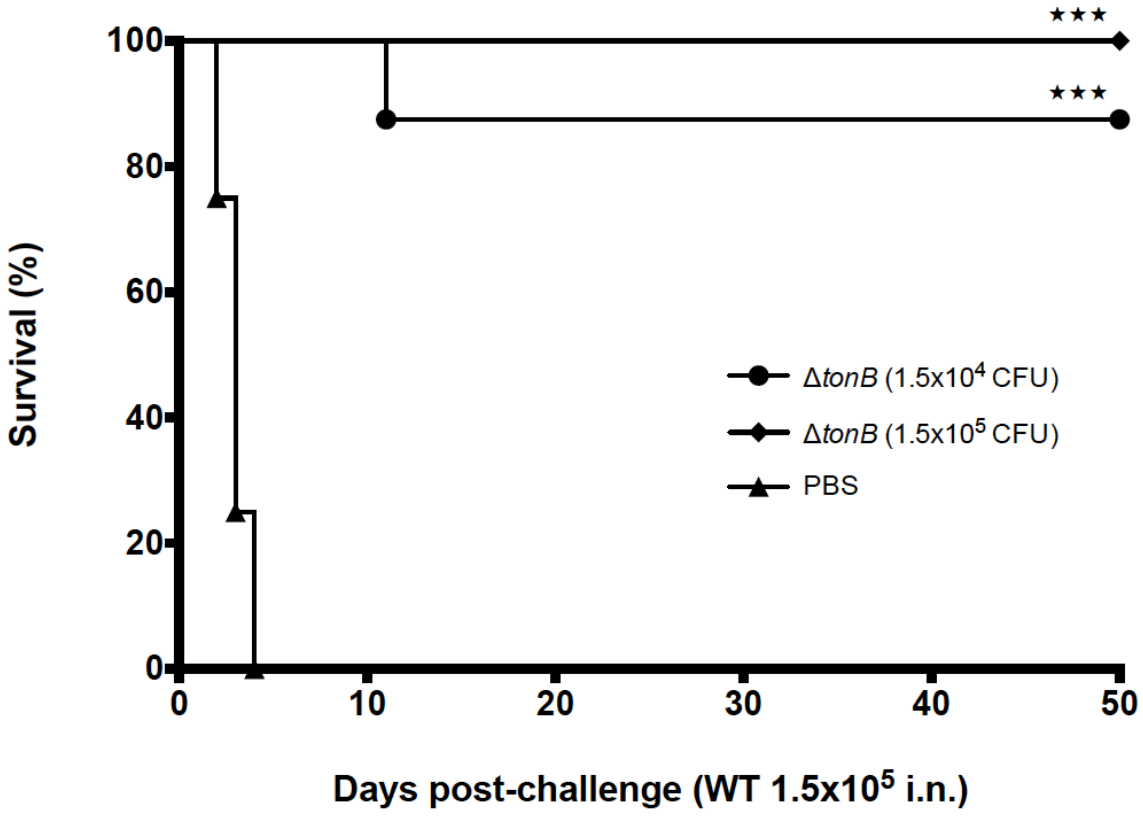

Figure 6. *B. mallei* Δ*tonB* mutant (1.5x10^5 CFU) provides 100% protect against wild type challenge. Mice (n=8) were immunized i.n. with PBS (solid triangle), 1.5x10^4 CFU (solid circle) or 1.5x10^5 CFU (solid diamond) of Δ*tonB*. Three weeks later, BALB/c mice were challenged with 1.5x10^5 CFU of a *B. mallei* WT luminescent reporter strain (CSM001). The statistical significance of differences in survival times was determined by plotting Kaplan-Meier curves, followed by a log rank test. ★★★★ $p < 0.0001$.

985 However, in BALB/c mice immunized with the Δ*tonB* mutant at a dose of 1.5 x 10^5 CFU
986 or 1.5 x 10^4 CFU, survival was 100% (*** p = 0.0003) and 87.5% (*** p = 0.0003),
987 respectively.

988 To evaluate dissemination and colonization of the *B. mallei* CSM001 strain, we
989 monitored vaccinated and naïve BALB/c mice for bioluminescence signals at 72-h post
990 challenge and every 7 days thereafter until the experiment ended. At 72-h post challenge,
991 PBS-treated BALB/c mice exhibited a luminescent signal associated with anatomical
992 locations corresponding to the lungs, liver, spleen and brain. However, this luminescent
993 signal was never detected at these locations in BALB/c mice immunized with the *B.*
994 *mallei* Δ*tonB* (Figure 7). To evaluate whether Δ*tonB* mutant immunization resulted in the

995 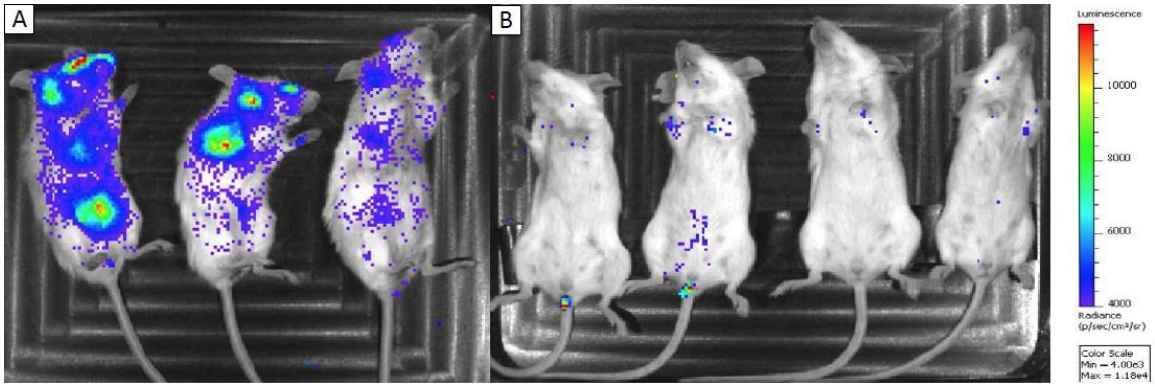

996 Figure 7. IVIS Images show reduced bacterial burden in *B. mallei* Δ*tonB* vaccinated
997 mice 72 h post challenge with luminescent wild-type. Mice immunized with
998 PBS (A) or Δ*tonB* (B) and subsequently challenged with CSM001were
999 imaged for bioluminescent signal at 72 h post challenge and every 7 days
1000 thereafter until the experiment end. The intensity of emission is represented
1001 as a pseudocolor image.

1002 production of sterile immunity, BALB/c mice surviving the experimental challenge were
1003 euthanized and organs harvested from survivors to be analyzed for gross pathology and
1004 bacterial persistence. Although the lungs and livers showed no signs of gross pathology,
1005 surviving BALB/c mice presented with splenomegaly accompanied by multiple splenic
1006 abscesses (Figure 8) mirroring that we previously described in the spleen at stage 3 of
1007 murine melioidosis infection [102]. Bacteria were isolated from the lungs, liver and

spleen of BALB/c mice immunized with 1.5 x 10^5 CFU of *B. mallei* Δ*tonB* and only from the spleen in BALB/c mice immunized with 1.5 x 10^4 CFU of the Δ*tonB* mutant (data not shown). Based on the phenotypic yellow pigment Pxb resistance and Km sensitivity, we were able to conclude that all bacteria recovered corresponded to *B. mallei* Δ*tonB* and not the CSM001 luminescent wild-type strain. In an attempt to eliminate long-term persistence of the *B. mallei* Δ*tonB* mutant, as well as the organ pathology, a vaccine titration study was initiated to identify the lowest Δ*tonB* mutant immunization dose that still provides 100% protection. The vaccine titration study used the following *B. mallei* Δ*tonB* mutant doses for immunization: 1.5 x 10^4 CFU, 1.5 x 10^3 CFU, or 1.5 x 10^2 CFU.

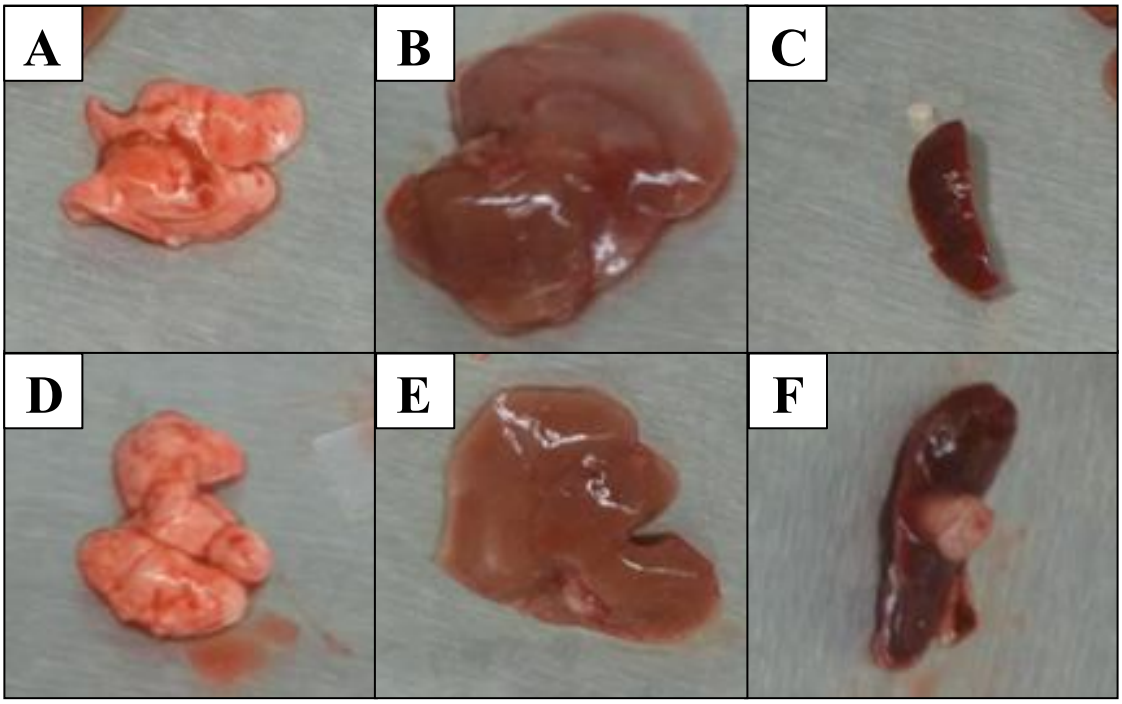

Figure 8. Effects of Δ*tonB* mutant vaccination on mouse gross pathology. BALB/c mice were inoculated with either PBS (A) or 1.5x10^5 CFU of Δ*tonB* (B). At day 21, the lung (bottom right), liver (top) and spleen (bottom left) were extracted and visually assessed for affects due to treatment. The visual difference in lungs and livers of both treatment groups were relatively unremarkable. The spleens of Δ*tonB* mutant treated animals were enlarged and contained one or multiple abscesses.

At day 21, before *B. mallei* CSM001 (1.5 x 10^4 CFU) challenge, and 48 h after challenge, three mice from each immunization group were euthanized and organs and serum harvested for histopathological and cytokine analysis. In accordance with the previous vaccination study, all PBS-treated BALB/c mice challenged with *B. mallei* CSM001 died by day 4, with a median survival of 3 days. The titration curve exhibits a significant dose-dependent increase in survival in Δ*tonB*- treated BALB/c mice challenged with *B. mallei* CSM001 (Figure 9).

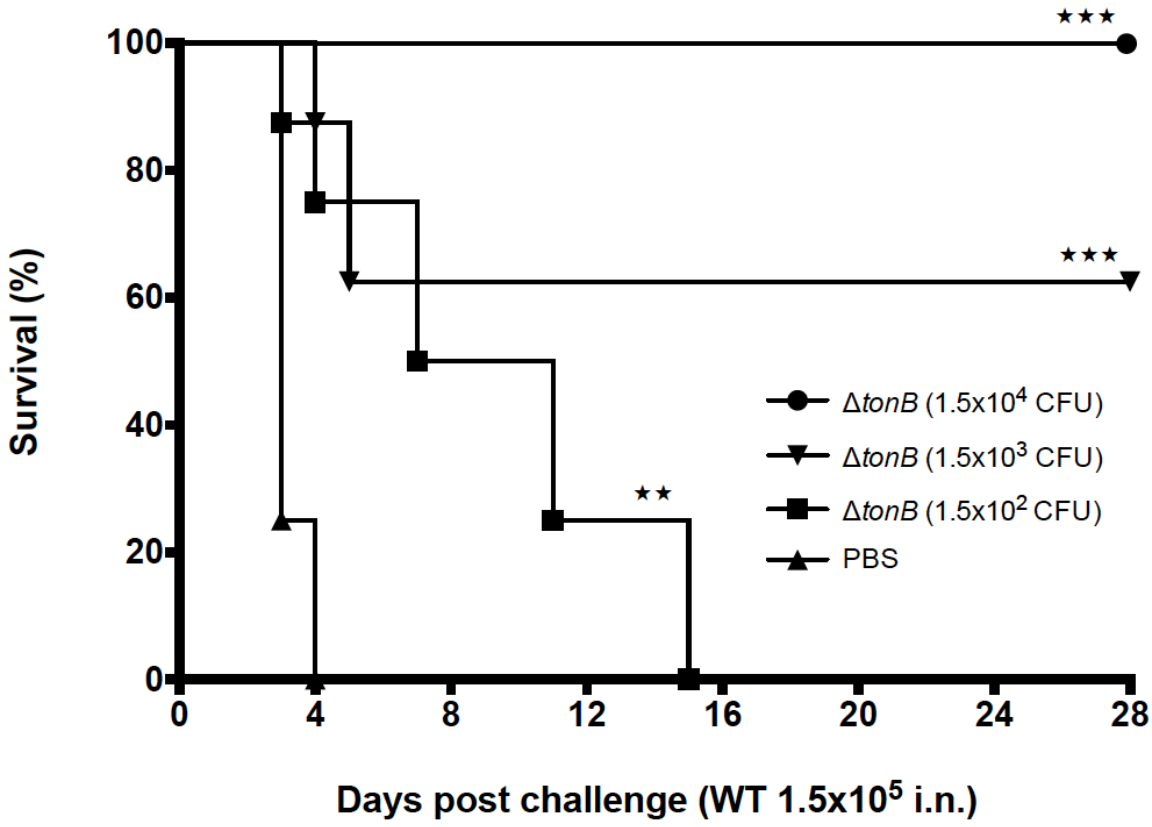

Figure 9. *B. mallei* Δ*tonB* mutant (1.5x10^4 CFU) provides 100% protect against wild type challenge. Mice were immunized i.n. with PBS (solid triangle), 1.5x10^4 CFU (solid circle), 1.5x10^3 CFU (solid inverted triangle) or 1.5x10^2 CFU (solid square) of *B. mallei* Δ*tonB*. Three weeks later, BALB/c mice were challenged with 1.5x10^5 CFU of a *B. mallei* WT luminescent reporter strain (CSM001). The statistical significance of differences in survival times was determined by plotting Kaplan-Meier curves, followed by a log rank test. ★★★ $p < 0.001$, ★★ $p < 0.01$.

All BALB/c mice immunized with 1.5 x 10^2 CFU expired by day 15, with an increased mean survival of 9 days (** p = 0.0016). In BALB/c mice immunized with 1.5 x 10^3 CFU or 1.5 x 10^4 CFU, survival increased to 62.5% (** p = 0.0016) and 100% (*** p = 0.00016), respectively, by the end point of 28 days. In addition to the cytokine and histopathological analysis described below, an assessment of bacterial burden in surviving animals showed the spleen and, to a lower extent, the liver chronically infected with the vaccine strain but not the wild-type strain (data not shown).

Serum immunoglobulin analysis

To determine differences in the antibody composition of PBS- and *B. mallei* Δ*tonB* mutant-treated BALB/c mice, serum was analyzed by using an ELISA. To probe for *B. mallei*-specific antibodies, we coated the ELISA plates with 10 µg/well of antigen acquired from heat-inactivated *B. mallei* lysate. When assayed at a 1:10,000 dilution and compared to the wild type, lysate from *B. mallei* Δ*tonB*-treated BALB/c mice had significantly higher titers of all *B. mallei*-specific antibodies tested (Figure 10). Mean differences in absorbance for IgG1, IgG2a, and IgM were 5.4 (p = 0.0009)-, 4.8 (p = 0.0106)-, and 10.9 (p = 0.0028)-fold higher, respectively, in *B. mallei* Δ*tonB*-vaccinated mice.

Histopathological analysis

The BALB/c mice tissues (lungs, liver and spleen) from the vaccine titration study (n=3 per treatment) at 0 h and 48 h post-challenge were histologically analyzed. Representative images of the lungs, liver and spleen from PBS- and Δ*tonB*-immunized BALB/c mice are presented in Figure 11. At 0 h, the lungs, livers and spleens of PBS-treated BALB/c mice were unremarkable, presenting as normal healthy tissue with normal architecture (Figure 11A-C). BALB/c mice immunized with the Δ*tonB* mutant presented with the following mild-to- moderate changes in pathology: perivascular and

peribronchial inflammatory infiltrates in the lung sections (Figure 11D), hepatitis with multifocal necrosis and scattered abscesses in the liver sections (Figure 11E), and

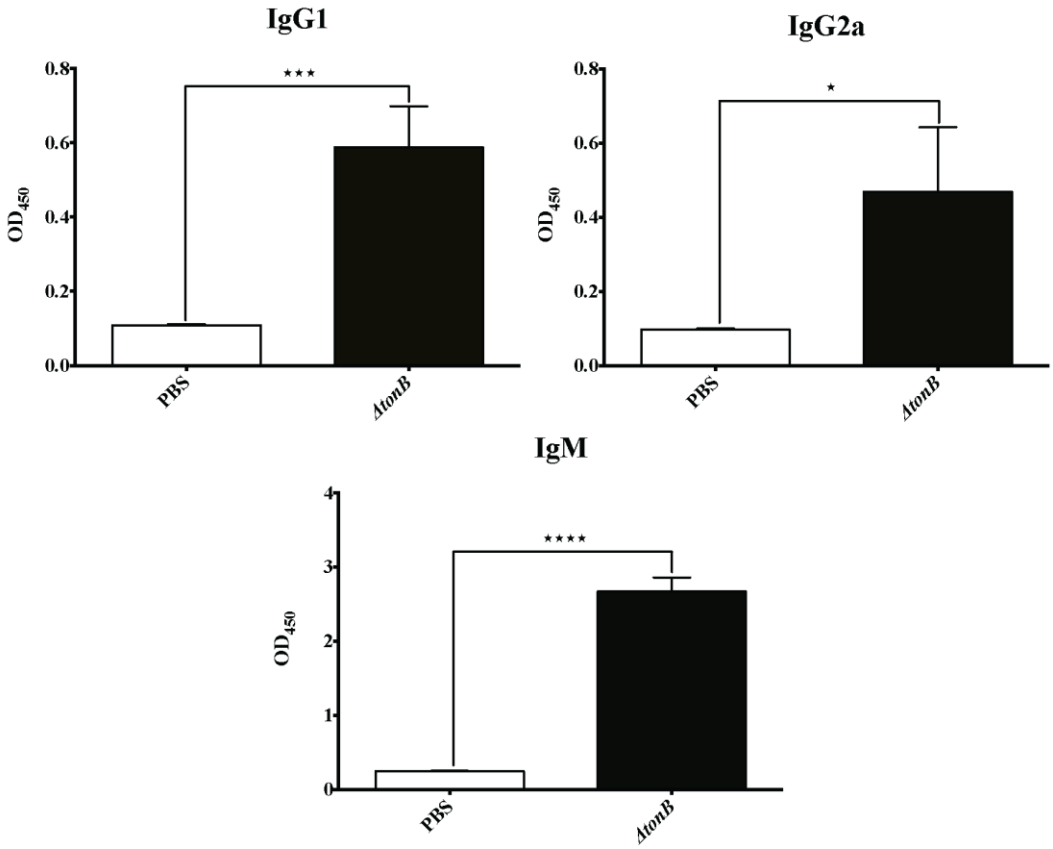

Figure 10. *B. mallei* specific Ig levels in *B. mallei* Δ*tonB* mutant vs PBS vaccinated mice before challenge. Serum samples from BALB/c mice taken at 21 days post PBS or *B. mallei* Δ*tonB* mutant vaccination were diluted 1:10,000 and analyzed for *B. mallei* specific IgG1 (A), IgG2a (B) and IgM (C) using a class specific HRP-conjugated anti-mouse Ig monoclonal antibody. Bars plotted with their SD represent the mean of three animals. Statistical significance was determined by the unpaired t test with equal SD. ⋆ $p < 0.05$ ⋆⋆⋆ $p < 0.001$, ⋆⋆⋆⋆ $p < 0.0001$.

necrosis of follicles and accumulation of neutrophils in spleen sections (Figure 11F). At 48 h, PBS-treated BALB/c mice showed moderate-to-severe pathological changes, such as abscesses and multifocal inflammatory infiltrates in the lungs (Figure 11G and Figure 12A), areas of hepatocellular necrosis, occasional abscesses with necrotic cores and areas of focal necrosis in the liver (Figure 11H), and congestion of the red pulp, proliferation of

large foamy macrophages (inset of Figure 12C) and necrosis affecting the mantle zone (Figure 11I and Figure 12C). Similarly, *B. mallei* Δ*tonB*-immunized BALB/c mice showed moderate-to-severe changes in pathology, but with a few differences. In the

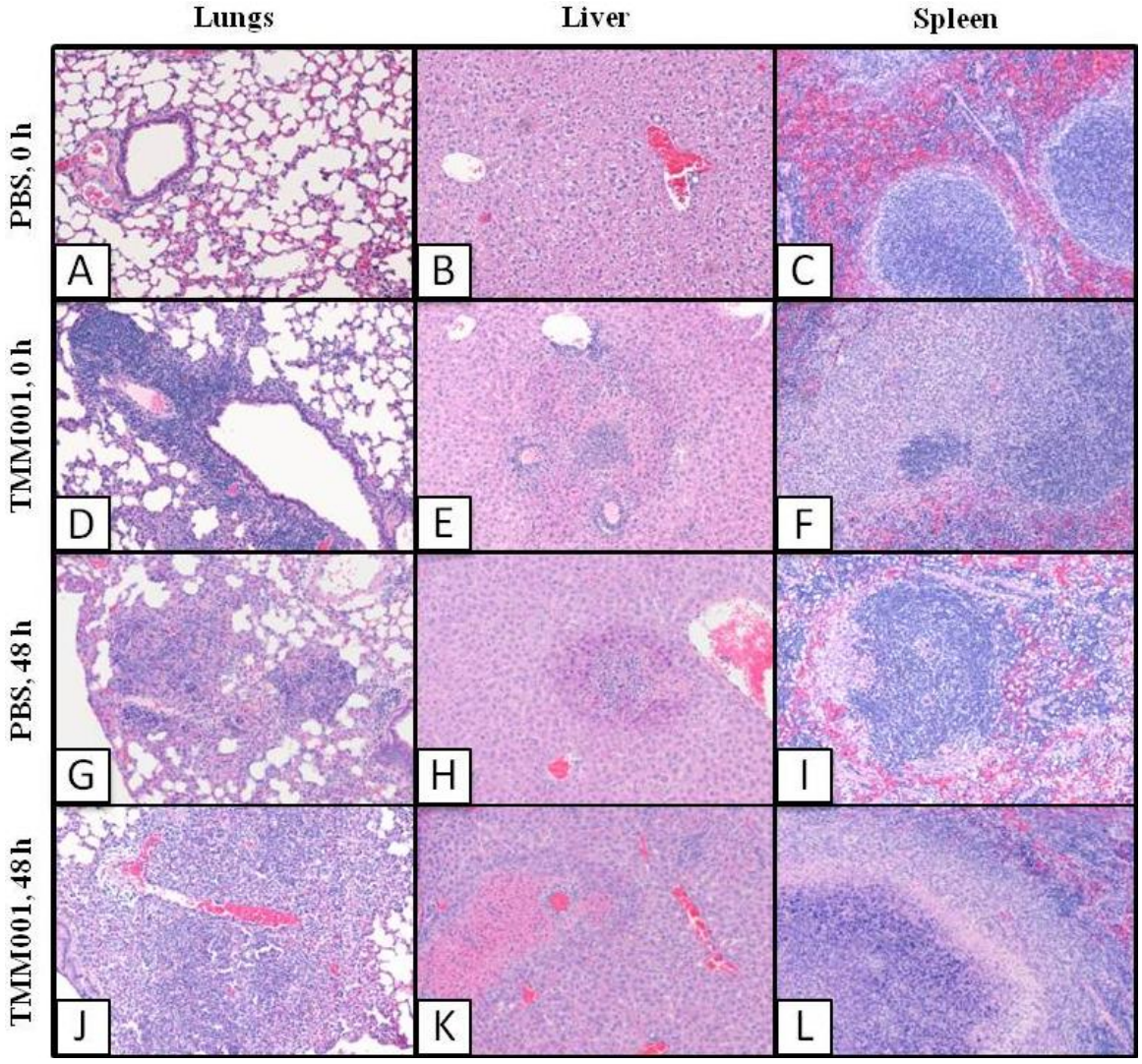

Figure 11. Representative images of CSM001 infected mice organ pathology. Figures A-L display the types of pathology seen in H&E stained lungs, liver and spleen of CSM001 ($1.5x10^5$ CFU) challenged BALB/c mice previously immunized with PBS or Δ*tonB* ($1.5x10^4$ CFU) at 0 h and 48 h post challenge.

lungs, large, multifocal inflammatory infiltrates, as well as abscesses, were present with focal consolidation observed as well (Figure 11J and Figure 12B). The liver presented

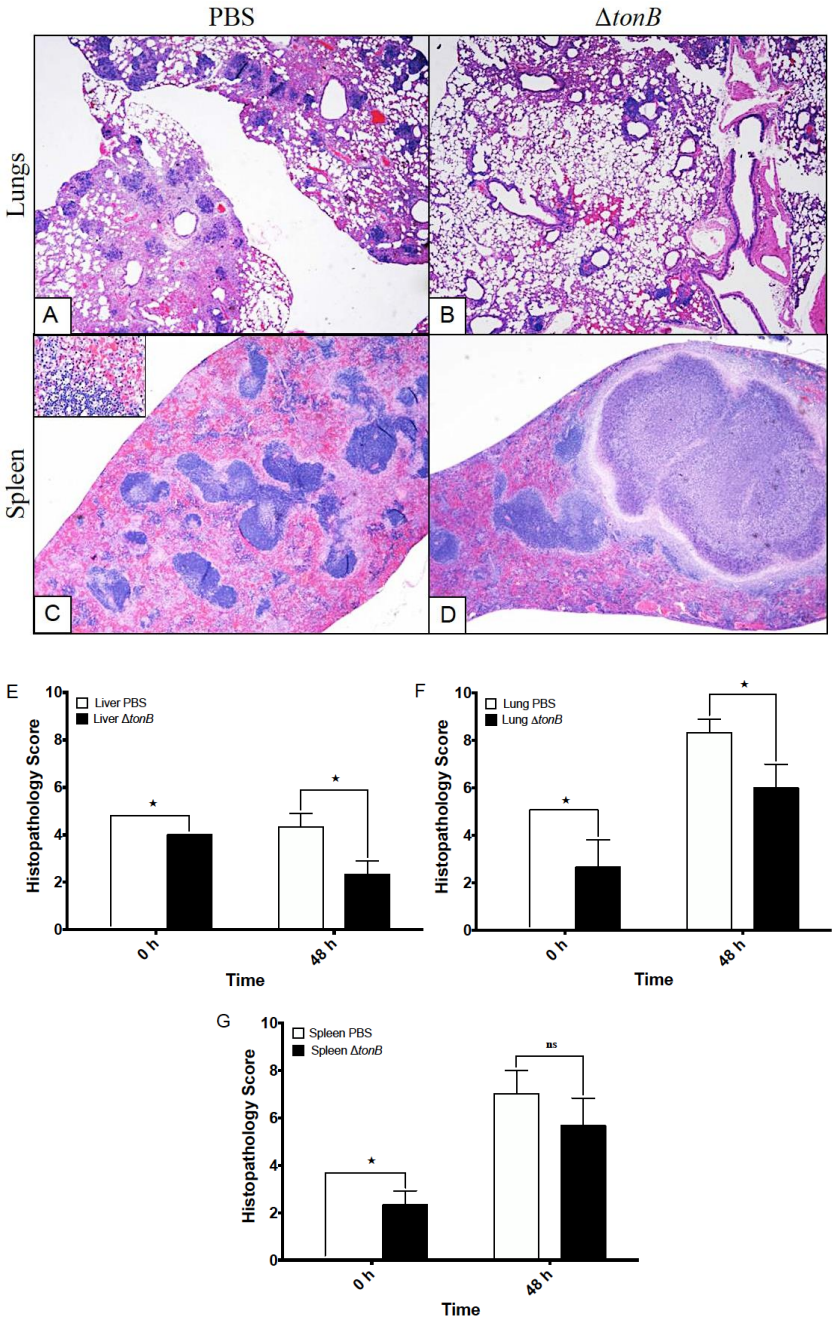

Figure 12. Histopathology of *B. mallei* Δ*tonB* mutant vs PBS vaccinated mice 48 h post challenge. H&E stained lung (A, B) and spleen (C, D) of CSM001 ($1.5x10^5$ CFU) challenged mice previously immunized with PBS (A, C) or Δ*tonB* ($1.5x10^4$ CFU) (B, D) 48 h post challenge. Scale bar = 100μM. Scores (E-G) were assigned for the lung, liver and spleen tissue sections after microscopic examination. Bars plotted with their SD are representative of three animals. Statistical significance was determined by the Mann-Whitney's test. ⋆ $p < 0.05$.

with hepatitis and multiple foci of hepatocellular necrosis (Figure 11K), and large granulomas were formed in the spleen (Figure 11L and Figure 12D). Histopathology scores showed significant differences due to treatment over time in the lungs (★★★★ $p \leq 0.0001$), liver (★★★★ $p \leq 0.0001$) and spleen (★★ $p \leq 0.001$). When comparing the differences in treatment at 0 h and 48 h, the lungs (★ $p = 0.05$), liver (★ $p = 0.05$) and spleen (★ $p = 0.05$) showed a robust trend toward significance as seen in Figure 12E-G.

Serum Cytokine Analysis

Cytokine analysis was conducted on the serum of vaccine titration study mice (n=3 per treatment) collected at 48 h post wild-type challenge. The majority of cytokines were highly expressed in the serum of PBS-treated BALB/c mice compared to those immunized with the *B. mallei* Δ*tonB* (Figure 13). Of those to note, IL-6 ($p = 0.049$), GM-CSF ($p = 0.037$), MCP-1 ($p = 0.022$), and RANTES ($p = 0.032$) were significantly up regulated in PBS-immunized mice, which is consistent with our previous studies (Figure 13) [102]. Furthermore, values for serum G-CSF were well above the standard, and thus the values were set to the highest extrapolated value. Analytes, IL-1β ($p = 0.097$), G-CSF, ($p = 0.067$) and KC ($p = 0.05$) showed a trend of up-regulated expression in PBS- vs Δ*tonB*–treated BALB/c mice (Figure 13). Of those more highly expressed in Δ*tonB* mutant-treated BALB/c mice, IL-12 (p40) showed the greatest significance in differential expression with a p value equal to 0.0005.

Cross Protection Study

Since *B. mallei* is a host-adapted clone of *B. pseudomallei*, the Δ*tonB* mutant was tested for its protective potential in an acute inhalational model of murine melioidosis. BALB/c mice were vaccinated with 1.5×10^4 CFU of *B. mallei* Δ*tonB*. At 21 days post-immunization, BALB/c mice were challenged with 3 LD_{50} (9.0×10^2 CFU) of *B.*

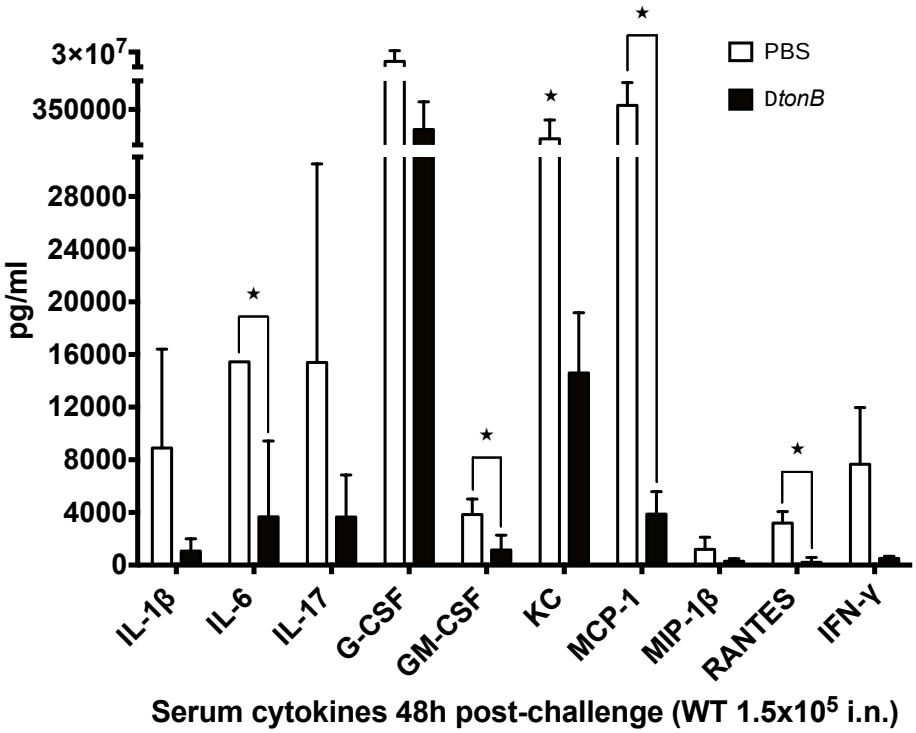

Figure 13. Cytokine/chemokine profile of B. mallei ΔtonB mutant vs PBS vaccinated mice 48 h post challenge. Serum chemokines/cytokines with higher expression levels in CSM001 (1.5x105 CFU) challenged BALB/c mice previously receiving PBS vs immunization with TMM001 (ΔtonB) (1.5x104 CFU) at 48 h post challenge. Bars plotted with their SD are representative three animals. Statistical significance was determined by one-way ANOVA followed by the Dunnett's test. ★ $p \leq 0.05$.

pseudomallei strain K96243 [103]. In accordance with previous data, all PBS-treated BALB/c mice died by 5 days post-challenge with a median survival of 5 days (Figure 14). In BALB/c mice immunized with the *ΔtonB* mutant, survival was increased to 75% (★★★, $p \leq 0.001$) at the end point of 36 days. As with the previously *B. mallei* Δ*tonB* vaccination studies, bacteria were recovered from immunized BALB/c mice who presented with splenomegaly accompanied by abscesses.

DISCUSSION

To date, immune correlates of protection for *B. mallei* and *B. pseudomallei* are not clearly defined. Due to their intracellular lifestyle, these pathogens use an array of

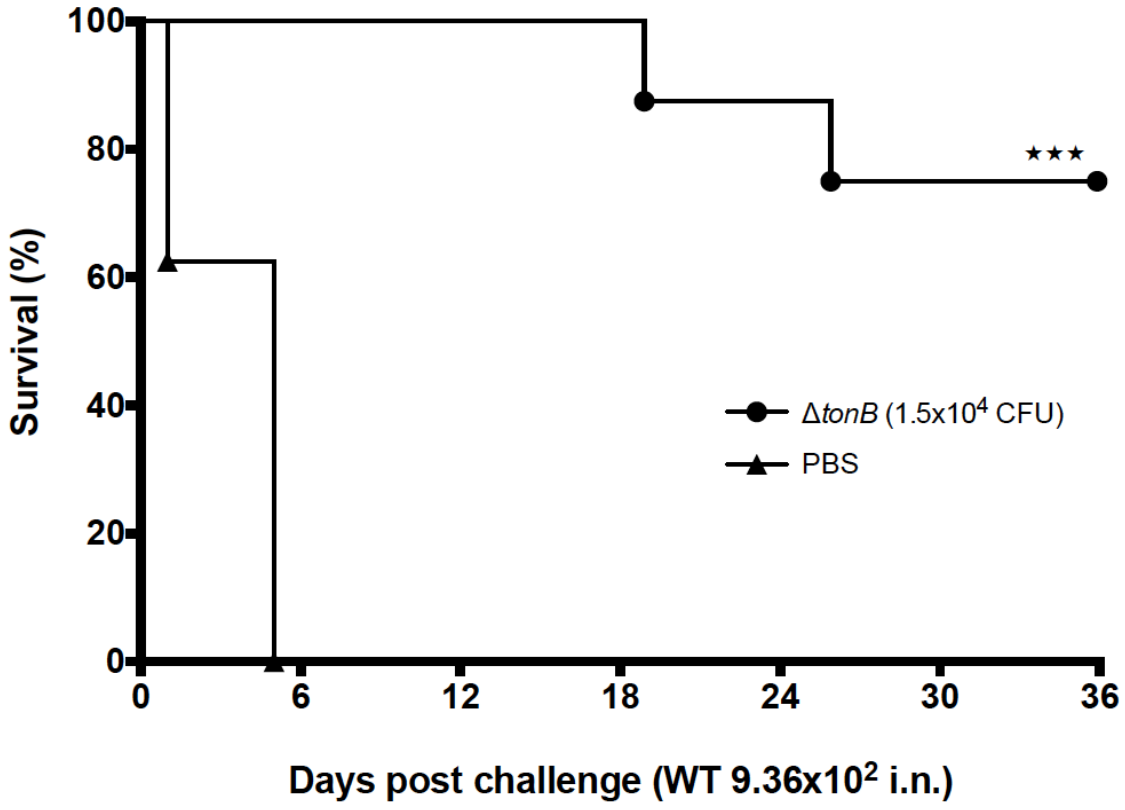

Figure 14. *B. mallei* Δ*tonB* mutant provides increased protection against *B. pseudomallei* wild type challenge. Mice were vaccinated i.n. with PBS (solid triangle) (n=7) or 1.5x104 CFU (solid circle) of TMM001 (Δ*tonB*) (n=8). Three weeks later, BALB/c mice were challenged (day 0) with 9.36 x 10^2 CFU of *B. pseudomallei* K96243. Statistical significant differences in survival times were determined by plotting Kaplan-Meier curves, followed by a log rank test. ★★★ $p < 0.0001$.

virulence factors to invade, replicate, and cause pathogenesis from within host cells, which can impede immune detection and, in some cases, protection. An extensive review of the literature suggested to us that an ideal vaccine for both pathogens would induce robust humoral and cell-mediated responses [106,113]. Thus, we decided to examine live attenuated vaccines, as these are often cited as the most efficacious approach to vaccine development against intracellular pathogens, since they mimic natural infection, inducing both humoral and cell-mediated immunity, without causing disease. Moreover, this thorough exposure to the live attenuated strain allows the immune system to customize a

protective response, in addition to generating an immune memory for lifelong protection against infection.

In the present study, we set out to create such a vaccine by targeting the B. mallei protein TonB. Anchored in the cytoplasmic membrane, TonB plays an essential role in energizing the outer membrane receptors responsible for the active transport of extracellular iron containing-complexes into the periplasm of the cell. Introduction of a 591-bp deletion in the *B. mallei tonB* gene (BMAA1801) generated a mutant strain disrupted in its ability to assimilate hemin, hemoglobin, lactoferrin, and transferin for growth under iron-chelated conditions. In contrast, growth halos were produced around filter disks saturated with $FeSO_4$, which showed the *B. mallei* Δ*tonB* mutant capable of utilizing sources whose important mechanisms are independent of the TonB protein. Aerobically growing bacterial mutants with non-functioning transport systems were found to become iron starved in the absence of free iron sources, such as $FeSO_4$ [114]. This condition was reported to lead to a distinct stress response characterized by the de-repression or induction of genes involved in iron acquisition [115]. In a futile attempt to acquire iron, said mutants were found to respond by hypersecreting siderophores [114-120]. This is consistent with our findings in the CAS agar assay that show the Δ*tonB* mutant producing yellow halos, a result synonymous with siderophore secretion, and these were 4-mm large in diameter, at a minimum, when compared to wild-type halos (Figure 3). The latter finding is consistent with the morphologically distinct, yellow colonies of the *B. mallei* Δ*tonB* mutant, when compared to those from the wild-type, which are white-beige (Figure 1). This change in morphology is reported to result from the constitutive production and accumulation of iron-bound siderophores, which are yellow-to-brown vs. iron-free siderophores which are uncolored [119-121]. The accumulation of iron-bound siderophores shows the *B. mallei* Δ*tonB* mutant unable to dissociate iron from siderophores, which provides further evidence of a disruption in iron transport and assimilation (Table 2).

In growth curve experiments, it was found that the *B. mallei* Δ*tonB* mutant was incapable of maintaining wild-type growth kinetics (Figure 2). Upon supplementing the starter culture with free iron, the *B. mallei* Δ*tonB* mutant exhibited increased growth rates more reminiscent of the wild-type, which is illustrated by a shorter lag phase and prolonged maintenance of wild-type growth kinetics. In a separate growth curve study, our lab showed the full rescue of the *B. mallei* Δ*tonB* mutant phenotype after both the starter and sub-culture were supplemented with free iron (data not shown). Thus, the direct correlation between free iron and the *B. mallei* Δ*tonB* mutant growth rate shows the importance of TonB and its role of facilitating iron transport in fitness.

In regard to virulence, a survival study in BALB/c mice showed an inverse correlation between the percentage of survival and *B. mallei* Δ*tonB* mutant dose and/or concentration of free iron (Figure 4). Compared to previous survival studies in BALB/c mice challenged with the wild-type, the *B. mallei* Δ*tonB* mutant strain is 30 times more attenuated with triple the dose, resulting in 100% survival. Decreased mortality observed in animals challenged with the *B. mallei* Δ*tonB* mutant grown in LBG alone illustrates the importance of iron and its TonB-mediated acquisition to virulence.

To prevent infection, vertebrate hosts employ a process known as iron withholding, a form of nutritional immunity that sequesters free iron from the environment [110]. The inaccessibility of free iron causes the invading pathogen to undergo a period of iron starvation which induces and/or increases the expression of iron acquisition systems to survive [108]. The absence of functional TonB-dependent iron acquisition systems could have rendered the *B. mallei* Δ*tonB* mutant incapable of overcoming this state of iron deficiency, resulting in decreased fitness of the mutant. This notion is supported by the diminished ability of the *B. mallei* Δ*tonB* mutant to survive, colonize, and disseminate to target organs (Figure 5) and could account for its attenuated virulence. Further, upon artificial complementation with exogenous iron, the

1217 *B. mallei* Δ*tonB* mutant phenotype was partially rescued, with the most noticeable
1218 difference in the later time points found in the spleen.

1219 In a series of vaccine titration studies, it was empirically determined that a dose of
1220 1.5 x 10^4 CFU of the *B. mallei* Δ*tonB* mutant resulted in 100% protection (Figure 9) and
1221 wild-type clearance following challenge. Protected animals developed strong *B. mallei*-
1222 specific IgG1, IgG2a, and IgM responses (Figure 10), which were attributed to *B. mallei*
1223 Δ*tonB* mutant-mediated protection. The observation and correlation of strong IgG and
1224 IgM elicitation and protection are cited often in *Burkholderia* vaccine studies
1225 [34,43,122,123]. In human cases, it was found that patients with less severe, localized
1226 infection produced detectable *Burkholderia*-specific IgM antibody titers, whereas none
1227 were detected in patients suffering from acute disseminated infection [122]. Thus, it is
1228 possible to suggest that *B. mallei* Δ*tonB* mutant vaccination protects against lethal
1229 infection by neutralizing bacteria and/or preventing their dissemination to target organs
1230 via antibody-mediated mechanisms.

1231 *B. mallei* Δ*tonB* mutant immunization resulted in pathological differences that
1232 may explain increased survival and protection. In general, histopathological scoring
1233 shows a robust trend toward significant differences in the pathology seen in the lungs,
1234 liver and spleen of control vs. *B. mallei* Δ*tonB*-immunized animals (Figure 12 e-g).
1235 Further analysis of these tissues revealed two discriminatory elements of pathology
1236 between vaccine treatments. First, despite the finding that the lungs and livers from both
1237 treatment groups displayed the same type of tissue damage, the pathological changes in
1238 the *B. mallei* Δ*tonB*-immunized mice were much less severe (Figure 11). And second,
1239 the differential alteration in spleen architecture implied the treatment groups responded
1240 differently to infection. For example, splenic tissues from PBS-treated mice show a
1241 diffuse response to injury (i.e. diffuse severe histiocytosis), while splenic tissue from *B.*
1242 *mallei* Δ*tonB* mutant immunized BALB/c mice show a focal response to injury (i.e.
1243 granuloma formation) (Figure 11c-d). These histological observations suggested to us

that immunization with the *B. mallei* Δ*tonB* mutant may result in the induction of an immune response that reduces the severity of tissue damage, in addition to confining infection to preventing disseminated disease, an important cause of morbidity and mortality in many diseases [122,124-126].

These histopathological differences between control and *B. mallei* Δ*tonB* mutant vaccinated mice are mirrored by the differences observed in their serum cytokine and chemokine expression. A comparison of the expression profiles showed unprotected control animals having higher expression levels of the following cytokines: IL-1β, IL-6, GM-CSF, KC, MCP-1, RANTES and G-CSF (Figure 13). Pleiotropic in nature, macrophage-derived pro-inflammatory cytokines IL-1β and IL-6 possess both potent immunological and inflammatory properties [127-130]. Unregulated levels of pro-inflammatory cytokines can disrupt the antimicrobial activity/degrees of host immunopathology balance and directly contribute to disease immunopathogenesis and progression. In models of murine melioidosis, it has been established that high levels of pro-inflammatory cytokines IL-1β and IL-6 are preceded by *B. pseudomallei* dissemination and concur with acute sepsis and mortality [131,132]. In addition, clinical evidence has shown a correlation between elevated serum levels of IL-1β and IL-6 and poor prognosis in patients with septic melioidosis [133-135]. Produced by activated macrophages, IL-1β is an important mediator of the inflammatory response involved in an array of processes, such as cell proliferation, differentiation, and apoptosis [136]. The deleterious role of IL-1β has been attributed to a variety of causes, such as excessive recruitment of neutrophils, which are speculated to support intracellular growth of *B. pseudomallei*; tissue damage; and inhibition of IFN-γ, an essential protective factor against *B. pseudomallei* and *B. mallei* infection [137]. Furthermore, IL-1 is a potent inducer of the cytokine cascade, which promotes the production of IL-6, GM-CSF, and G-CSF (CSF responses) [138]. Secreted by activated macrophages, IL-6 is a pro-inflammatory cytokine that functions to mediate fever and acute phase responses [139].

During bacterial infection, IL-6 is able to induce MCP-1 production and has also been implicated in the suppression of IFN-γ and IL-12, a cytokine well know for it protective properties against *B. pseudomallei* and *B. mallei* infection [140-142]. In line with our results, previous work in the lab conducted by Judy et al. [103] showed that cytokines IL-1β, IL-6, G-CSF, KC, MCP-1 and RANTES, were detected in much higher levels at 1-3 days post *B. pseudomallei* challenge in the lungs of unprotected control animals vs those of CpG-treated animals. The cytokine profile of control mice seems to be indicative of a highly inflammatory environment. These results are consistent, not only in this study, but in our previous work on the natural history *B. pseudomallei* virulence, in which the serum of infected animals showed dramatic increase in KC, G-CSF, and MCP-1 (20). Given the role of these cytokines for recruitment and activation of neutrophils and monocyte/macrophage populations, these cytokines were correlated with observed leukocyte infiltration and pathology at sites of infection [102]. Lastly, since *B. mallei* and *B. pseudomallei* are genetically closely related, the *B. mallei* Δ*tonB* mutant was further tested for its potential to provide protection in an acute inhalational model of murine melioidosis (Figure 14). The significant cross protection seen in *B. mallei* Δ*tonB* mutant-vaccinated mice provides an optimistic outlook for the development for a single vaccine for both pathogens.

Our vaccine is unique in that immunization provided considerable protection and clearance of wild-type, while the *B. mallei* Δ*tonB* mutant was able to persist in all long-term surviving animals. This persistence may be an attribute of long-term protection as a result of increasing the immune system's accessibility to protective antigen or contributing to the development in an environment adverse to wild-type colonization via chronic elicitation of the immune response. This notion is supported by previous live attenuated vaccine studies that showed survivors are generally all colonized at the end of the study [36,42,143]. Furthermore, the failure to provide systemic, long-term protection has been attributed to the rapid clearance of the attenuated vaccine strain [42,143] .

Based on these and previously reported results, our studies are now focused on reducing the long-term persistence of the *B. mallei* Δ*tonB* mutant. The current objective is to further optimize our vaccine strain by the following strategies: (1) introducing additional mutations into the backbone, (2) investigating alternative routes of administration, and (3) investigating alternative vaccine strategies, such as the incorporation of a prime-boost regiment or a two-pronged approach in which vaccination consists of a combination of two immunization routes. Overall, we believe the present study represents a good starting point for projects in which the *B. mallei* Δ*tonB* mutant could be further optimized to become an effective vaccine against glanders and melioidosis.

Chapter 7: Monitoring Therapeutic Treatments against *Burkholderia* Infections Using Imaging Techniques

INTRODUCTION

In developing vaccines, researchers have looked to the employment of adjuvants to generate and/or improve protective immunity. There has been significant interest in using cytosine-phosphate-guanine (CpG)-containing oligodeoxynucleotides (ODNs) as an adjuvant for preventative therapeutic measures [103,144-155]. CpG provides protection from a variety of pathogens, such as *Klebsiella pneumoniae, Yersinia pestis, Listeria monocytogenes, Burkholderia pseudomallei,* respiratory syncytial virus and human immunodeficiency virus, by enhancing non-specific immunity commonly associated with a strong polarized Th1-cell response, including increased production of IFN-γ and Th1-associated antibody isotypes [144-150]. Pre- and post-vaccination with CpG has been shown to protect and in some cases may contribute to the cessation of disease transmission [144]. Mimicking bacterial DNA, CpG ODNs activate toll-like receptor (TLR) 9 signaling and thus, function as potent stimulators of innate immunity [156,157]. CpG ODNs are categorized in A-, B- and C-classes, based on varying properties of length, sequence, backbone and formation of secondary or tertiary structures. Although all act as TLR-9 agonists, the three classes have been described as eliciting different innate immune responses [157]. Class-A is characterized by strong natural killer (NK) cell and precursor dendritic cell (pDC) activation, high levels of IFN-α production, and limited B cell activation, whereas class-B is categorized by strong B cell activation, moderate NK and pDC activation with moderate IL-12 and limited IFN-α production [158-163]. Class-C has intermediate properties of both class-A and -B and thus is categorized by a strong B cell, antigen presenting cells (APC) and NK cell activation, induction of pDC IFN-α production and preferential development and differentiation of T helper 1 (Th1) cells [156,159,164,165]. The activation of innate

immunity by the administration of CpG has been shown to provide protection against an array of intracellular pathogens [144-150]. Against low aerosol challenge of *B. mallei*, BALB/c mice pre-treated with CpG had lower levels of bacterial burden in the lungs and increased survival compared to controls [166]. The protection provided by CpG pre-treatment was associated with enhanced levels of IL-12 and IFN-γ, IFN-γ-inducible protein 10 and IL-6 [153]. Similar results were seen in an acute fatal sepsis model of *B. pseudomallei* infection in BALB/c mice where CpG pre-treatment conferred more than 90% protection which was attributed to elevated levels of IL-12 and IFN-γ [152]. In an attempt to define immune correlates of protection provided by CpG pre-treatment, Judy et al. [101] showed that protection against an acute respiratory model of *B. pseudomallei* infection in BALB/c mice is linked to elevated levels of IL-12 and recruitment of inflammatory monocytes and neutrophils to lungs prior to infection. Because *B. mallei* is considered a dwarfed clone of *B. pseudomallei*, data from experiments ascertaining the protective efficacy of CpG treatment in an acute model of glanders should reflect the infectious trends seen in melioidosis [167].

In the present study, the protective potential of CpG pre-treatment was evaluated in an acute respiratory BALB/c mouse model of *B. mallei* infection. In addition to assessing class-C CpG ODN protective capabilities and the role inflammatory cell recruitment is playing during murine glanders, our study has focused on the implementation of *in vivo* imaging techniques to monitor disease progression and treatment. Since our previous study showed that CpG class-C provides the greatest protection against *B. pseudomallei*, this CpG ODN was chosen for evaluation. The bioluminescent *B. mallei* reporter strain CSM001 was used to monitor real time bacterial infection combined with a new technique that employs a Neutrophil-Specific Fluorescent Imaging Agent to visualize neutrophil trafficking *in vivo*.

RESULTS

Class-C CpG ODNs treatment increases percent survival in BALB/c mice.

Using the pre-established acute respiratory challenge (i.e., intranasal) model of glanders [104], two groups of 10 BALB/c mice were treated intranasally (i.n.) with 20 µg of class-C CpG or PBS. Twenty four hours after treatment, BALB/c mice were infected i.n with 1 x 10^4 CFU of *B. mallei* CSM001. This combination of class-C CpG ODN treatment and CSM001 challenge was used in all the following studies unless otherwise

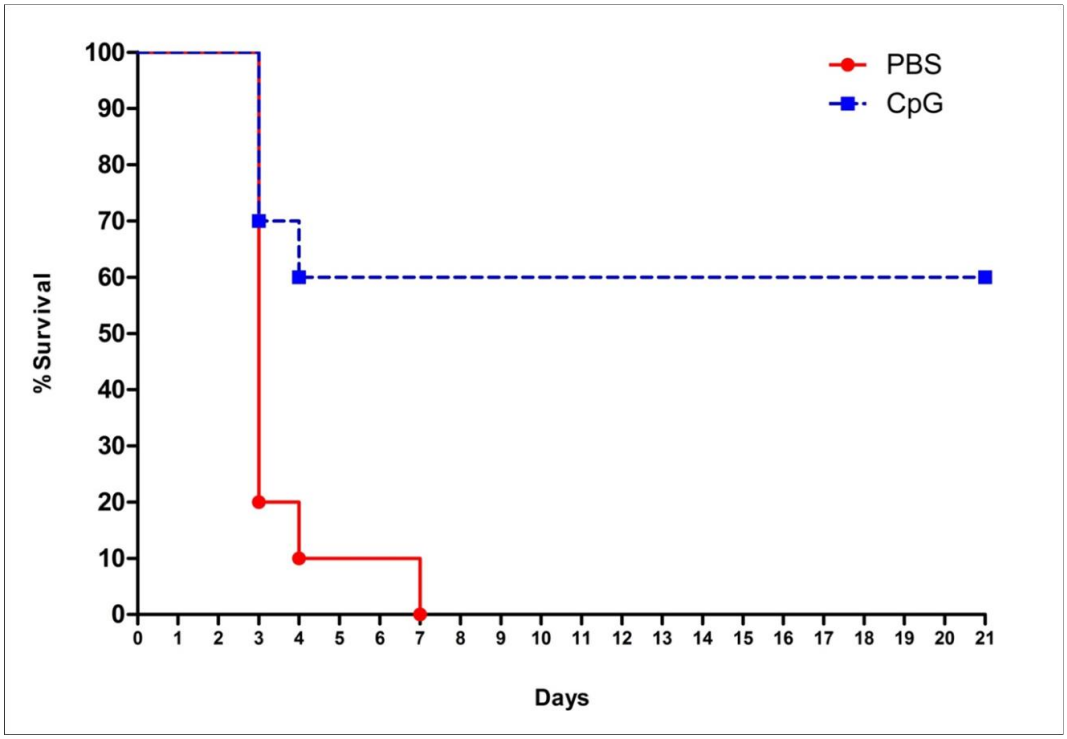

Figure 15: Survival of BALB/c mice immunized with Class-C CpG and challenged with CSM001. Mice were immunized i.n. with PBS or CpG 24 h prior to i.n. challenge with 1.5 x 10^5 CFU of CSM001. CpG immunized mice showed 60% survival at day 21, whereas in the control group, mice began to die at day 3 with 0% survival by day 7. Both a Log-rank test (p= 0.0029) and a Gehan-Breslow-Wilcoxon test (p=0.0094) found both Kaplan-Meier survival curves to be statistically different.

mentioned. As previously demonstrated with this model, the majority of deaths in the control group occurred on days 3 and 4, with all PBS-treated animals succumbing to infection by day 7 (Figure 15). On the other hand, treatment with class-C CpG resulted

in increased protection shifting the curve from 0% to 60% survival until the study was terminated at day 21.

Class-C CpG ODNs treatment reduces bacterial load in BALB/c mice.

To assess the effects of class-C CpG ODN treatment on CSM001's ability to establish infection and colonize target organs, BALB/c mice were treated and infected as described in the experimental section. At 24, 48 and 72 h post-infection, 3 animals per group were euthanized, their lungs, livers and spleens homogenized, serial diluted in PBS and plated

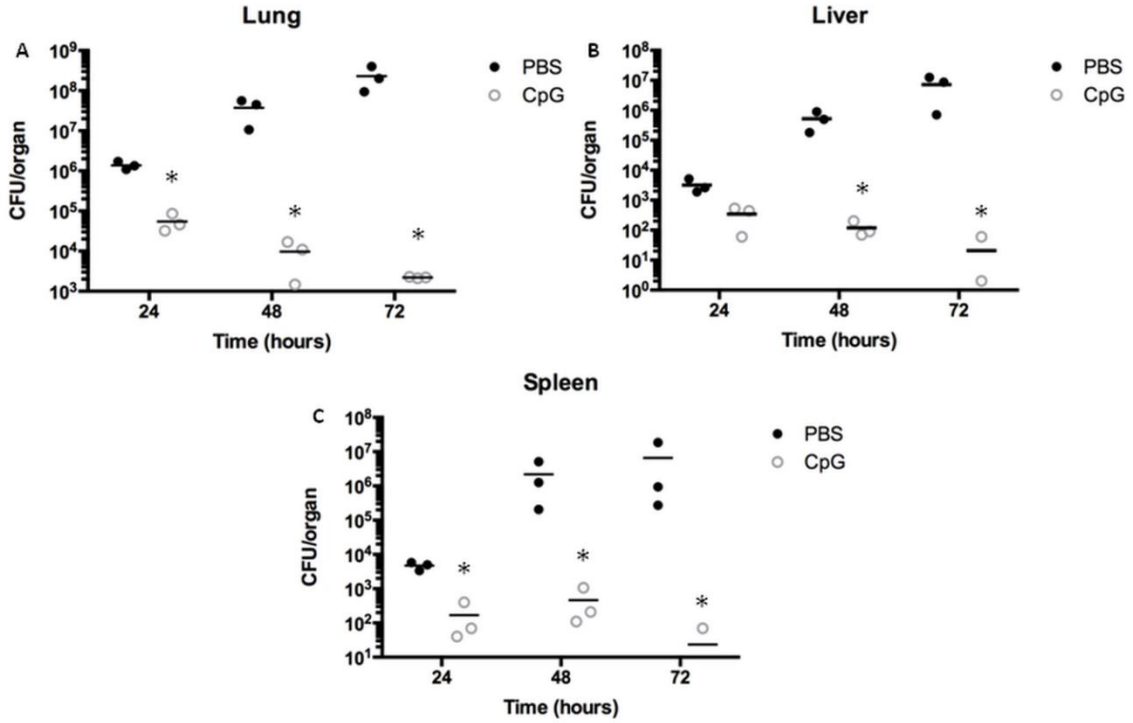

Figure 16: Bacterial burden of BALB/c mice immunized with Class-C CpG and challenged with CSM001. Bacterial burden in the lungs (A), liver (B) and spleen (C) was ascertained in three mice per group per time point. To determine statistical differences, values were log transformed and then subjected to a paired two tailed Student t test. *, $p < .05$.

on LBG agar supplemented with kanamycin (Km). BALB/c mice treated with class-C

CpG ODN showed significantly reduced levels of bacteria in the lung, liver and spleen at every time point, as compared to PBS-treated BALB/c mice (Figure 16). Bacterial numbers peaked at mean values of 1.38×10^6 CFU, 3.43×10^2 CFU and 1.70×10^2 CFU in the lung, liver and spleen, respectively; in class-C CpG ODN treated mice at 24 h and then receded to low levels in the lung or undetectable levels in the liver and spleen by 72 h post-infection. On the other hand, bacterial numbers in PBS-treated mice continued to increase exponentially over the sampling period peaking at 72 h with a mean value of 2.31×10^8 CFU, 7.23×10^6 CFU and 6.60×10^6 CFU in the lung, liver and spleen, respectively.

Class-C CpG ODNs treatment leads to higher neutrophil-specific fluorescence signal in BALB/c mice

Class-C CpG ODNs immunized mice challenge with *B. pseudomallei* wild-type showed increased neutrophil and inflammatory monocyte trafficking to the lung, reduced bacterial burden and increased survival time compared to control mice treated with PBS [168]. Due to the close relatedness of these two pathogens, we then focused on the visual analysis of neutrophil trafficking in BALB/c mice treated with class-C CpG ODN or PBS and infected with *B. mallei* CSM001. Three hours prior to imaging, two BALB/c mice from each group were administered the Neutrophil-Specific, Fluorescent Imaging Agent via tail vein injection. At 24, 48 and 72 h, BALB/c mice were anesthetized and monitored for bioluminescent bacteria and fluorescent neutrophil-specific signal, using an *in vivo* imaging system (IVIS Spectrum) to collect and quantifying the photons emitted by neutrophils and CSM001 within the animals (Figure 17).

Nothing significant was visualized at 24 h (Figure 17a, 17c) or 48 h (data not shown); however, at 72 h, *B. mallei* CSM001 organisms are seen in the head region, lungs, livers and spleens of CpG treated mice. In addition, trafficking and recruitment of neutrophils to the site of infection at 72h (Figure 17b) is also seen in similar areas. By

overlaying these images, it is possible to see dissemination, trafficking and co-localization of bacteria and neutrophils. This ability is extremely informative when study progression of bacterial infection and host responses to combat and control bacterial dissemination. Thus, these results support the value of *in vivo* imaging technology. PBS-treated animals expired before the 72 h and thus were not imaged.

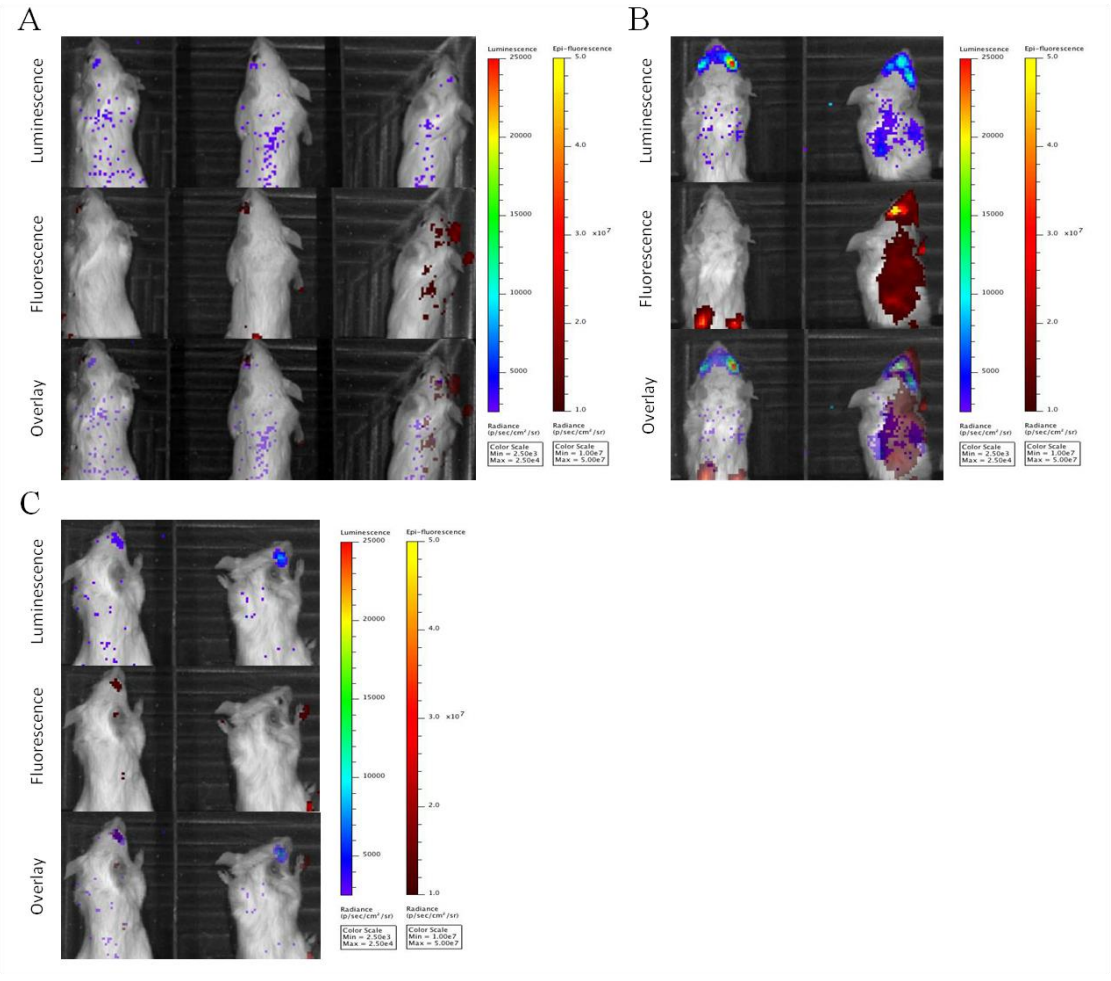

Figure 17: *In vivo* whole body imaging of BALB/c mice immunized with Class-C CpG or PBS and challenged with *B. mallei* CSM001. *In vivo* whole body bioluminescence and fluorescence images of Class-C CpG treated (A, B) and PBS treated (C) were taken at 24 h (A ,C) and 72 h (B) post-infection. The intensity of emission is represented as a pseudocolor image. The luminescence and fluorescent images were then overlaid to visualize bacteria and neutrophil localization.

Class-C CpG ODNs treatment leads to increase levels of inflammatory monocytes during early infection of BALB/c mice.

The influx of neutrophils, inflammatory monocytes and alveolar macrophage populations associated with class-C CPG ODNs treatment and *B. mallei* infection was assessed by flow cytometry of cells found in lung tissue. As shown in Figure 19, a hierarchical gating strategy was used to quantitate numbers of specific populations within lung tissue based on surface marker expression.

Acquired samples were first selected based on side scatter and forward scatter characteristics consistent with leukocytes (Gate 1) (Figure 19a). The Gate 1 cell populations were further separated based on expression of F4/80 (Gate2, F480+ and Gate 3, F4/80-) to distinguish monocyte and macrophage populations (F4/80+) from neutrophils (F4/80-). Neutrophil numbers were further determined from the F4/80- population based on lack of CD11c expression (Gate 4) and expression of CD11b (Gate 5) and Ly6 G/C (Figure 19b). Data are shown as number of events (cells) from the same volume of total lung homogenate as described in the experimental section. The use of these markers additionally enabled assessment of alveolar macrophages that are phenotypically defined as F4/80+CD11b-CD11c+.

Twenty four hours (Time 0 h) after pre-treatment with class-C CpG ODN, the numbers of inflammatory monocytes (F4/80+Ly6 G/C+) increased in BALB/c mice compared with those treated with PBS (Figure 18d). At 72 h, an inverse trend is seen with PBS-treated mice showing significantly higher numbers of inflammatory monocytes (Figure 18d). Although neutrophil levels were 1.7 times higher at 0 h in class-C CpG ODN treated vs PBS treated BALB/c mice, this increase was not statistically significant due to animal variability (Figure 18c). Following challenge with *B. mallei*; however, neutrophil numbers were increased in both treatment groups by 72 h post-infection. PBS-treated mice had significantly higher numbers of alveolar macrophages numbers at 0 and 72 h compared to class-C CpG ODN treated mice (Figure 18e).

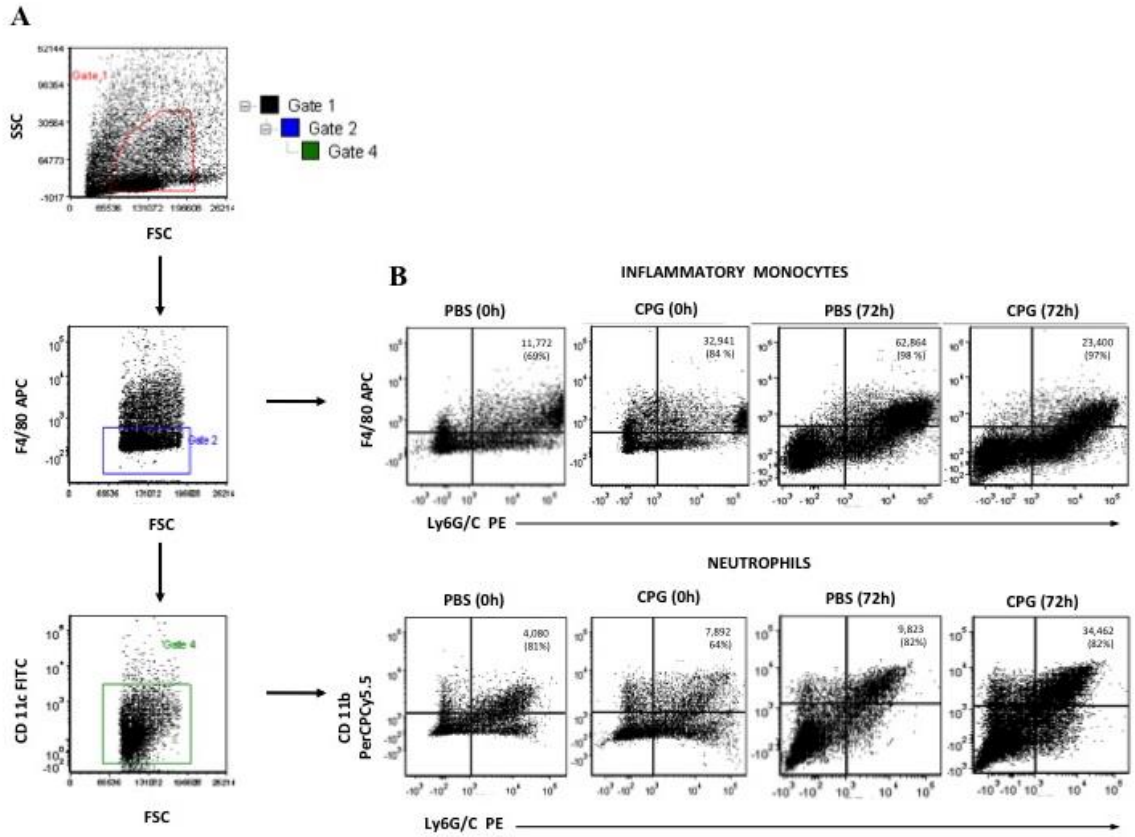
A
SSC
FSC
Gate 1
Gate 2
Gate 4
F4/80 APC
CD 11c FITC
B
INFLAMMATORY MONOCYTES
PBS (0h)
CPG (0h)
PBS (72h)
CPG (72h)
11,772 (69%)
32,941 (84 %)
62,864 (98 %)
23,400 (97%)
Ly6G/C PE
NEUTROPHILS
4,080 (81%)
7,892 (64%)
9,823 (82%)
34,462 (82%)
CD 11b PerCPCy5.5

1474

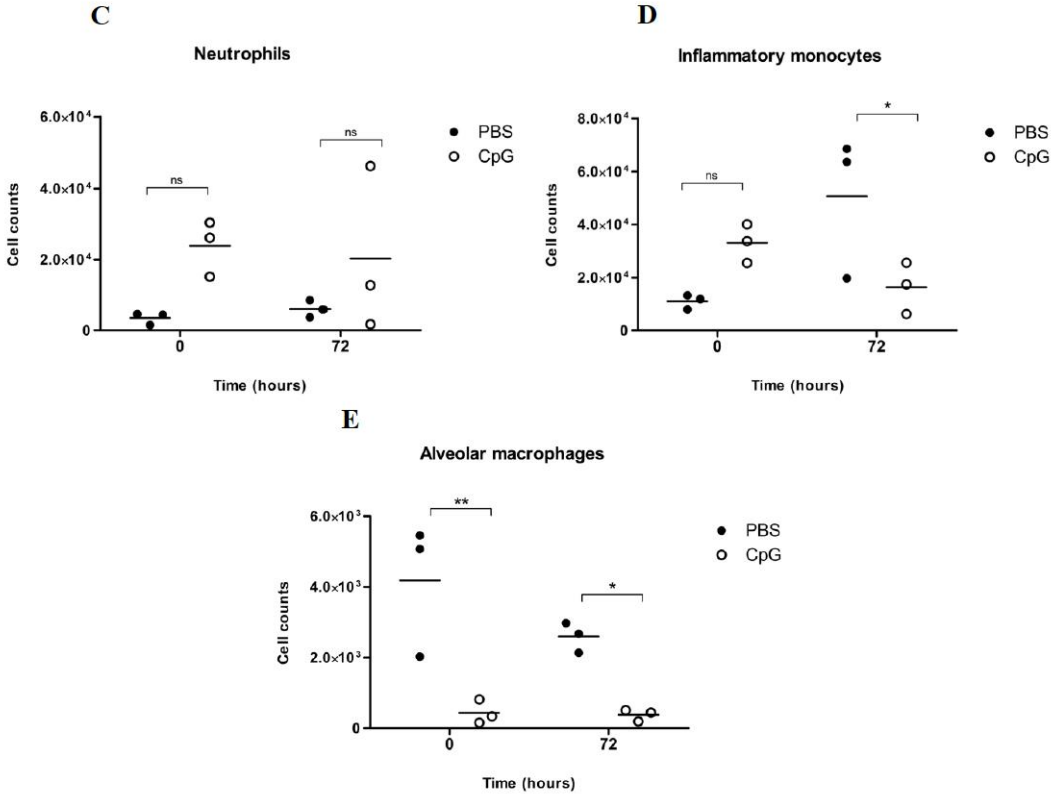
C
Neutrophils
Cell counts
Time (hours)
PBS
CpG
ns
D
Inflammatory monocytes
*
E
Alveolar macrophages
**

1475

Figure 18: Flow cytometry analysis of inflammatory cell populations in BALB/c mice immunized with Class-C CpG or PBS and challenged with *B. mallei* CSM001.Cells from the lung were isolated at 0 h (before infection) and 72 h (after infection). Cells were labeled with Ly6G/C-PE, CD11c-FITC, CD11b-PerCPCy5.5, F4/80-APC monoclonal antibodies or corresponding isotype controls and analyzed using FCS Express v4.0 Flow Research Edition (De Nova Software). Panel A (Gate1) shows gating of leukocytes from PBS treated group by selecting cells that display the appropriate forward and side scatter characteristics. The inflammatory monocyte population (F4/80+ Ly6G/C+) as depicted in panel 4B (upper plots) was obtained from cells in gate 1. Cell populations were further separated based on lack of the F4/80 marker (gate 2) and lack of the CD11c (gate 4) in order to obtain the neutrophil population (CD11c, F4/80–, CD11b+, Ly6G/C+) as shown in panel B (lower plots). Results are representative of 3 animals per group. Shown in panels C, D and E are neutrophil, inflammatory monocytes and alveolar macrophage numbers respectively of PBS (solid circles) or Class-C CpG (open circles) pre-treated animals at 0 h and 72 h after infection. Data are shown as mean ± SEM. One-way ANOVA followed by a Dunnett's multiple comparison tests for group comparisons (Graph Pad Software v4.0). Statistically significant value is designated *, $p < 0.05$.

Class-C CpG ODNs treatment results in decreased tissue damage in the lungs

Lungs sections from *B. mallei*-infected BALB/c mice treated with class-C CpG ODN or PBS were compared at 24, 48 and 72 h after challenge (Figure 19). At 24 h, lungs from class-C CpG ODN- and PBS-treated BALB/c mice show mild to moderate and moderate to focally severe, respectively, perivascular and peribronchial inflammation with a considerable neutrophilic component. Interstitial inflammatory infiltrates, which are mostly neutrophils, are present with numerous scattered micro-abscesses throughout the lung parenchyma (Figure 19a and 19d). Collection of neutrophils and cellular debris within the bronchial lumen are also seen in PBS-treated BALB/c mice (Figure 19a). At 48 and 72 h, areas of necrosis begin to form in microabscesses in both treatment, although, necrotic areas in the lungs of CpG treated BALB/c mice (Figure 19e and 19f) are much smaller and localized compared to lungs of PBS treated BALB/c mice (Figure 19b and 19c).

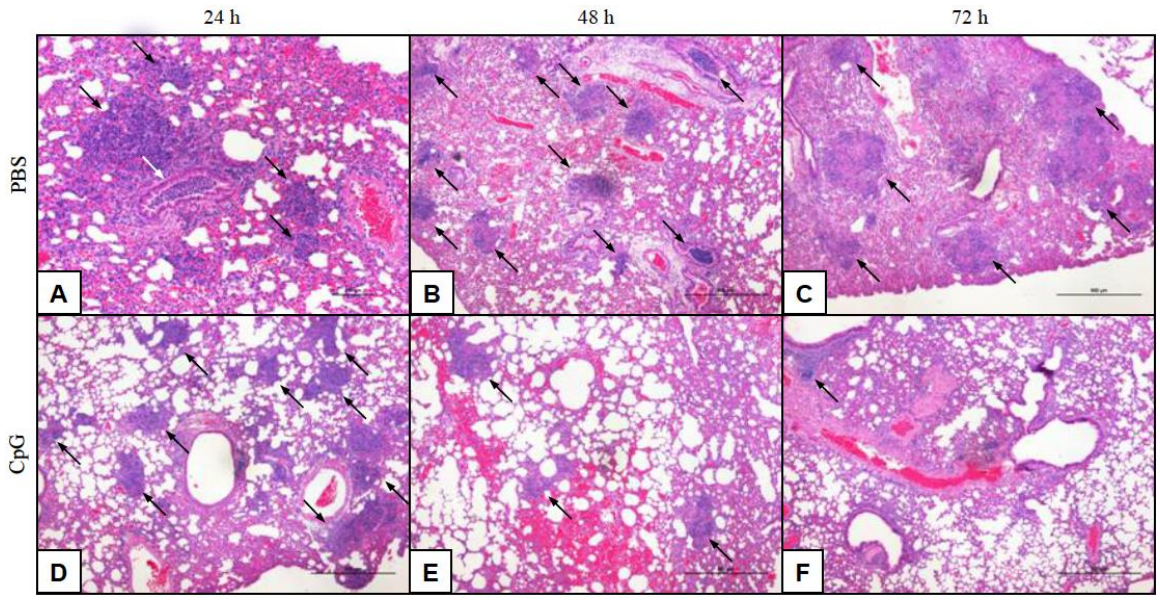

Figure 19: Histological analysis of lungs from BALB/c mice immunized with Class-C CpG or PBS and challenged with *B. mallei* CSM001. Representative images of Hematoxylin and Eosin stained mouse lungs sections from *B. mallei*-infected mice pre-treated with PBS (A–C) or class-C CpG ODN (D–F) at 24 h (A, D), 48 h (B, E) and 72 h (C, F) after challenge. Magnification 40x and scale bar = 100µM. Each panel is representative of the tissue pathology observed in three mice per treatment group. Arrows highlight pathology described in the text.

DISCUSSION

B. mallei is the causative agent of glanders, a disease with high mortality rates in untreated infections [169]. Despite *B. mallei*'s classification as a biothreat agent, there is currently no licensed pre- and post-exposure vaccine that may protect against infection. There are very little data on the efficacy of treating human glanders with antibiotics. Currently, the treatment regimen consists of long-term administration of mixed antibiotics that, if diagnosed early and accurately, is often only partially effective [170]. In the case of *B. pseudomallei* and *B. mallei*, there has been significant interest in using the cytosine-guanine (CpG)-containing oligodeoxynucleotides (ODNs) as adjuvant for preventative therapeutic measures [103,145,151-155,161,171,172]. The interest resides in the fact that CpG interacting with TLR-9 receptors, primarily expressed on B cells and

DCs, stimulates the secretion/production of Ig, cytokine and chemokines and biases host immune reactivity in favor of Th1 responses (IL-12 and IFN-γ) [173]. CpG treatment has been shown to rapidly activate T cells, B cells, macrophage proliferation, and secretion of antibodies as well as an array of Th1-associated cytokines [161]. In addition, CpG is speculated to stimulate non-specific innate inflammatory responses to aid in development of antigen specific immunity. Of the three classes of CpG, class-C attains properties intermediated to those in class-A and -B CpG which include B-cell and NK-cell activation, in addition to induction of IFN-α secretion from DCs [156].

Our previous studies have demonstrated that of the different classes of CpG, the class-C provided better protection against an acute respiratory murine model of *B. pseudomallei* infection [103], and therefore, a similar model was chosen for analysis in the present study. Also, the BALB/c mouse model was previously optimized in our laboratory for acute respiratory *B. mallei* infection and bioluminescent imaging [99]. BALB/c mice are a good animal model to study infection since *B. mallei* exhibits an organ-tropism, localizing specifically to the lung, liver and spleen [106]. In addition, BALB/c mice are susceptible to aerosol and due to the symptoms exhibited after infection; this becomes a clinical relevant model for vaccine/therapeutic testing. Thus, in this study, class-C CpG ODN was assessed for the ability to protect against *B. mallei* in the acute respiratory model of BALB/c infection. Protection was evaluated by percentage of survival, bacterial burden, real-time bacterial dissemination and lung histopathology. In an attempt to dissect immune processes of protection, treated and untreated groups were further monitored in real time for neutrophil trafficking and quantified for their neutrophil, inflammatory monocyte and macrophage populations. In addition, this study highlights, for the first time, the use of a new multi-modal imaging technique which employs neutrophil-specific, fluorescent imaging agent, to monitor neutrophil trafficking *in vivo* simultaneously with luminescent *B. mallei* dissemination.

CpG treatment has resulted in the prolonged survival in an array of animal models infected with a variety of intracellular and extracellular pathogens such as *B. pseudomallei, B. mallei, Klebsiella pneumoniae Listeria monocytogenes, Yersinia pestis, Francisella tularensis, and mycobacteria* [103,106,145,146,149,152-154,174,175]. This protection is attributed to the rapid and early induction of innate immunity which provides increased resistance through controlling infection and lowering/preventing the dissemination of pathogens to target organs. Consistent with previous findings [103], class-C CpG treatment resulted in increased survival of BALB/c mice (Figure 15) with lowered and/or undetectable levels of *B. mallei* present in target organs (Figure 16). As expected with the selected infective dose (10^4 CFUs), the majority of PBS treated animals died on day 3 with 0% surviving on day 7 (Figure 15. Although some animals also died around day 3, protective effects of class-C CpG ODN treatment increased survival to 60% in BALB/c mice until the experiment was terminated on day 21. In parallel with the survival study, mice from each treatment group were sacrificed at different time points to assess the effect of class-C CpG treatment on bacterial load in the lungs, liver and spleen (Figure 16). Bacterial burden in all organs showed inverse trend in the mean values between class-C CpG treated and untreated groups as time progressed. From 24 to 72 h, bacterial burden in untreated BALB/c mice increases exponentially, whereas in class-C CpG-treated BALB/c mice the opposite effect is seen, with bacterial burden decreasing exponentially over time with the exception of the 48 h time point in the spleen, where bacterial burden seemed to increase slightly and then, in the case of two animals, decreased to undetectable levels. Consistently, class-C CpG displays the potential to decrease bacterial number by 6- to 7- logs as seen in all organs by 72 h post-infection. Our results indicated that increased survival in BALB/c mice may be attributed to class-C CpG ODNs ability to control infection in the lungs and/or prevent/reducing *B. mallei's* dissemination to target organs.

The use of CpG DNA with a variety of vaccines has improved protective immunity in many animal challenge models. CpG act as an immune adjuvant, accelerating and boosting cellular immune and antigen-specific antibody responses independent of the infecting pathogen [99,103,144,145,147-154,156-161,163-165,167,173-175]. In the absence of this influx, bacteria are able to multiply and disseminate freely until an appropriate immune response can be elicited, as was the case for the PBS-treated BALB/c mice. By the time an immune response was induced, the infection was too advanced, causing animals to eventually succumb to infection. Previous experiments on CpG treatment in models of *B. pseudomallei* infection attribute the rapid trafficking of neutrophils to protection [103,175]. As the primary antimicrobial effector cell of innate immunity, neutrophils serve as a first line of defense against pathogens that has infiltrated the body [175,176]. When an inflammatory response is initiated, neutrophils leave the circulatory system and migrate to the site of infection for containment and clearance of the invading pathogen. Classically, neutrophils are viewed as phagocytes that ingest microbes and kill them by different mechanisms [144,159]. Further, neutrophils also provide signals that play a role in innate immune system activation and function, which are important for communication with other innate immune cells (i.e., macrophages, DCs) and the adaptive immune system (T cells and B cells) [176,177].

Due to these characteristics and previous supporting evidence gathered with *B. pseudomallei* [103], neutrophil trafficking in response to *B. mallei* infection was observed and characterized. To accomplish this, a new technique for monitoring neutrophil trafficking *in vivo* in real time was optimized using a neutrophil-specific, fluorescent imaging agent. This reagent is a Cyanine7-conjugate, PEG-modified hexapeptide that specifically binds the formylpeptide receptor (FPR) of neutrophils [178]. The main novelty that comes from this experiment is the fact that the dye allows real time monitoring of neutrophils activation and trafficking. Because the dye is non-toxic and

the fluorescence signal corresponds to neutrophil number, the same animal can be monitored throughout the duration of the experiment, giving semi-quantitative data, which lowers the number of animals needed for an experiment and also negates the need for animal sacrifice when looking at neutrophil localization.

However, a more in depth look at the cell populations was taken, were the lungs of treatment groups at 0 (pre-infection) and 72 h post-infection were extracted and processed for flow cytometric analysis. In accordance with earlier studies [103] class-C CpG ODN pre-treatment in BALB/c mice resulted in a substantial increase in inflammatory monocytes at time zero vs. PBS-treated BALB/c mice (Figure 18C). Neutrophil numbers increased prior to infection due to CpG treatment (Figure 18D), which we had previously observed; this increase was not statistically different than PBS treated mice. The lack of differences in the number of events could be explained by sample timing. When optimizing the use of the Neutrophil-Specific, Fluorescent Imaging Agent, the highest fluorescence's intensity was observed 24 h after CpG treatment; thus, the 24 h pre-treatment time point was chosen for this assay. However, in previous studies of acute respiratory models of *B. pseudomallei* infection, where neutrophils numbers were higher in CpG treated mice vs. PBS treated mice at time zero, CpG treatment was administered 48 h before sampling. Thus, given our sampling time points, the window of detecting difference in the neutrophil numbers seen previously may have been missed. To assess class-C CpG treatment effect on lung architecture, histopathological lung sections were examined at 24, 48 and 72 h post-infection (Figure 19). In general, both treatment groups show the same types of inflammatory processes in the lung; although in the PBS treatment animals the pathology seems to be more severe (Figure 19A–C). At 24 h, lungs from class-C CpG ODN- and PBS-treated BALB/c mice (Figure 19A, D) show mild to moderate and moderate to focally severe, respectively, perivascular and peribronchial inflammation with a considerable neutrophilic component (Figure 20b). Interesting trends are noticed in both treatments. In the PBS-treatment, higher numbers of

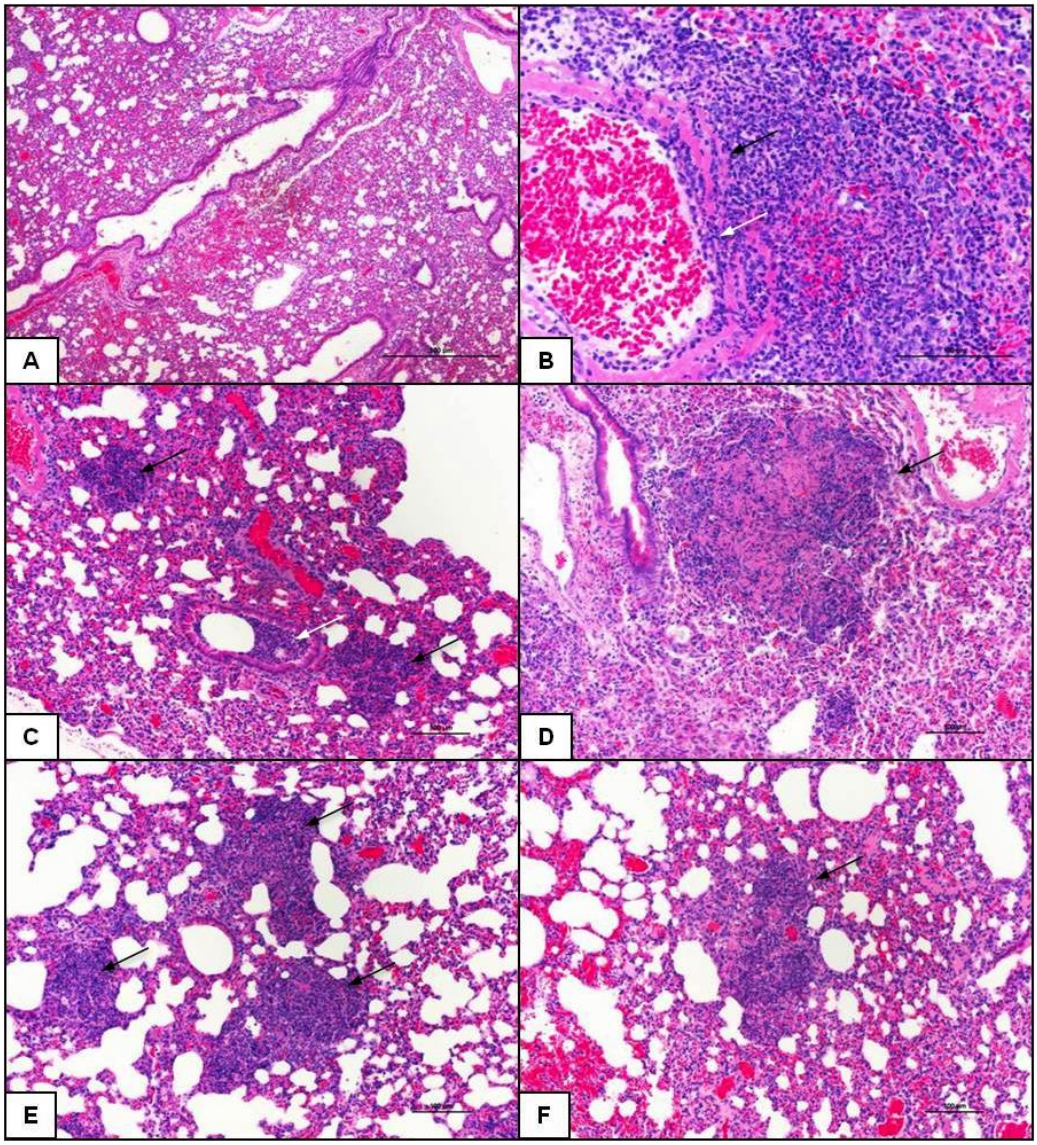

Figure 20: Representative examples of lung tissue pathology seen in infected BALB/c mice. Representative images of Hematoxylin and Eosin stained mouse lungs sections that highlight the following pathology: normal lung (A), Perivasculitis (black arrow) and vasculitis with neutrophil component (white arrow) (B), scattered microabscesses (black arrows) and cell debris in bronchial lumen with neutrophil component (white arrow) (C), areas of necrosis (black arrows) (D), microabscesses (black arrows) (E) and small necrotic foci (black arrow) (F). Magnification 40x and scale bar = 100 µM.

microabscesses are observed in the lungs at 48 h compared to 24h and 72 h. On the other hand, in class-C CpG ODN treated BALB/c mice; the highest number of microabscesses is observed at 24 h and progressively decreases at 48 and 72 h. This is supported by the

early recruitment of immune cells which kill and contain the infection early and thus negates the constant stimulation and influx of inflammatory cells [179]. Further, this would explain the higher number of clear air-sacs, reduction in microabscesses and inflammatory cells and tissue damage in class-C CpG ODN animals.

In conclusion, pre-treatment of CpG 24 h before CSM001 challenge, reduced bacteria burden and tissue damage in target organs which resulted in a 60% increase in protection compared to mock treated animals. This protection can be attributed to an increase in inflammatory monocytes and neutrophils, as illustrated by the successful implementation of a dye that allowed the simultaneous visualization of neutrophils and bacteria. The application of multi-modal imaging could provide a new novel tool for non-invasive monitoring of the dynamics of neutrophils accumulation in the lung over time following induction of infection. This additional capability could prove to be highly valuable as we work toward developing therapeutic interventions for the treatment of *Burkholderia* respiratory infections.

Conclusions and Future Directions

The goal of this study was to generate a vaccine that could cross protect and provide sterile immunity against *B. mallei* and *B. pseudomallei* infection. To achieve this goal, I generated a *B. mallei* Δ*tonB* mutant that is attenuated in growth, *in vivo* colonization and virulence when tested in murine models of respiratory glanders. When evaluated as a vaccine, the *B. mallei* Δ*tonB* mutant provided 100% protected that resulted in wild-type clearance in vaccinated mice challenged with a lethal dose of wild-type *B. mallei*. The *B. mallei* Δ*tonB* mutant was also able to provide substantial cross protection to vaccinated mice challenge with a lethal dose of *B. pseudomallei*. Evaluating the protection generated by *B. mallei* Δ*tonB* mutant vaccination, immunized mice had significantly increased levels of *B. mallei* specific IgG1, IgG2 and IgM. In *Burkholderia* infected subjects, both animal and human, increased serum IgG1, IgG2 and IgM levels has been associated with localized infection, increased protection and an overall better prognosis of survival. These results are consistent with the histopathology data that show more localized and less severe pathology the lungs, liver and spleen of wild-type challenged mice previously vaccinated with the *B. mallei* Δ*tonB* mutant vs. mice vaccinated with PBS. In agreement with these results, the cytokine/chemokine profiles of mice challenge with wild-type *B. mallei* show higher levels of inflammatory analytes in the PBS mice vaccinated animals vs. *B. mallei* Δ*tonB* mutant vaccinated animals that showed high levels of IL-12, a cytokine extensively reported in the literature for its ability to control pathogen growth and dissemination, and to provide protection.

The *B. mallei* Δ*tonB* mutant has showed great potential as a vaccine candidate against *B. mallei* and *B. pseudomallei* infection. However, it does have a few drawbacks that can be addressed with further optimization. In addition to the draw backs that plague every live attenuated vaccine, such as concerns about wild-type reversion and use on the immunocompromised, the *B. mallei* Δ*tonB* mutant is unique in the fact that it shows long

term persistence. All live attenuated vaccines candidate developed for glanders and melioidosis have attributed the failure to fully protect, particularly in the chronic phase, to the rapid clearance of the organism from the host. Based on these conclusions, long-term persistence of the *B. mallei* Δ*tonB* mutant may play a huge role in generating protective immunity. For example, the long term persistence may increase the immune systems exposure to protective antigen or lead to the periodic elicitation of protective immunity, which may result in immune memory and generation of an enhanced, educated immune response 100% effective in fighting wild-type infection. Although to reduce the probability of chronic infection, the *B. mallei* Δ*tonB* mutant's long-term persistence must be addressed. To create a *B. mallei* Δ*tonB* mutant that can persist short term, additional mutations must introduced. Recently, *B. mallei* Δ*tonB* Δ*hcp1* double mutant was generated to reduce not only probability of reversion but also persistence. In the chance that this double mutant does not produce expected outcome, I believe future studies should include the comparison of *B. mallei* gene expression under iron rich and iron depleted conditions. From these results we can down select our gene targets for mutagenesis by choosing those most up-regulate under iron depleted conditions. Furthermore, I believe different routes and approaches to vaccination must be considered. Alternative administration, such as i.p or s.c., of the *B. mallei* Δ*tonB* mutant could result in decreased persistence. In the case that the introduction of an additional mutation into the *B. mallei* Δ*tonB* mutant results in reduced protection, I think it's important to investigate a prime-boost vaccination strategy or us a two-pronged approach in which vaccination consist of a combination of two routes of immunization. For example, a vaccine regiment that incorporated both i.n. and s.c. immunizations may see great protection locally and systemically. Overall, I believe this work represent a good starting point in which the *B. mallei* Δ*tonB* mutant could be further optimized to become an effective vaccine for glanders and melioidosis.

References

1. Neubauer H, Sprague LD, Zacharia R, Tomaso H, Al Dahouk S, et al. (2005) Serodiagnosis of *Burkholderia mallei* infections in horses: state-of-the-art and perspectives. J Vet Med B Infect Dis Vet Public Health 52: 201-205.
2. Whitlock GC, Estes DM, Torres AG (2007) Glanders: off to the races with *Burkholderia mallei*. FEMS Microbiol Lett 277: 115-122.
3. Brett PJ, Woods DE (2000) Pathogenesis of and immunity to melioidosis. Acta Trop 74: 201-210.
4. Cheng AC, Currie BJ (2005) Melioidosis: epidemiology, pathophysiology, and management. Clin Microbiol Rev 18: 383-416.
5. Dance DA (2000) Melioidosis as an emerging global problem. Acta Trop 74: 115-119.
6. Lehavi O, Aizenstien O, Katz LH, Hourvitz A (2002) Glanders - a potential disease for biological warfare in humans and animals. Harefuah 141: 88-91.
7. Arun S, Neubauer H, Gürel A, Ayyildiz G, Kusçu B, et al. (1999) Equine glanders in turkey. Vet Rec 144: 255-258.
8. Neubauer H, L. D. Sprague, R. Zacharia, H. Tomaso, S. Al Dahouk, R. Wernery, U. Wernery, and H. C. Scholz. (2005) Serodiagnosis of *Burkholderia mallei* infections in horses: state-of-the-art and perspectives. J Vet Med B Infect Dis Vet Public Health 52: 201-205.
9. Peacock SJ (2006) Melioidosis. Curr Opin Infect Dis 19: 421-428.
10. Chaowagul W, White NJ, Dance DA, Wattanagoon Y, Naigowit P, et al. (1989) Melioidosis: a major cause of community-acquired septicemia in northeastern Thailand. J Infect Dis 159: 890-899.
11. Chierakul W, Winothai W, Wattanawaitunechai C, Wuthiekanun V, Rugtaengan T, et al. (2005) Melioidosis in 6 tsunami survivors in southern Thailand. Clin Infect Dis 41: 982-990.
12. Pruekprasert P, Jitsurong S (1991) Case report: septicemic melioidosis following near drowning. Southeast Asian J Trop Med Public Health 22: 276-278.
13. Currie BJ, Jacups SP (2003) Intensity of rainfall and severity of melioidosis, Australia. Emerg Infect Dis 9: 1538-1542.
14. Wiersinga WJ, van der Poll T, White NJ, Day NP, Peacock SJ (2006) Melioidosis: insights into the pathogenicity of *Burkholderia pseudomallei*. Nat Rev Microbiol 4: 272-282.
15. White NJ (2003) Melioidosis. Lancet, 361: 1715-1722.
16. Srinivasan A, Kraus CN, DeShazer D, Becker PM, Dick JD, et al. (2001) Glanders in a military research microbiologist. N Engl J Med 345: 256-258.
17. Mandell GL, Douglas RG, Bennett JE (1995) Mandell, Douglas and Bennett's principles and practice of infectious diseases. New York: Churchill Livingstone.
18. Kenny DJ, Russell P, Rogers D, Eley SM, Titball RW (1999) In vitro susceptability of *Burkholderia mallei* in comparison to those of other pathogenic *Burkholderia* spp. Antimicrob Agents Chemother 43: 2773-2775.
19. Leelarasamee A (2004) Recent development in melioidosis. Curr Opin Infect Dis 17: 131-136.

20. Mekalanos JJ (1992) Environmental signals controlling expression of virulence determinants in bacteria. J Bacteriol 174: 1-7.
21. Nierman WC, DeShazer D, Kim HS, Tettelin H, Nelson KE, et al. (2004) Structural flexibility in the *Burkholderia mallei* genome. Proc Natl Acad Sci U S A 101: 14246-14251.
22. Woods DE, DeShazer D, Moore RA, Brett PJ, Burtnick MN, et al. (1999) Current studies on the pathogenesis of melioidosis. Microbes Infect 1: 157-162.
23. Woods DE, Jones AL, Hill PJ (1993) Interaction of insulin with *Pseudomonas pseudomallei*. Infect Immun 61: 4045-4050.
24. Pier G (2004) Vaccines and vaccination. In: Pier GB LJ, Wetzler LM, editor. Immunology, Infection, and Immunity. DC, USA: ASM Press. pp. 497-528.
25. Amemiya K, Bush GV, DeShazer D, Waag DM (2002) Nonviable *Burkholderia mallei* induces a mixed Th1- and Th2-like cytokine response in BALB/c mice. Infect Immun 70: 2319-2325.
26. Sarkar-Tyson M, Smither SJ, Harding SV, Atkins TP, Titball RW (2009) Protective efficacy of heat-inactivated *B. thailandensis*, *B. mallei* or *B. pseudomallei* against experimental melioidosis and glanders. Vaccine 27: 4447-4451.
27. Sarkar-Tyson M, Thwaite JE, Harding SV, Smither SJ, Oyston PC, et al. (2007) Polysaccharides and virulence of *Burkholderia pseudomallei*. J Med Microbiol 56: 1005-1010.
28. Reckseidler S, DeShazer D, Sokol PA, Woods DE (2001) Detection of bacterial virulence genes by subtractive hybridisation: Identification of capsular polysaccharide of *Burkholderia pseudomallei* as a major virulence determinant. Infect Immun 69: 34-44.
29. DeShazer D, Brett PJ, Woods DE (1998) The type II O-antigenic polysaccharide moiety of *Burkholderia pseudomallei* lipopolysaccharide is required for serum resistance and virulence. Mol Microbiol 30: 1081-1100.
30. Atkins T, Prior R, Mack K, Russell P, Nelson M, et al. (2002) Characterisation of an acapsular mutant of *Burkholderia pseudomallei* identified by signature tagged mutagenesis. J Med Microbiol 51: 539-547.
31. Atkins T, Prior RG, Mack K, Russell P, Nelson M, et al. (2002) A mutant of *Burkholderia pseudomallei,* auxotrophic in the branched chain amino acid biosynthetic pathway, is attenuated and protective in a murine model of melioidosis. Infect Immun 70: 5290-5294.
32. Rodrigues F, Sarkar-Tyson M, Harding SV, Sim SH, Chua HH, et al. (2006) Global map of growth-regulated gene expression in *Burkholderia pseudomallei*, the causative agent of melioidosis. J Bacteriol 188: 8178-8188.
33. Haque A, Chu K, Easton A, Stevens MP, Galyov EE, et al. (2006) A live experimental vaccine against *Burkholderia pseudomallei* elicits CD4+ T cell-mediated immunity, priming T cells specific for 2 type III secretion system proteins. J Infect Dis 194: 1241-1248.
34. Ulrich RL, Amemiya K, Waag DM, Roy CJ, DeShazer D (2005) Aerogenic vaccination with a *Burkholderia mallei* auxotroph protects against aerosol-initiated glanders in mice. Vaccine 23: 1986-1992.

35. Cuccui J, Easton A, Chu KK, Bancroft GJ, Oyston PC, et al. (2007) Development of signature-tagged mutagenesis in *Burkholderia pseudomallei* to identify genes important in survival and pathogenesis. Infect Immun 75: 1186-1195.
36. Breitbach K, Kohler J, Steinmetz I (2008) Induction of protective immunity against *Burkholderia pseudomallei* using attenuated mutants with defects in the intracellular life cycle. Trans R Soc Trop Med Hyg 102 Suppl 1: S89-94.
37. Ulett GC, Labrooy JT, Currie BJ, Barnes JL, Ketheesan N (2005) A model of immunity to *Burkholderia pseudomallei*: unique responses following immunization and acute lethal infection. Microbes Infect 7: 1263-1275.
38. Barnes JL, Ketheesan N (2007) Development of protective immunity in a murine model of melioidosis is influenced by the source of *Burkholderia pseudomallei* antigens. Immunol Cell Biol 85: 551-557.
39. Healey GD, Elvin SJ, Morton M, Williamson ED (2005) Humoral and cell-mediated adaptive immune responses are required for protection against *Burkholderia pseudomallei* challenge and bacterial clearance postinfection. Infect Immun 73: 5945-5951.
40. Liu B, Koo GC, Yap EH, Chua KL, Gan YH (2002) Model of differential susceptibility to mucosal *Burkholderia pseudomallei* infection. Infect Immun 70: 504-511.
41. Stevens MP, Friebel A, Taylor LA, Wood MW, Brown PJ, et al. (2003) A *Burkholderia pseudomallei* type III secreted protein, BopE, facilitates bacterial invasion of epithelial cells and exhibits guanine nucleotide exchange factor activity. J Bacteriol 185: 4992-4996.
42. Norris MH, Propst KL, Kang Y, Dow SW, Schweizer HP, et al. (2011) The *Burkholderia pseudomallei* Delt*aasd* mutant exhibits attenuated intracellular infectivity and imparts protection against acute inhalation melioidosis in mice. Infect Immun 79: 4010-4018.
43. Silva EB, Goodyear A, Sutherland MD, Podnecky NL, Gonzalez-Juarrero M, et al. (2013) Correlates of immune protection following cutaneous immunization with an attenuated *Burkholderia pseudomallei* vaccine. Infect Immun 81: 4626-4634.
44. Propst KL, Mima T, Choi KH, Dow SW, Schweizer HP (2010) A *Burkholderia pseudomallei* delta*purM* mutant is avirulent in immunocompetent and immunodeficient animals: candidate strain for exclusion from select-agent lists. Infect Immun 78: 3136-3143.
45. Rich JR, Withers SG (2009) Emerging methods for the production of homogeneous human glycoproteins. Nat Chem Biol 5: 206-215.
46. Amemiya K, Meyers JL, Trevino SR, Chanh TC, Norris SL, et al. (2006) Interleukin-12 induces a Th1-like response to *Burkholderia mallei* and limited protection in BALB/c mice. Vaccine 24: 1413-1420.
47. Amemiya K, Meyers JL, Trevino SR, Chanh TC, Norris SL, et al. (2006) Interleukin-12 induces a Th1-like response to *Burkholderia mallei* and limited protection in BALB/c mice. Vaccine 24: 1413-1420.
48. Waag DM, McCluskie MJ, Zhang N, Krieg AM (2006) A CpG oligonucleotide can protect mice from a low aerosol challenge dose of *Burkholderia mallei*. Infect Immun 74: 1944-1948.

49. Goodyear A, Kellihan L, Bielefeldt-Ohmann H, Troyer R, Propst K, et al. (2009) Protection from pneumonic infection with *Burkholderia* species by inhalational immunotherapy. Infect Immun 77: 1579-1588.
50. Atkins T, Prior RG, Mack K, Russell P, Nelson M, et al. (2002) A mutant of *Burkholderia pseudomallei,* auxotrophic in the branched chain amino acid biosynthetic pathway, is attenuated and protective in a murine model of melioidosis. Infect Immun 70: 5290-5294.
51. Ulrich RL, Amemiya K, Waag DM, Roy CJ, DeShazer D (2005) Aerogenic vaccination with a *Burkholderia mallei* auxotroph protects against aerosol-initiated glanders in mice. Vaccine 23: 1986-1992.
52. Haque A, Easton A, Smith D, O'Garra A, Van Rooijen N, et al. (2006) Role of T cells in innate and adaptive immunity against murine *Burkholderia pseudomallei* infection. J Infect Dis 193: 370-379.
53. Haque A, Chu K, Easton A, Stevens MP, Galyov EE, et al. (2006) A live experimental vaccine against *Burkholderia pseudomallei* elicits CD4+ T cell-mediated immunity, priming T cells specific for 2 type III secretion system proteins. J Infect Dis 194: 1241-1248.
54. DeShazer D, Waag DM, Fritz DL, Woods DE (2001) Identification of a *Burkholderia mallei* polysaccharide gene cluster by subtractive hybridization and demonstration that the encoded capsule is an essential virulence determinant. Microb Pathog 30: 253-269.
55. Lopez J, Copps J, Wilhelmsen C, Moore R, Kubay J, et al. (2003) Characterization of experimental equine glanders. Microbes Infect 5: 1125-1131.
56. Ulrich RL, Deshazer D, Brueggemann EE, Hines HB, Oyston PC, et al. (2004) Role of quorum sensing in the pathogenicity of *Burkholderia pseudomallei*. J Med Microbiol 53: 1053-1064.
57. Ulrich RL, Deshazer D, Hines HB, Jeddeloh JA (2004) Quorum sensing: a transcriptional regulatory system involved in the pathogenicity of *Burkholderia mallei*. Infect Immun 72: 6589-6596.
58. Valade E, Thibault FM, Gauthier YP, Palencia M, Popoff MY, et al. (2004) The PmlI-PmlR quorum-sensing system in *Burkholderia pseudomallei* plays a key role in virulence and modulates production of the MprA protease. J Bacteriol 186: 2288-2294.
59. Ulrich RL, DeShazer D (2004) Type III secretion: a virulence factor delivery system essential for the pathogenicity of *Burkholderia mallei*. Infect Immun 72: 1150-1154.
60. Schell MA, Ulrich RL, Ribot WJ, Brueggemann EE, Hines HB, et al. (2007) Type VI secretion is a major virulence determinant in *Burkholderia mallei*. Mol Microbiol 64: 1466-1485.
61. Kim HS, Schell MA, Yu Y, Ulrich RL, Sarria SH, et al. (2005) Bacterial genome adaptation to niches: divergence of the potential virulence genes in three *Burkholderia* species of different survival strategies. BMC Genomics 6: 174.
62. Braun V (2005) Bacterial iron transport related to virulence. Contrib Microbiol 12: 210-233.
63. Tuanyok A, Kim HS, Nierman WC, Yu Y, Dunbar J, et al. (2005) Genome-wide expression analysis of iron regulation in *Burkholderia pseudomallei* and

Burkholderia mallei using DNA microarrays. FEMS Microbiol Lett 252: 327-335.
64. Schmitt MP, Holmes RK (1991) Iron-dependent regulation of diphtheria toxin and siderophore expression by the cloned *Corynebacterium diphtheriae* repressor gene *dtxR* in *C. diphtheriae* C7 strains. Infect Immun 59: 1899-1904.
65. Goldberg MB, Boyko SA, Calderwood SB (1990) Transcriptional regulation by iron of a *Vibrio cholerae* virulence gene and homology of the gene to the *Escherichia coli* fur system. J Bacteriol 172: 6863-6870.
66. Storey DG, Frank DW, Farinha MA, Kropinski AM, Iglewski BH (1990) Multiple promoters control the regulation of the *Pseudomonas aeruginosa regA* gene. Mol Microbiol 4: 499-503.
67. Bagg A, Neilands JB (1987) Molecular mechanism of regulation of siderophore-mediated iron assimilation. Microbiol Rev 51: 509-518.
68. Crichton RR, Charloteaux-Wauters M (1987) Iron transport and storage. Eur J Biochem 164: 485-506.
69. Letain TE, Postle K (1997) TonB protein appears to transduce energy by shuttling between the cytoplasmic membrane and the outer membrane in *Escherichia coli*. Mol Microbiol 24: 271-283.
70. Braun V (2001) Iron uptake mechanisms and their regulation in pathogenic bacteria. Int J Med Microbiol 291: 67-79.
71. Weinberg ED (1984) Iron withholding: a defense against infection and neoplasia. Physiol Rev 64: 65-102.
72. Aisen P, Leibman A, Zweier J (1978) Stoichiometric and site characteristics of the binding of iron to human transferrin. J Biol Chem 253: 1930-1937.
73. Martin RB, Savory J, Brown S, Bertholf RL, Wills MR (1987) Transferrin binding of Al^{3+} and Fe^{3+}. Clin Chem 33: 405-407.
74. Kretchmar SA, Reyes ZE, Raymond KN (1988) The spectroelectrochemical determination of the reduction potential of diferric serum transferrin. Biochim Biophys Acta 956: 85-94.
75. Braun V, Braun M (2002) Active transport of iron and siderophore antibiotics. Curr Opin Microbiol 5: 194-201.
76. Kadner RJ, Heller KJ (1995) Mutual inhibition of cobalamin and siderophore uptake systems suggests their competition for TonB function. J Bacteriol 177: 4829-4835.
77. Postle K (1993) TonB protein and energy transduction between membranes. J Bioenerg Biomembr 25: 591-601.
78. Larsen RA, Myers PS, Skare JT, Seachord CL, Darveau RP, et al. (1996) Identification of TonB homologs in the family Enterobacteriaceae and evidence for conservation of TonB-dependent energy transduction complexes. J Bacteriol 178: 1363-1373.
79. Stojiljkovic I, Srinivasan N (1997) *Neisseria meningitidis tonB, exbB,* and *exbD* genes: Ton-dependent utilization of protein-bound iron in *Neisseriae*. J Bacteriol 179: 805-812.
80. Braun V (1995) Energy-coupled transport and signal transduction through the gram-negative outer membrane via TonB-ExbB-ExbD-dependent receptor proteins. FEMS Microbiol Rev 16: 295-307.

81. Postle K, Kadner RJ (2003) Touch and go: tying TonB to transport. Mol Microbiol 49: 869-882.
82. Alvarez B, Alvarez J, Menendez A, Guijarro JA (2008) A mutant in one of two *exbD* loci of a TonB system in *Flavobacterium psychrophilum* shows attenuated virulence and confers protection against cold water disease. Microbiology 154: 1144-1151.
83. Seliger SS, Mey AR, Valle AM, Payne SM (2001) The two TonB systems of *Vibrio cholerae*: redundant and specific functions. Mol Microbiol 39: 801-812.
84. Gorbacheva VY, Faundez G, Godfrey HP, Cabello FC (2001) Restricted growth of *ent*(-) and *tonB* mutants of *Salmonella* enterica serovar Typhi in human Mono Mac 6 monocytic cells. FEMS Microbiol Lett 196: 7-11.
85. Henderson DP, Payne SM (1994) *Vibrio cholerae* iron transport systems: roles of heme and siderophore iron transport in virulence and identification of a gene associated with multiple iron transport systems. Infect Immun 62: 5120-5125.
86. Hsieh PF, Lin TL, Lee CZ, Tsai SF, Wang JT (2008) Serum-induced iron-acquisition systems and TonB contribute to virulence in *Klebsiella pneumoniae* causing primary pyogenic liver abscess. J Infect Dis 197: 1717-1727.
87. Jarosik GP, Sanders JD, Cope LD, Muller-Eberhard U, Hansen EJ (1994) A functional *tonB* gene is required for both utilization of heme and virulence expression by *Haemophilus influenzae* type b. Infect Immun 62: 2470-2477.
88. Pradel E, Guiso N, Menozzi FD, Locht C (2000) *Bordetella pertussis* TonB, a Bvg-independent virulence determinant. Infect Immun 68: 1919-1927.
89. Reeves SA, Torres AG, Payne SM (2000) TonB is required for intracellular growth and virulence of *Shigella dysenteriae*. Infect Immun 68: 6329-6336.
90. Takase H, Nitanai H, Hoshino K, Otani T (2000) Requirement of the *Pseudomonas aeruginosa tonB* gene for high-affinity iron acquisition and infection. Infect Immun 68: 4498-4504.
91. Torres AG, Payne SM (1997) Haem iron-transport system in enterohaemorrhagic *Escherichia coli* O157:H7. Mol Microbiol 23: 825-833.
92. Torres AG, Redford P, Welch RA, Payne SM (2001) TonB-dependent systems of uropathogenic *Escherichia coli*: aerobactin and heme transport and TonB are required for virulence in the mouse. Infect Immun 69: 6179-6185.
93. Tsolis RM, Baumler AJ, Heffron F, Stojiljkovic I (1996) Contribution of TonB- and Feo-mediated iron uptake to growth of *Salmonella typhimurium* in the mouse. Infect Immun 64: 4549-4556.
94. Beddek AJ, Sheehan BJ, Bosse JT, Rycroft AN, Kroll JS, et al. (2004) Two TonB systems in *Actinobacillus pleuropneumoniae*: their roles in iron acquisition and virulence. Infect Immun 72: 701-708.
95. Enard C, Expert D (2000) Characterization of a *tonB* mutation in *Erwinia chrysanthemi* 3937: TonB(Ech) is a member of the enterobacterial TonB family. Microbiology 146 (Pt 8): 2051-2058.
96. Hamad MA, Zajdowicz SL, Holmes RK, Voskuil MI (2009) An allelic exchange system for compliant genetic manipulation of the select agents *Burkholderia pseudomallei* and *Burkholderia mallei*. Gene 430: 123-131.
97. Yabuuchi E, Kosako Y, Oyaizu H, Yano I, Hotta H, et al. (1992) Proposal of *Burkholderia* gen. nov. and transfer of seven species of the genus *Pseudomonas*

homology group II to the new genus, with the type species *Burkholderia cepacia* (Palleroni and Holmes 1981) comb. nov. Microbiol Immunol 36: 1251-1275.
98. Holden MT, Titball RW, Peacock SJ, Cerdeno-Tarraga AM, Atkins T, et al. (2004) Genomic plasticity of the causative agent of melioidosis, *Burkholderia pseudomallei*. Proc Natl Acad Sci U S A 101: 14240-14245.
99. Massey S, Johnston K, Mott TM, Judy BM, Kvitko BH, et al. (2011) In vivo Bioluminescence Imaging of *Burkholderia mallei* Respiratory Infection and Treatment in the Mouse Model. Front Microbiol 2: 174.
100. Simon R, Priefer, U., Puhler, A. (1983) Broad Host Range Mobilization System for *In Vivo* Genetic Engineering: Transposon Mutagenesis in Gram Negative Bacteria. Nat Biotech 1: 8.
101. Alexander DB, Zuberer DA (1991) Use of chrome azurol S reagents to evaluate siderophore production by rhizosphere bacteria. Biology and Fertility of Soils 12: 39-45.
102. Massey S, Yeager LA, Blumentritt CA, Vijayakumar S, Sbrana E, et al. (2014) Comparative *Burkholderia pseudomallei* natural history virulence studies using an aerosol murine model of infection. Sci Rep 4: 4305.
103. Judy BM, Taylor K, Deeraksa A, Johnston RK, Endsley JJ, et al. (2012) Prophylactic application of CpG oligonucleotides augments the early host response and confers protection in acute melioidosis. PLoS One 7: e34176.
104. Massey S, Johnston K, Mott TM, Judy BM, Kvitko BH, et al. (2011) In vivo Bioluminescence Imaging of *Burkholderia mallei* Respiratory Infection and Treatment in the Mouse Model. Front Microbiol 2: 174.
105. Mott TM, Johnston RK, Vijayakumar S, Estes DM, Motamedi M, et al. (2013) Monitoring Therapeutic Treatments against Infections Using Imaging Techniques. Pathogens 2: 383-401.
106. Bondi SK, Goldberg JB (2008) Strategies toward vaccines against *Burkholderia mallei* and *Burkholderia pseudomallei*. Expert Rev Vaccines 7: 1357-1365.
107. Schell MA, Lipscomb L, DeShazer D (2008) Comparative genomics and an insect model rapidly identify novel virulence genes of *Burkholderia mallei*. J Bacteriol 190: 2306-2313.
108. Skaar EP (2010) The battle for iron between bacterial pathogens and their vertebrate hosts. PLoS Pathog 6: e1000949.
109. Sritharan M (2006) Iron and bacterial virulence. Indian J Med Microbiol 24: 163-164.
110. Griffiths E (1991) Iron and bacterial virulence--a brief overview. Biol Met 4: 7-13.
111. Wooldridge KG, Williams PH (1993) Iron uptake mechanisms of pathogenic bacteria. FEMS Microbiol Rev 12: 325-348.
112. Kvitko BH, Goodyear A, Propst KL, Dow SW, Schweizer HP (2012) Burkholderia pseudomallei known siderophores and hemin uptake are dispensable for lethal murine melioidosis. PLoS Negl Trop Dis 6: e1715.
113. Silva EB, Dow SW (2013) Development of *Burkholderia mallei* and *pseudomallei* vaccines. Front Cell Infect Microbiol 3: 10.
114. Thomas MG, O'Toole GA, Escalante-Semerena JC (1999) Molecular characterization of *eutF* mutants of *Salmonella typhimurium* LT2 identifies eutF lesions as partial-loss-of-function *tonB* alleles. J Bacteriol 181: 368-374.

115. Ochsner UA, Wilderman PJ, Vasil AI, Vasil ML (2002) GeneChip expression analysis of the iron starvation response in *Pseudomonas aeruginosa*: identification of novel pyoverdine biosynthesis genes. Mol Microbiol 45: 1277-1287.
116. Wexler M, Yeoman KH, Stevens JB, de Luca NG, Sawers G, et al. (2001) The *Rhizobium leguminosarum tonB* gene is required for the uptake of siderophore and haem as sources of iron. Mol Microbiol 41: 801-816.
117. Wiggerich HG, Klauke B, Koplin R, Priefer UB, Puhler A (1997) Unusual structure of the *tonB-exb* DNA region of *Xanthomonas campestris* pv. campestris: *tonB*, *exbB*, and *exbD1* are essential for ferric iron uptake, but *exbD2* is not. J Bacteriol 179: 7103-7110.
118. Wiggerich HG, Puhler A (2000) The *exbD2* gene as well as the iron-uptake genes *tonB*, *exbB* and *exbD1* of *Xanthomonas campestris* pv. campestris are essential for the induction of a hypersensitive response on pepper (Capsicum annuum). Microbiology 146 (Pt 5): 1053-1060.
119. Lesuisse E, Knight SA, Courel M, Santos R, Camadro JM, et al. (2005) Genome-wide screen for genes with effects on distinct iron uptake activities in *Saccharomyces cerevisiae*. Genetics 169: 107-122.
120. Gauthier GM, Sullivan TD, Gallardo SS, Brandhorst TT, Vanden Wymelenberg AJ, et al. (2010) SREB, a GATA transcription factor that directs disparate fates in *Blastomyces dermatitidis* including morphogenesis and siderophore biosynthesis. PLoS Pathog 6: e1000846.
121. Zhou LW, Haas H, Marzluf GA (1998) Isolation and characterization of a new gene, sre, which encodes a GATA-type regulatory protein that controls iron transport in *Neurospora crassa*. Mol Gen Genet 259: 532-540.
122. Ho M, Schollaardt T, Smith MD, Perry MB, Brett PJ, et al. (1997) Specificity and functional activity of anti-*Burkholderia pseudomallei* polysaccharide antibodies. Infect Immun 65: 3648-3653.
123. Zhang S, Feng SH, Li B, Kim HY, Rodriguez J, et al. (2011) *In Vitro* and *In Vivo* studies of monoclonal antibodies with prominent bactericidal activity against *Burkholderia pseudomallei* and *Burkholderia mallei*. Clin Vaccine Immunol 18: 825-834.
124. Crump JA, Reller LB (2003) Two decades of disseminated tuberculosis at a university medical center: the expanding role of mycobacterial blood culture. Clin Infect Dis 37: 1037-1043.
125. Pandey V, Rao SP, Rao S, Acharya KK, Chhabra SS (2010) *Burkholderia pseudomallei* musculoskeletal infections (melioidosis) in India. Indian J Orthop 44: 216-220.
126. von Reyn CF, Kimambo S, Mtei L, Arbeit RD, Maro I, et al. (2011) Disseminated tuberculosis in human immunodeficiency virus infection: ineffective immunity, polyclonal disease and high mortality. Int J Tuberc Lung Dis 15: 1087-1092.
127. Ehlers S, Mielke ME, Blankenstein T, Hahn H (1992) Kinetic analysis of cytokine gene expression in the livers of naive and immune mice infected with *Listeria monocytogenes*. The immediate early phase in innate resistance and acquired immunity. J Immunol 149: 3016-3022.

128. Xiong H, Kawamura I, Nishibori T, Mitsuyama M (1994) Cytokine gene expression in mice at an early stage of infection with various strains of *Listeria* spp. differing in virulence. Infect Immun 62: 3649-3654.
129. Iizawa Y, Brown JF, Czuprynski CJ (1992) Early expression of cytokine mRNA in mice infected with *Listeria monocytogenes*. Infect Immun 60: 4068-4073.
130. Golovliov I, Sandstrom G, Ericsson M, Sjostedt A, Tarnvik A (1995) Cytokine expression in the liver during the early phase of murine tularemia. Infect Immun 63: 534-538.
131. Ulett GC, Ketheesan N, Hirst RG (2000) Cytokine gene expression in innately susceptible BALB/c mice and relatively resistant C57BL/6 mice during infection with virulent *Burkholderia pseudomallei*. Infect Immun 68: 2034-2042.
132. Ulett GC, Ketheesan N, Hirst RG (2000) Proinflammatory cytokine mRNA responses in experimental *Burkholderia pseudomallei* infection in mice. Acta Trop 74: 229-234.
133. Simpson AJ, Smith MD, Weverling GJ, Suputtamongkol Y, Angus BJ, et al. (2000) Prognostic value of cytokine concentrations (tumor necrosis factor-alpha, interleukin-6, and interleukin-10) and clinical parameters in severe melioidosis. J Infect Dis 181: 621-625.
134. Friedland JS, Suputtamongkol Y, Remick DG, Chaowagul W, Strieter RM, et al. (1992) Prolonged elevation of interleukin-8 and interleukin-6 concentrations in plasma and of leukocyte interleukin-8 mRNA levels during septicemic and localized *Pseudomonas pseudomallei* infection. Infect Immun 60: 2402-2408.
135. Wiersinga WJ, Dessing MC, Kager PA, Cheng AC, Limmathurotsakul D, et al. (2007) High-throughput mRNA profiling characterizes the expression of inflammatory molecules in sepsis caused by *Burkholderia pseudomallei*. Infect Immun 75: 3074-3079.
136. Contassot E, Beer HD, French LE (2012) Interleukin-1, inflammasomes, autoinflammation and the skin. Swiss Med Wkly 142: w13590.
137. Ceballos-Olvera I, Sahoo M, Miller MA, Del Barrio L, Re F (2011) Inflammasome-dependent pyroptosis and IL-18 protect against *Burkholderia pseudomallei* lung infection while IL-1beta is deleterious. PLoS Pathog 7: e1002452.
138. Caldwell J, Emerson SG (1994) IL-1 alpha and TNF alpha act synergistically to stimulate production of myeloid colony-stimulating factors by cultured human bone marrow stromal cells and cloned stromal cell strains. J Cell Physiol 159: 221-228.
139. Rincon M (2012) Interleukin-6: from an inflammatory marker to a target for inflammatory diseases. Trends Immunol 33: 571-577.
140. Biswas P, Delfanti F, Bernasconi S, Mengozzi M, Cota M, et al. (1998) Interleukin-6 induces monocyte chemotactic protein-1 in peripheral blood mononuclear cells and in the U937 cell line. Blood 91: 258-265.
141. Nagabhushanam V, Solache A, Ting LM, Escaron CJ, Zhang JY, et al. (2003) Innate inhibition of adaptive immunity: *Mycobacterium tuberculosis*-induced IL-6 inhibits macrophage responses to IFN-gamma. J Immunol 171: 4750-4757.
142. Mondal S, Roy A, Pahan K (2009) Functional blocking monoclonal antibodies against IL-12p40 homodimer inhibit adoptive transfer of experimental allergic encephalomyelitis. J Immunol 182: 5013-5023.

143. Scott AE, Laws TR, D'Elia RV, Stokes MG, Nandi T, et al. (2013) Protection against experimental melioidosis following immunization with live *Burkholderia thailandensis* expressing a manno-heptose capsule. Clin Vaccine Immunol 20: 1041-1047.
144. Becker Y (2005) CpG ODNs treatments of HIV-1 infected patients may cause the decline of transmission in high risk populations - a review, hypothesis and implications. Virus Genes 30: 251-266.
145. Deng JC, Moore TA, Newstead MW, Zeng X, Krieg AM, et al. (2004) CpG oligodeoxynucleotides stimulate protective innate immunity against pulmonary *Klebsiella* infection. J Immunol 173: 5148-5155.
146. Hickey AJ, Lin JS, Kummer LW, Szaba FM, Duso DK, et al. (2013) Intranasal prophylaxis with CpG oligodeoxynucleotide can protect against *Yersinia pestis* infection. Infect Immun 81: 2123-2132.
147. Klinman DM, Conover J, Coban C (1999) Repeated administration of synthetic oligodeoxynucleotides expressing CpG motifs provides long-term protection against bacterial infection. Infect Immun 67: 5658-5663.
148. Pun PB, Bhat AA, Mohan T, Kulkarni S, Paranjape R, et al. (2009) Intranasal administration of peptide antigens of HIV with mucosal adjuvant CpG ODN coentrapped in microparticles enhances the mucosal and systemic immune responses. Int Immunopharmacol 9: 468-477.
149. Ray NB, Krieg AM (2003) Oral pretreatment of mice with CpG DNA reduces susceptibility to oral or intraperitoneal challenge with virulent Listeria monocytogenes. Infect Immun 71: 4398-4404.
150. Yamaguchi Y, Harker JA, Wang B, Openshaw PJ, Tregoning JS, et al. (2012) Preexposure to CpG protects against the delayed effects of neonatal respiratory syncytial virus infection. J Virol 86: 10456-10461.
151. Elkins KL, Rhinehart-Jones TR, Stibitz S, Conover JS, Klinman DM (1999) Bacterial DNA containing CpG motifs stimulates lymphocyte-dependent protection of mice against lethal infection with intracellular bacteria. J Immunol 162: 2291-2298.
152. Wongratanacheewin S, Kespichayawattana W, Intachote P, Pichyangkul S, Sermswan RW, et al. (2004) Immunostimulatory CpG oligodeoxynucleotide confers protection in a murine model of infection with *Burkholderia pseudomallei*. Infect Immun 72: 4494-4502.
153. Waag DM, McCluskie MJ, Zhang N, Krieg AM (2006) A CpG oligonucleotide can protect mice from a low aerosol challenge dose of *Burkholderia mallei*. Infect Immun 74: 1944-1948.
154. Rozak DA, Gelhaus HC, Smith M, Zadeh M, Huzella L, et al. (2010) CpG oligodeoxyribonucleotides protect mice from *Burkholderia pseudomallei* but not *Francisella tularensis* Schu S4 aerosols. J Immune Based Ther Vaccines 8: 2.
155. Easton A, Haque A, Chu K, Patel N, Lukaszewski RA, et al. (2011) Combining vaccination and postexposure CpG therapy provides optimal protection against lethal sepsis in a biodefense model of human melioidosis. J Infect Dis 204: 636-644.

156. Liu Y, Luo X, Yang C, Yu S, Xu H (2011) Three CpG oligodeoxynucleotide classes differentially enhance antigen-specific humoral and cellular immune responses in mice. Vaccine 29: 5778-5784.
157. Cooper CL, Ahluwalia NK, Efler SM, Vollmer J, Krieg AM, et al. (2008) Immunostimulatory effects of three classes of CpG oligodeoxynucleotides on PBMC from HCV chronic carriers. J Immune Based Ther Vaccines 6: 3.
158. Bernasconi NL, Onai N, Lanzavecchia A (2003) A role for Toll-like receptors in acquired immunity: up-regulation of TLR9 by BCR triggering in naive B cells and constitutive expression in memory B cells. Blood 101: 4500-4504.
159. Vollmer J, Weeratna R, Payette P, Jurk M, Schetter C, et al. (2004) Characterization of three CpG oligodeoxynucleotide classes with distinct immunostimulatory activities. Eur J Immunol 34: 251-262.
160. Krug A, Rothenfusser S, Hornung V, Jahrsdörfer B, Blackwell S, et al. (2001) Identification of CpG oligonucleotide sequences with high induction of IFN-alpha/beta in plasmacytoid dendritic cells. Eur J Immunol 31: 2154-2163.
161. Gursel M, Verthelyi D, Gürsel I, Ishii KJ, Klinman DM (2002) Differential and competitive activation of human immune cells by distinct classes of CpG oligodeoxynucleotide. J Leukoc Biol 71: 813-820.
162. Asselin-Paturel C, Brizard G, Chemin K, Boonstra A, O'Garra A, et al. (2005) Type I interferon dependence of plasmacytoid dendritic cell activation and migration. J Exp Med 201: 1157-1167.
163. Ballas ZK, Rasmussen WL, Krieg AM (1996) Induction of NK activity in murine and human cells by CpG motifs in oligodeoxynucleotides and bacterial DNA. . J Immunol 157: 1840-1845.
164. Hartmann G, Battiany J, Poeck H, Wagner M, Kerkmann M, et al. (2003) Rational design of new CpG oligonucleotides that combine B cell activation with high IFN-alpha induction in plasmacytoid dendritic cells. Eur J Immunol 33: 1633-1641.
165. Marshall JD, Fearon K, Abbate C, Subramanian S, Yee P, et al. (2003) Identification of a novel CpG DNA class and motif that optimally stimulate B cell and plasmacytoid dendritic cell functions. J Leukoc Biol 73: 781-792.
166. Amemiya K, Bush GV, DeShazer D, Waag DM (2002) Nonviable *Burkholderia mallei* induces a mixed Th1- and Th2-like cytokine response in BALB/c mice. Infect Immun 70: 2319-2325.
167. Galyov EE, Brett PJ, Deshazer D (2010) Molecular insights into *Burkholderia pseudomallei* and *Burkholderia mallei* pathogenesis. Annu Rev Microbiol 64 495-517.
168. Judy BM, Taylor K, Deeraksa A, Johnston RK, Endsley JJ, et al. (2012) Prophylactic application of CpG oligonucleotides augments the early host response and confers protection in acute melioidosis. PLoS One 7: e34176.
169. Estes DM, Dow SW, Schweizer HP, Torres AG (2010) Present and future therapeutic strategies for melioidosis and glanders. Expert Rev Anti Infect Ther 8: 325-338.
170. Deitchman S, Sokas R (2001) Glanders in a military research microbiologist. N Engl J Med 345: 1644.

171. Utaisincharoen P, Kespichayawattana W, Anuntagool N, Chaisuriya P, Pichyangkul S, et al. (2003) CpG ODN enhances uptake of bacteria by mouse macrophages. Clin Exp Immunol 132: 70-75.
172. Puangpetch A, Anderson R, Huang YY, Sermswan RW, Chaicumpa W, et al. (2012) Cationic liposomes extend the immunostimulatory effect of CpG oligodeoxynucleotide against *Burkholderia pseudomallei* infection in BALB/c mice. Clin Vaccine Immunol 19: 675-683.
173. Krieg AM (2002) CpG motifs in bacterial DNA and their immune effects. Annu Rev Immunol 20: 709-760.
174. Wedlock DN, Denis M, Skinner MA, Koach J, de Lisle GW, et al. (2005) Vaccination of cattle with a CpG oligodeoxynucleotide-formulated mycobacterial protein vaccine and *Mycobacterium bovis* BCG induces levels of protection against bovine tuberculosis superior to those induced by vaccination with BCG alone. Infect Immun 73: 3540-3546.
175. Ren T, Liang YJ, Cai YY, Li CY, Mei J, et al. (2008) A study on the mechanisms of mycobacterial clearance induced by CpG-oligodeoxynucleotides in mice. Zhonghua Jie He He Hu Xi Za Zhi 31: 46-50.
176. Appelberg R (2007) Neutrophils and intracellular pathogens: beyond phagocytosis and killing. Trends Microbiol 15: 87-92.
177. Kumar V, Sharma A (2010) Neutrophils: Cinderella of innate immune system. Int Immunopharmacol 10: 1325-1334.
178. Xiao L, Zhang Y, Liu Z, Yang M, Pu L, et al. (2010) Synthesis of the Cyanine 7 labeled neutrophil-specific agents for noninvasive near infrared fluorescence imaging. Bioorg Med Chem Lett 20: 3515-3517.
179. Blasi F, Tarsia P, Aliberti S (2005) Strategic targets of essential host-pathogen interactions. Respiration 72: 9-25.